
Modeling, simulation and validation of
generic wind turbine models based on
international guidelines



DOCTORAL THESIS

Alberto Lorenzo Bonache

Instituto de Investigación en Energías Renovables

Escuela Técnica Superior de Ingenieros

Industriales de Albacete

Universidad de Castilla – La Mancha

June 2019

Modeling, simulation and validation
of generic wind turbine models
based on international guidelines

Author

Alberto Lorenzo Bonache

Directed by

**Emilio Gómez Lázaro
Andrés Honrubia Escribano**

**Instituto de Investigación en Energías Renovables
Escuela Técnica Superior de Ingenieros
Industriales de Albacete
Universidad de Castilla – La Mancha**

June 2019

*... and I would come back,
but I have already covered a long road.*

*... y volvería,
pero ya anduve mucho trecho.*

Cada día, Rosendo Mercado

Acknowledgements

Looking back on when I wrote the acknowledgments of degree and master's final theses, of barely half a dozen lines, I remember the real headache they involved. Now, the idea of having to write at least one page causes me real terror... or laziness, I find it hard to discern. But the time has come, let's go for the final touch.

Since this may be the only section where I have real creative freedom, I will take a few licenses. The first will be to deprive them of solemnity. All those people to whom I am grateful for accompanying me through this process, in one way or another, should already know. If you don't feel that way, I'm not. Just in case, here's a little summary in which I don't intend, by any means, to cover everyone.

To my family in general and to my parents in particular, for having made me a person capable of standing on my own, with values and strength impossible to achieve without you. Special mention to Rufo, Tilo and Rita, because regardless of your dog nature, you have given me more happiness than most people. I am now dating Ana, who has a special line for being the

first time that she appears in my acknowledgments. Thank you very much, Anita, above all, for your smile. To my friends... I don't know whether or not to thank you for having given me so much beer over the years, because it's not good for the mind, of course. You have compensated by exercising it with references to the Simpsons (I think they also deserve thanks). To all my colleagues, I also thank you for all those tips and lessons over the years. I am going to especially thank my tutors, Emilio and Andrés, for their work and, above all, because they have to sign many papers yet. Thanks also to all those who once put stones in my way. Falling is one more squat, and it makes me stronger. By the way, thanks to Ana M^a Sánchez, my nutritionist, and Sergio Peinado, my online personal trainer, because without you I would have a deplorable health right now. As for the rest of people, do not keep it in mind if you do not show up, I am better with this than I thought and you cannot all fit in. And finally, I want to stop for a moment to thank in a very special way to that person without whom I would not be here. José Garrigós, you are the real reason why I, as many others, chose this profession. You taught us the value of effort and hard work, showing to all of us that getting something is not easy. We will never forget your classes, your exams and, above all, your advice.

Thank you all, sincerely.

Agradecimientos

Echando la vista atrás a cuando escribí los agradecimientos de TFG y TFM, de apenas media docena de líneas, recuerdo el auténtico quebradero de cabeza que supusieron. Ahora, la idea de tener que escribir, al menos, una página me causa verdadero terror... o pereza, me cuesta discernirlo. Pero llegó la hora, vamos a por el toque final.

Como puede que este sea el único apartado en el que tenga auténtica libertad creativa, me tomaré ciertas licencias. La primera de ellas será quitarles la solemnidad. Todas aquellas personas a las que les estoy agradecido por acompañarme durante este proceso, de una manera o de otra, ya deberían saberlo. Si no os sentís así, es que no lo estoy. Por si acaso, aquí va un pequeño resumen en el que no pretendo, ni mucho menos, abarcar a todo el mundo.

A mi familia en general y a mis padres en particular, por haber hecho de mí una persona capaz de valerme por mí mismo, con unos valores y una fortaleza imposible de alcanzar sin vosotros. Mención especial a Rufo, a Tilo y a Rita, porque a pesar de vuestra naturaleza perruna, me habéis dado más

alegrías que la mayoría de las personas. Me cito ahora con Ana, a la que le toca una línea especial por ser la primera vez que aparece en mis agradecimientos. Muchas gracias Anita, sobre todo, por tu sonrisa. A mis amigos... pues no sé si agradecer o no el hecho de haberme suministrado tanta cerveza a lo largo de los años, pues no es bueno para la mente, claro. Lo habéis compensado ejercitándola con referencias a los Simpsons (creo que estos últimos también se merecen un agradecimiento). A todos mis compañeros de trabajo, también les tengo que agradecer por todos esos consejos y lecciones a lo largo de estos años. Voy a agradecer especialmente a mis tutores, Emilio y Andrés, por su trabajo y, sobre todo, porque tienen que firmar muchos papeles aun. Gracias también a todos aquellos que alguna vez pusieron piedras en mi camino. Caerme supone una sentadilla más, y me hace más fuerte. Por cierto, gracias a Ana M^a Sánchez, mi nutricionista, y a Sergio Peinado, el fuertaco mayor, porque sin vosotros ahora mismo tendría una salud deplorable. En cuanto al resto de personas, no me lo tengáis en cuenta si no aparecéis, esto se me da mejor de lo que pensaba y no cabéis todos. Y para terminar, quiero pararme un momento para agradecer de forma muy especial a esa persona sin la que no estaría aquí. José Garrigós, eres la auténtica razón por la que yo, y muchos más, elegimos esta profesión. Nos enseñaste el valor del esfuerzo y el trabajo duro, demostrándonos que conseguir algo cuesta. Nunca olvidaremos tus clases, tus exámenes y, sobre todo, tus consejos.

Gracias a todos, de verdad.

Summary

In these days, wind energy is one of the most reliable and profitable among renewable energy sources. During the last decades, its growth has been unstoppable. At the end of 2018, 591.5 GW of wind power were installed worldwide, according to the Global Wind Energy Council (GWEC). From them, 51.3 GW were installed in 2018, with 2015 being the year in which most wind capacity was ever installed (63.6 GW). With hindsight, in 2001, only 23.9 GW of total capacity was installed worldwide. This fast development, together with all the social and environmental benefits, involves the emergence of new challenges for power systems.

The proper integration of wind energy in power systems constitutes an important issue to power system operators, such as Transmission System Operators (TSOs) or Distribution System Operators (DSOs). Wind Power Plants (WPP) layout, consisting in several small generators which add up to a considerable installed power, opposes to conventional generation units, which are usually equipped with a unique electrical generator. Not only this characteristic defines the particular behavior of WPP, but also does the high use of power electronics. These features involve particular behaviors facing grid events, such as Low Voltage Ride Through (LVRT), also known as voltage dips. To face these events and guaranteeing the security and continuity of power supply, TSOs and DSOs conduct dynamic simulations of their power systems. In the current Doctoral Thesis, the focus is the transient stability of power systems, for which Wind Turbine (WT) and WPP dynamic simulation models are needed.

Traditionally, these models are developed and owned by WT manufacturers. This fact involves a series of inconveniences. On the one hand, they are designed to cover the vendor's needs, which do not have to be the same than those of power system operators. Furthermore, each vendor defines the specific model for each of their manufactured WT models (i.e., there exist a huge number of models). On the other hand, vendor models are usually very complex, and defined by a large number of parameters. Moreover, they are developed in the simulation software which better fits their purpose. Last

but not least, all these models, parameters and software are usually confidential, with the manufacturers being extremely zealous regarding their external use. In order to solve these issues and to cover power system operators needs, international entities, such as the International Electrotechnical Commission (IEC) and the Western Electricity Coordinating Council (WECC), have developed generic, also known as simplified or standard, WT and WPP models.

In contrast to vendor models, generic WT models are designed to be publicly available, relatively simple (i.e., they should use low computational resources and be defined by a limited number of parameters) and easily implementable in any simulation software. They are designed to conduct transient stability analysis of power systems, facing events such as voltage dips. Concretely, these models are developed to conduct large-disturbance short term voltage stability studies. The first international guideline regarding this topic was the “*WECC Wind Power Plant Dynamic Modeling Guide*” (2010), which firstly defined these models. Later, in 2014 the “*Second Generation of Generic Wind Turbine Models*” was published, improving the performance of the models from the previous version. Later, in 2015, the IEC published the International Standard IEC 61400-27-1 “*Electrical simulation models - Wind turbines*”. Although the main goal of the two entities is the same (i.e., the definition of generic WT models based on the previous requirements), their focus is different. On the one hand, the WECC is focused on the simplicity of the models. This means that they should be defined by the least possible number of blocks and parameters, with the consequent implications in the accuracy (especially during transient periods) and simulation time. On the other hand, the IEC intends to provide as accurate a response as possible, regardless of the generic models limitations.

Under this framework, the current Doctoral Thesis aims to cover three main aspects. First, the modeling of generic WT models based on the two international guidelines (IEC and WECC) is addressed, focusing on Doubly Fed Induction Generator (DFIG) and Full-Converter (FC) technologies. This choice is not arbitrary. Currently, DFIG technology, also known as Type 3, is the most widespread in power systems worldwide. Additionally, FC technology, also known as Type 4, is more and more used due to its advantages and the reduction in power electronics price, especially in offshore WPPs. Second, the comparison between the two perspectives is discussed. This involves analyzing the modeling differences, as well as studying their consequences, not only on accuracy, but also on simplicity and simulation time. Finally, the validation of the WT models with field data collected in wind farms, following the IEC 61400-27-1 guidelines, is performed to evaluate their accuracy.

Resumen

En la actualidad, la energía eólica es una de las fuentes de energía renovable más fiables y rentables. Durante las últimas décadas, su crecimiento ha sido imparable. A finales de 2018, la potencia eólica total instalada en todo el mundo era de 591,5 GW, según el GWEC. De ellos, 51,3 GW fueron instalados sólo en 2018, siendo 2015 un año récord, en el que se instalaron 63,6 GW de potencia eólica. En retrospectiva, en 2001, sólo existían 23,9 GW de capacidad total en todo el mundo. Este rápido desarrollo, junto con todos los beneficios sociales y ambientales asociados al uso de energías renovables, implica la aparición de nuevos desafíos para los sistemas eléctricos actuales.

La correcta integración de la energía eólica en los sistemas eléctricos constituye una tarea muy importante para los operadores de estos sistemas, como son los operadores de transporte y distribución. El diseño de los parques eólicos, que consiste en pequeños generadores que suman una potencia instalada considerable, es muy diferente a las unidades de generación convencionales, que suelen estar equipadas con un único gran generador eléctrico. Junto con esta disposición particular, el importante uso de sistemas de electrónica de potencia también define el comportamiento de los parques eólicos. Estas características involucran determinados comportamientos cuando ocurren eventos en la red, como los huecos de tensión. Para hacer frente a estos eventos y garantizar la seguridad y continuidad del suministro de energía, los operadores de los sistemas eléctricos realizan simulaciones dinámicas de sus sistemas. La presente Tesis Doctoral se centra en el estudio de la estabilidad transitoria de los sistemas eléctricos, para lo cual se necesitan modelos dinámicos de aerogeneradores y parques eólicos.

Tradicionalmente, estos modelos han sido desarrollados por los fabricantes de aerogeneradores. Esto implica una serie de inconvenientes. Por un lado, están diseñados para cubrir las necesidades específicas del fabricante, que no tienen por qué ser las mismas que las de los operadores del sistema eléctrico. Además, cada fabricante define un modelo específico para cada uno de sus modelos fabricados (es decir, existen un gran número de modelos). Por otro lado, los modelos de fabricantes suelen ser considerablemente complejos, y

están definidos por un gran número de parámetros. Además, se desarrollan en el software de simulación que mejor se adapta a sus necesidades. Por último, pero no por ello menos importante, todos estos modelos, parámetros y software suelen ser confidenciales, siendo los fabricantes extremadamente celosos con su uso externo. Para resolver estos problemas y cubrir las necesidades de los operadores del sistema eléctrico, entidades internacionales, como la IEC y el WECC, han desarrollado modelos genéricos, también conocidos como simplificados o estándar, de aerogeneradores y parques eólicos. Estos modelos han sido desarrollados para realizar análisis de grandes perturbaciones de tensión a corto plazo (huecos de tensión) en sistemas eléctricos.

A diferencia de los modelos de los fabricantes, los modelos genéricos están diseñados para ser públicos, relativamente sencillos (es decir, deben utilizar pocos recursos computacionales y estar definidos por un número limitado de parámetros) y ser fácilmente implementados en cualquier software de simulación. El primer documento internacional que trataba acerca de este tema fue el “*WECC Wind Power Plant Dynamic Modeling Guide*” (2010), donde se definieron por primera vez estos modelos genéricos. Posteriormente, en 2014 se publicó el documento “*Second Generation of Generic Wind Turbine Models*”, mejorando la respuesta de los modelos de la versión anterior. Por último, en 2015, la IEC publicó la IEC 61400-27-1 “*Electrical simulation models - Wind turbines*”. Aunque el objetivo principal de las dos entidades es el mismo, la definición de modelos genéricos de aerogeneradores que cubrieran los requisitos anteriores, su enfoque es diferente. Por un lado, el WECC se centró en la simplicidad de los modelos. Esto significa que deben definirse por el menor número posible de bloques y parámetros, con las consecuentes implicaciones en la precisión (especialmente en los períodos transitorios) y en el tiempo de simulación. Por otra parte, la IEC pretende dar una respuesta lo más precisa posible, a pesar de las limitaciones de los modelos genéricos.

Con todo lo anterior, la presente Tesis Doctoral pretende cubrir tres objetivos principales. En primer lugar, se aborda el modelado de modelos genéricos de aerogeneradores basados en las dos directrices internacionales (IEC y WECC), con especial interés en las tecnologías DFIG y FC. Esta elección no es arbitraria. Actualmente, la tecnología DFIG, conocida como Tipo 3, es la más extendida en los sistemas eléctricos en todo el mundo. Además, la tecnología FC, conocida como Tipo 4, es cada vez más utilizada debido a sus ventajas, así como a la reducción del precio de la electrónica de potencia, especialmente en parques eólicos marinos. En segundo lugar, se comparan ambas perspectivas (IEC y WECC). Esto implica el análisis de las diferencias de modelado, así como el estudio de sus consecuencias, no sólo en la precisión, sino también en la simplicidad y el tiempo de simulación. Por último, se realiza la validación de los modelos con datos de campo recogidos en aerogeneradores reales, siguiendo las consideraciones de la IEC 61400-27-1, para evaluar la precisión de los modelos genéricos.

Table of contents

Acknowledgements	VII
Agradecimientos	IX
Summary	XI
Resumen	XIII
1. Introduction	1
1.1. Motivation	1
1.2. Justification	3
1.3. Objectives	4
1.4. Thesis Outline	5
2. State of the art	7
2.1. International guidelines associated with generic WT models	7
2.2. Generic WT and WPP models in scientific literature	11
2.3. Summary of the state of the art and discussion	14
3. Methodology	15
3.1. Development of generic WT models	15
3.1.1. Generic Type 3 model	16
3.1.2. Generic Type 4 model	21
3.1.3. Annex – Generic models schemes	24
3.2. IEC 61400-27-1 Validation Methodology	38
3.3. <i>Simulink</i> [®] <i>Design Optimization</i> TM tool	41
4. Results	45
4.1. Published results	45
4.1.1. Paper I - IEC Type 3 parameter analysis	46
	XV

4.1.2. Paper II - IEC and WECC Type 3 comparison	70
4.1.3. Paper III - Type 4 Validation	82
4.2. Additional analysis - Transient response study	92
4.2.1. Proposal of extension of the IEC 61400-27-1 validation methodology	92
4.2.2. Results	94
4.2.3. Conclusions	104
5. Conclusions, summary of contributions and future work	107
5.1. Conclusions	107
5.2. Summary of contributions	110
5.2.1. Contributions to journals, conferences and seminars . .	110
5.2.2. Contributions to the 2 nd Edition of the IEC 61400-27-1	112
5.3. Future work	116
Bibliography	117
List of Acronyms	130

List of figures

1.1. Evolution of global installed wind capacity.	2
2.1. Main components of Types 1 and 2 WTs.	8
2.2. IEC and WECC membership distribution worldwide	10
3.1. Main components of a DFIG WT.	16
3.2. Main components of a FC WT.	21
3.3. Type 4 system that modifies the active power reference during and after the fault.	23
3.4. Modular structures of generic Type 3 models.	24
3.5. General structure of generic Type 3 models implemented in Simulink [®]	25
3.6. Control systems of generic Type 3 models implemented in Simulink [®]	26
3.7. Mechanical two mass model implemented in Simulink [®]	27
3.8. One dimensional aerodynamic model implemented in Simulink [®]	27
3.9. Active power control models implemented in Simulink [®]	28
3.10. Torque PI control modes implemented in Simulink [®]	29
3.11. Pitch control models implemented in Simulink [®]	30
3.12. Reactive power control models implemented in Simulink [®]	31
3.13. Current limitation system models implemented in Simulink [®]	32
3.14. Type 3 - Electrical generator models implemented in Simulink [®]	33
3.15. IEC 61400-27-1 reference frame rotational model model im- plemented in Simulink [®]	34
3.16. IEC 61400-27-1 reactive power limitation model implemented in Simulink [®]	34
3.17. Modular structures of generic Type 4 models.	35
3.18. General structure of generic Type 4 models implemented in Simulink [®]	36

3.19. IEC 61400-27-1 Type 4 Active power control model implemented in Simulink [®]	37
3.20. IEC 61400-27-1 Type 3A electrical generator model implemented in Simulink [®]	37
3.21. IEC 61400-27-1 Validation methodology time windows	39
3.22. Limitation of ME against MAE.	40
3.23. <i>Simulink[®] Design OptimizationTM</i> variables set.	42
3.24. <i>Simulink[®] Design OptimizationTM</i> example.	43
3.25. <i>Simulink[®] Design OptimizationTM</i> with 6 cases at a time.	44
4.1. Active power for case FL1.	95
4.2. Active power for case PL2.	96
4.3. Active power for case FL2.	96
4.4. Reactive power for case FL3.	98
4.5. Reactive power for case PL3.	99
4.6. Reactive power for case PL1.	99
4.7. Active power errors calculated according to IEC methodology and transient errors, in pu.	101
4.8. Reactive power errors calculated according to IEC methodology and transient errors, in pu.	103
5.1. IEC 61400-27-1 Delay flag and timer.	113
5.2. Proposals for delay flag systems.	114
5.3. IEC 61400-27-1 Pitch control system.	115
5.4. IEC 61400-27-1 First order filter with limitation detection (G.10).	116

List of tables

3.1. WECC control flags.	18
3.2. IEC control parameters.	19
3.3. Generic Type 3 figures' reference.	20
3.4. Generic Type 4 figures' reference.	23
3.5. Time windows for error calculations.	40
4.1. Journal Metrics – Paper I.	46
4.2. Journal Metrics – Paper II.	70
4.3. Journal Metrics – Paper III.	82
4.4. Characteristics of the test cases analyzed.	92
4.5. Active power MAE and MXE during fault period with IEC and transient validation methodology.	102
4.6. Active power MAE and MXE during post-fault period with IEC and transient validation methodology.	102
4.7. Reactive power MAE and MXE during fault period with IEC and transient validation methodology.	104
4.8. Reactive power MAE and MXE during post-fault period with IEC and transient validation methodology.	104

Introduction

The first Chapter of the present Doctoral Thesis introduces its field of study. Motivation, justification and objectives are included as well. Finally, the Thesis outline is also detailed, briefly describing each Chapter of the Doctoral Thesis.

1.1. Motivation

During the last decades, the growth of wind energy worldwide has been unstoppable. According to GWEC [1], at the end of 2018, more than 590 GW of wind power were installed worldwide. With hindsight, in the year 2001, only 23.9 GW of wind power existed in the world. This fast growth is shown in Figure 1.1. In 2018, 51.3 GW of wind power were installed worldwide, being 2015 a record year with 63.6 GW installed. This development is supported by the fact that wind energy is one of the most profitable sources of electricity [2, 3]. Lastly but not last, the social and environmental benefits linked to wind energy have been widely discussed during the last decades, especially with the climate change goals established by the European Union or the Kyoto Protocol [4, 5].

This fast development involves that power systems in which wind energy is a relevant source of generation have to be prepared for the new challenges that arise [6, 7]. For this purpose, power system operators have developed strict grid codes with which to control the impact of renewable energy power plants [8]. Wind Power Plants (WPP), among other renewable energy sources, present some characteristics which involve particular behaviors that differ with those of traditional generation power plants (e.g., nuclear, natural gas, hydroelectric...) facing different grid events [9]. One of these features is related to the fact that a WPP consists of a group of several WTs of, relatively, small power. In comparison, traditional power plants are usually equip-

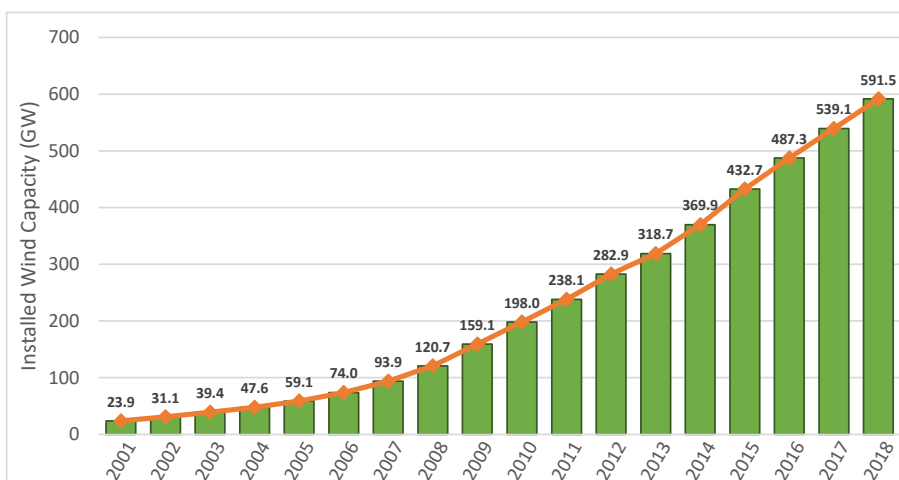


Figure 1.1: Evolution of global installed wind capacity. Source [1].

ped with a unique electrical generator of large power. Additionally, WTs are usually equipped with power converters with a considerable influence on their response. For example, Doubly Fed Induction Generator (DFIG) WTs are equipped with a power converter rated at 30-40 % of their nominal power [10], meanwhile Full-Converter (FC) WTs are connected to the grid via a converter rated at the nominal power of the WT. These two topologies are the most relevant in current power systems: DFIG technology is the most widespread topology nowadays [11], and FC technology is more and more used (especially in offshore WPP [12]) due to its flexibility advantages and reduction in the price of power electronics [13]. In order to evaluate the impact of WPP when a grid event (e.g., short-circuits, voltage dips, loss of loads or generation...) occurs, power system operators (Transmission System Operators (TSOs) and Distribution System Operators (DSOs)) conduct transient system stability analysis via simulation. For this purpose, they need dynamic models which accurately represent the response of WTs and WPP.

Simulation models for WTs and WPP have existed for years [14–16]. Nevertheless, there was a lack of standardized, relatively simple and publicly available models. Contrarily, these models were usually developed by WT manufacturers [17, 18]. Manufacturers develop their models aiming to cover their own needs, which do not necessarily correspond to those from TSOs or DSOs [19–21]. Furthermore, for each manufactured WT model, vendors usually develop a simulation model. Hence, the number of different simulation models that are needed to conduct an analysis of a complex grid (e.g., a country) may be considerably large. Additionally, vendor models are usually complex, and defined by a considerable number of parameters, since they are developed to cover a wide range of analyses. Besides, the simulation software in which these models are developed depends on each manufacturer,

and may even be an own software (i.e., not available for external users). Lastly, it is worth mentioning that all these vendor models, parameters or software are usually confidential [22, 23]. Manufacturers are mostly zealous about the external use of their tools and resources. All of the above leads to the need of new models which are appropriate to be used by power system operators [24, 25].

In order to provide TSOs and DSOs with the necessary simulation models to conduct transient system stability analysis, the International Electrotechnical Commission (IEC) and the Western Electricity Coordinating Council (WECC) have developed generic, also known as standard or simplified, WT and WPP models [26]. The WECC published the “*WECC Wind Power Plant Dynamic Modeling Guide*” [27] in 2010, which firstly described the generic WT and WPP models. However, these first models did not accurately represent the actual behavior of WTs. Thus, with the aid of several manufacturers (ABB, General Electric, REPower...), the model response was improved [28]. Then, with the improvements from that first version, the “*WECC Second generation of wind turbine models*” [29] was published in 2014. In parallel, the IEC worked in the 1st Edition of the International Standard IEC 61400-27-1 “*Electrical simulation models - Wind turbines*” [30], which was finally published in 2015. Both entities aim the same: the definition of standardized, relatively simple and publicly available generic WT and WPP models, which should be easily implemented in any simulation software. These dynamic models are designed to conduct transient stability analysis of power systems, facing short-term events such as voltage dips or loss of loads or generation [28, 31, 32]. Finally, generic WT models are designed under a series of assumptions which involve certain limitations on their application (e.g., only three-phase faults can be studied, wind speed must be considered constant, stator flux dynamics are neglected for DFIG WTs...) [33].

1.2. Justification

The relatively recent publication of these documents, especially the Standard IEC 61400-27-1, involves a lack of implementation works. The modeling and implementation of new models is necessary in order to find issues and improvements implementable in future versions [34, 35]. This fact is accentuated because of the current work in the development of the 2nd Edition of the IEC 61400-27-1, which is being conducted by Working Group (WG) 27 of Technical Committee (TC) 88 of the IEC, and it is supposed to be published in 2020. Together with this topic, the validation of generic WT models constitutes another important issue. Validation works are vital to test the capacities and limitations of generic WT models, especially their accuracy when their response is compared to field data [36–38]. Additionally, the vali-

dation methodology applied in the current Doctoral Thesis is the one briefly described in the Standard IEC 61400-27-1. The complete methodology is currently under development for its publication in the 1st Edition of the IEC 61400-27-2. Thus, the application of this methodology is of high interest not only to test the accuracy and proficiency of generic WT models, but also to the development of the validation methodology itself.

On another side, the existence of two documents related to the definition of generic models may seem unusual, since the aim of both is to provide standardized models. In fact, both entities (IEC and WECC) started the development of generic models in conjunction, with the aid of several manufacturers [39]. However, during the process, they identified differences in their point of views. On the one hand, the WECC is focused on simplicity. This means that the model should be defined by the least possible parameters and blocks. This involves less accuracy (especially during transient periods), but also a considerable improvement on simulation time and computational resources consumption. On the other hand, the IEC is focused on accuracy. Despite the limitations with which the generic models are developed, the IEC intends to emulate as accurate the real response of the WT as possible. Some detailed systems are implemented in the IEC generic models (especially in the DFIG model, which is the most complex among the four WT types) which pretend to represent some specific behaviors of the WT (e.g., crowbar system, complex electromagnetic torque control system, detailed electrical generator...). Meanwhile, the WECC studied the inclusion of these systems into their models, but it was dismissed since, from their point of view, the performance improvement does not outweigh the additional complexity [40–42]. Additionally, it is worth noting that WECC models are defined with particular software in mind (e.g., GE PSLFTM or Siemens PSS[®]E) [43], whereas the IEC defines the models in a more open manner. With these perspectives on the table, the comparison between them becomes a crucial topic, since each stakeholder (manufacturers, TSOs, DSOs, researchers...) needs to know which model to use depending on the required features [44].

1.3. Objectives

In addition to the background in the field of generic WT models detailed above, and the motivation and justification of the present work, the specific objectives of this Doctoral Thesis are enumerated as follows, with the ultimate goal of enhancing the development, performance and spread of generic WT models:

- To implement the generic WT models of DFIG and FC technologies based on the IEC and WECC guidelines.
- To conduct a detailed comparison between the IEC and WECC pers-

pectives regarding generic WT models.

- To conduct parametrization and validation studies to the generic WT models with field data, assessing their accuracy and limitations.
- To provide feedback to the IEC Committee in charge of the development of the future editions of the IEC 61400-27 (Parts 1 and 2).

1.4. Thesis Outline

This Doctoral Thesis is divided into five Chapters. This Introduction Chapter describes the current situation of the wind energy sector, with a particular focus on the situation of dynamic WT models. The motivation, justification and objectives are detailed as well.

Following this introduction, in Chapter 2, the state of the art on generic WT models is presented. The previous situation to the publication of the WECC “*Wind Power Plant Dynamic Modeling Guide*” and the IEC 61400-27-1 is outlined. Then, the background of the publication of the different guidelines is depicted, with special emphasis on the contrasting perspectives of the IEC and the WECC. Finally, the most relevant publications that have been published during these last years regarding generic WT models are presented, acknowledging their contribution to the topic studied in the present Doctoral Thesis.

In Chapter 3, the methodology followed is detailed. Generic DFIG and FC models following both guidelines (IEC and WECC) have been developed in MATLAB[®]/Simulink[®]. This Chapter includes a description of the developed models. The IEC 61400-27-1 validation methodology is depicted in this Chapter as well. Finally, the *Simulink[®] Design OptimizationTM*, used for the fine adjustment of the models’ parameters, is described.

Chapter 4 presents the results of the Doctoral Thesis. The present Doctoral Thesis is submitted as a thesis dissertation by *Compendium of Publications*. Thus, this Chapter is formed by the three papers published in indexed journals. An additional analysis is included, the results of which have been submitted to another indexed journal as well, but it is still in the review process.

Lastly, Chapter 5, presents the conclusions obtained during the development of this Doctoral Thesis. The contributions to the scientific literature that have been published are detailed, as well as those contributions to the future versions of the IEC 61400-27-1. Finally, the expected future works regarding the application of generic WT models for further studies are summarized.

State of the art

This Chapter presents the state of the art on generic WT models. The background of the international guidelines which are currently applicable (IEC and WECC) is discussed, followed by the most relevant publications which have been published since the inception of the models.

2.1. International guidelines associated with generic WT models

Generic WT and WPP models have been developed to cover TSOs and DSOs needs regarding transient stability analysis. The lack of public, standardized, relatively simple and easily implementable in any simulation software WT and WPP models led the International Electrotechnical Commission (IEC) and the Western Electricity Coordinating Council (WECC) to develop them. All these concerns were remarked in [23], which provides a detailed state of the art of the available models at that time, as well as the needs depending on each study. In [43], the North American Electric Reliability Corporation (NERC) highlights the need for this kind of models for non-manageable energy sources (e.g., wind or solar energy). This document underscores the past situation regarding the existing manufacturer models, the drawbacks of which have been depicted in Section 1.1. In fact, [43] remarks that the most relevant constraint on WT modeling is the manufacturer secrecy regarding their resources (e.g., parameters, models, software, field data...). Thus, the IEC and the WECC started the development of generic WT and WPP models collaboratively.

The first published document is the “*WECC Wind Power Plant Dynamic Modeling Guide*” [27], in 2010. The WECC’s first generation models of WTs are included in these guidelines. This document classifies all the existing WTs in four generic types, mainly according to their electrical generator:

- The models have to provide an accurate response at the point of connection of the WPP (i.e., active and reactive powers and currents, along with voltage). Hence, internal variables (e.g., turbine speed, controller signals, aerodynamic power...) do not represent an accurate behavior necessarily.
- They are designed to conduct simulations of transient voltage events (e.g., balanced grid faults, capacitor switching, loss of loads or generation...). Wind transient events cannot be accurately emulated (i.e., wind is considered constant during the entire simulation).
- Simulations should last for 10-30 s, with time steps between 1-10 ms.
- They are valid within a range of frequencies from DC to 10 Hz.
- They should be initialized by the power system power flow.

All features can be found at the beginning of each guideline.

On another note, some limitations were found when comparing these models' response with field data [45]. The highest concern was opening the models to cover the grid codes of different countries, since the WECC's generic models were defined with the aid of North-American manufacturers (e.g., GE, ABB, Siemens...). Fig. 2.2 shows the countries which are members of each entity. These concerns included the control of reactive power during faults, the technological development of the most advanced WT models (i.e., DFIG and FC) or improving the accuracy for validation purposes (more and more required by grid codes). Furthermore, the Electric Power Research Institute (EPRI) summarized all the issues concerning Type 3 and Type 4 in [41, 46], respectively. With all these comments, the WECC started the development of their second generation models.

The WECC's "*Second Generation of Generic Wind Turbine Models*" [29] was finally published in 2014, along with a document with more detailed guidelines [47]. All changes between first and second generation models are listed in [29], being the most important those related to reactive power control and aerodynamic and pitch angle controllers. The WECC continues working in the development of their generic models nowadays, with EPRI providing feedback to this new version [40].

Meanwhile, not only the WECC has been working in generic WT and WPP models. The IEC started working in the development of generic models in 2009 as well. Despite the WECC and the IEC began working in conjunction, the different points of view of the two working groups involved the development of two parallel documents. Since the publication of the first WECC's report [27], the IEC decided to work in their own models in order to adopt their perspective. It is worth noting that most of the issues commented to the WECC come from the IEC working group or European WT manufacturers [40, 41, 45, 46]. WG 27 of TC 88 published the 1st Edition of the

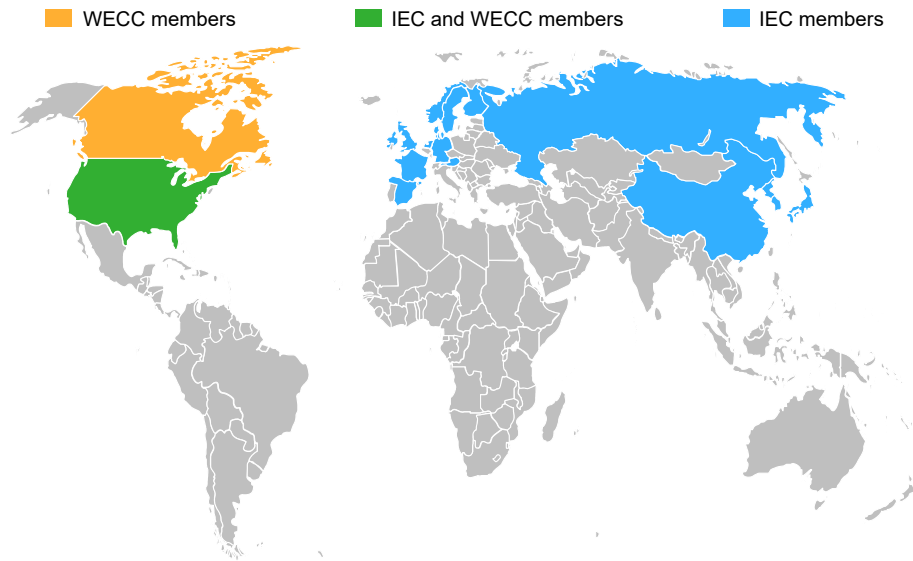


Figure 2.2: IEC and WECC membership distribution worldwide

International Standard IEC 61400-27-1 “*Electrical simulation models - Wind turbines*” [30] in February 2015. European WT manufacturers (e.g., GAME-SA, Vestas, Senvion...) collaborated in the development of the IEC Standard. This document includes the modeling of the four types of WTs and a brief description of the validation methodology. At that time, the idea of WG 27 TC 88 was the future publication of the 2nd Edition of the IEC 61400-27-1, together with the 1st Edition of the IEC 61400-27-2, which would have included the modeling of WPP. Thus, originally, the IEC 61400-27-1 would have included the modeling of WTs and the validation process, and the IEC 61400-27-2 would have included the modeling of WPPs. However, during their development, they found several redundancies and duplications with this structure. Hence, nowadays, the outline of the future versions of the IEC 61400-27 is as follows:

2nd Edition of the IEC 61400-27-1 Will include the modeling of the four types of WTs and WPPs.

1st Edition of the IEC 61400-27-2 Will include the detailed validation methodology.

These last editions are currently on Final Draft International Standard (FDIS) stage, with the voting of their approval in process [48, 49]. Their publication is expected in 2020. The models of the IEC 61400-27-1 are defined in a more open manner than those from the WECC guidelines. Every subsystem is depicted in detail, including systems such as timers, first-order filters with saturation or anti wind-up integrators, depicted in Annex G of

the IEC 61400-27-1 [30]. On the other hand, the IEC does not provide any value of the parameters included in the model.

With all the above, it may seem curious that the project of two international entities, which started to work in conjunction aiming for the same goal, has resulted in two different documents. The fact is that, despite the IEC and the WECC aspired to define generic WT and WPP models, the perspective of each of them differs. On the one hand, the WECC decided to describe models as simple as possible. This means, using the fewer computational resources and the minimum blocks and parameters. Naturally, this simplicity should be balanced with enough accurate results. On the other hand, the IEC disposed to make models as accurate as possible. This means that, despite the limitations linked to the definition of the generic models (i.e., wind variations cannot be emulated, stator flux is considered as constant, exclusion of the transformer dynamics...), they should provide a precise response. Indeed, this involves a larger number of blocks and parameters, together with the use of larger computational resources. For instance, in the case of the generic Type 3 models developed in the current Doctoral Thesis, the WECC's model is defined by 260 Simulink[®] blocks and 75 parameters, while the IEC's model is defined by 435 Simulink[®] blocks and 100 parameters (approximately, these numbers may change depending on the modeling approach). This leads to simulation times which can be doubled by the IEC generic Type 3 model. Nevertheless, especially in transient periods, the accuracy achieved with the IEC model is considerably better than that of the WECC. This result is discussed in Section 4.

These different perspectives allow the user to choose which model better adjusts to their needs. The current Doctoral Thesis investigates deeper about the differences between the models and their consequences in the response and simulation time.

2.2. Generic WT and WPP models in scientific literature

Most scientific works regarding generic WT and WPP models have been published since the release of the guidelines. Nevertheless, works previous to the international guidelines were published with the idea of using simplified models for transient stability studies. In [50], a simplified Type 3 WT model is presented, comparing it with a more detailed model. Furthermore, several manufacturers (especially North-American ones, such as GE or Siemens) started the development of their own simplified models [51–54]. It is worth noting that, at this time, models are known as simplified, but not standard. Thus, manufacturers developed simpler models for their own purposes, but not thinking about a standardization work. Finally, those manufacturers collaborated with the development of the first generation of WECC's WT

models, as shown in [55]. The closer the publication of the first generation WECC's guidelines, the more scientific publications regarding the standardization of the models were published [26, 45, 56–58].

Regardless of the publication of [27], manufacturers continued with the development of their own simplified models [31, 59, 60], which were similar to those from [27], but did not intend to perform a standardization. Additionally, status reports such as [24, 28, 61] were published, acknowledging the continuation of the WECC's models development. In [28], EPRI provided a status report of the development of the models, as well as the validation efforts. It is worth noting that the WECC's guidelines do not provide any validation methodology, and reports such as [28] conduct the validation of the models qualitatively, using the graphs of the responses. Furthermore, manufacturers were working with WECC's models as well. [62] validates a WECC's generic Type 4 model adapted to an ABB WT using a full-scale test (following the German - TR4 - validation guideline). One of the most complete works summarizing validation efforts can be found in [38], in which the WECC Wind Generation Modeling Task Force validates the four types of first generation models with data from several manufacturers (e.g., Mitsubishi, Vestas, Siemens, GE...) and detailed models (Hydro-Quebec). Furthermore, not only three-phase faults are simulated, but also the disconnection of capacitors and loads. Different studies were also conducted using WECC's models, such as [63], which uses the Type 3 model to analyze the aerodynamics of DFIG WTs. In [64], the adjustment and parametrization of a Type 4 generic WT model is conducted using field data. Additionally, from 2010 to 2014, works such as [65, 66] began to show the ongoing work of the second generation of WECC's generic models.

With the publication of the second WECC's report [29], the modeling and validation works with the second generation models continued. In [67], the validation of a generic Type 3 WT model following these last guidelines is conducted. This validation work does not cover the case of a voltage dip, but a voltage reference step and the disconnection of a capacitor bank. The comparison is also conducted between the first and the second generation models. To this end, [68] conducts a comparison between the second generation WECC Type 4 WT model and a detailed Electromagnetic Transients (EMT) model. Furthermore, in [69], members from WECC show a status report on these second generation models, summarizing the improvements and future work. Regarding future work, in [40], EPRI shows the proposed changes to Type 3 WT model, while in [70], a more detailed user guide is depicted by WECC members. As a side note, most of the proposed changes shown in [40] came from the IEC or European manufacturers (e.g., the crowbar system, see Section 3.1.1). Most of them were dismissed because of the focus on simplicity. That, as it has been previously pointed out, is the reason why the IEC was working on their own Standard.

The IEC working group was working on the development of generic WT and WPP models since 2009, in conjunction with the WECC. However, considering the different perspectives that the two entities had, they decided to work on their own Standard. Finally, in 2015, the IEC 61400-27-1 [30] was published. Nevertheless, scientific works regarding the IEC models started to be published years before the publication of the Standard. Most of them were congresses or workshop papers, in which the members of WG 27 of TC 88 showed the ongoing work. From 2011, these works, which revealed the in progress work, were published [32, 35, 71–75]. Later, using draft-version models, publications showing the IEC models began to be published. In [76], a generic Type 1 IEC model is described and modeled in the simulation software RTDS, studying both steady state and dynamic performance. Further works regarding the implementation and validation of an IEC 61400-27-1 Type 1 draft version model are shown in [77, 78]. In [79], the parametrization of a Type 3 using field data is presented. [80] shows the implementation and response of a Type 3 in MATLAB[®]/Simulink[®] and DIgSILENT-PowerFactory[™]. Detailed works concerning specific aspects of Type 3 generic models were published as well. In [81], the behavior of the crowbar system, as well as its consequences on the model response are analyzed. With regard to the Type 3 models, one of the most interesting works is the Doctoral Thesis of Dr. Jens Fortmann [82], in which the theoretics with which the generic IEC models were developed are depicted. Based on that thesis, [83] details the process of the DFIG modeling. More works regarding Type 3 draft version can be found in [45, 58, 84–86]. In [87], the WT manufacturer Siemens shows its perspective regarding the validation of the IEC 61400-27-1 Types 1 and 4 models with field data obtained from their real WTs. Finally, in 2015, the IEC 61400-27-1 was published.

Since the publication of the IEC 61400-27-1, different international working groups have been working in the modeling and validation of IEC models. In [36], an IEC Type 3 generic model is validated with a detailed manufacturer model. Later, the Type 3 model is validated with field data in [37]. It is worth noting that this paper applies for the first time the IEC 61400-27-1 validation methodology between a generic Type 3 model and field data. Not related with generic models but with validation methodology, [88, 89] conduct an interesting analysis of the available validation methodologies (including the IEC 61400-27-1 one), suggesting improvements for further versions. A very detailed review regarding generic WT models (both WECC and IEC) is presented in [90]. Additionally, works discussing the modeling of WPP have been published as well. In [91], the WPP model of the IEC 61400-27-1 (which will be deeper discussed in its 2nd Edition) is validated with a plant power factor controller. By the part of WECC, [92] provides some suggestions to conduct the WPP models validation. Moreover, the IEC and the WECC have been working jointly in the development of these WPP mo-

dels, as shown in [93]. Lastly, but not last, [44] was the first publication regarding the compatibility between WECC and IEC models. This topic has been widely studied in the current Doctoral Thesis, and [44] constitutes an important point of departure.

2.3. Summary of the state of the art and discussion

During the last years, two international entities have been actively working on the development of generic WT and WPP models. Despite a conjoined initial development, the different perspectives led to two different documents. As shown in the existing literature, generic WT and WPP models have been studied by, approximately, a decade. However, in the current literature, there is a lack of details of the modeling process. Almost none of the previous publications show a self-made model, but they use the guidelines images.

In contrast, the author of the current Doctoral Thesis has made a strong effort to develop and validate his own MATLAB[®]/Simulink[®] models, as well as explaining in detail the behavior and parametrization of every part of the models. Furthermore, an extensive comparison has been conducted between the WECC and the IEC models, not only regarding responses or results, but also with concern to the internal operation of every system. All these studies are backed up by the use of field data provided by a WT manufacturer, which has allowed to guarantee the correct response of the models. The results of this extensive modeling, development and validation of the IEC and WECC generic models are shown in the publications depicted in Section 4.

Methodology

This chapter describes the methodology used in this Doctoral Thesis. The generic Types 3 and 4 WT models described by the IEC and WECC guidelines have been modeled using MATLAB[®]/Simulink[®]. The Simulink[®] schemes of all systems which compose these models are shown. Furthermore, the IEC 61400-27-1 validation methodology is described as well. Finally, the *Simulink[®] Design OptimizationTM* tool, with which the fine adjustment of the models has been conducted, is presented.

This Chapter does not intend to extensively depict the behavior of all the systems which compose the generic WT models. That work has already been done in the publications shown in Section 4, as well as in other works of the author of the current Doctoral Thesis, summarized in Section 5.2. Rather, this Chapter, specifically the Annex 3.1.3, serves as a repository which includes the models developed in Simulink[®] for the current Doctoral Thesis.

3.1. Development of generic WT models

The generic WT models described by the WECC “*Second Generation of Generic Wind Turbine Models*” [29] and the IEC 61400-27-1 [30] have been modeled and developed in the simulation software MATLAB[®]/Simulink[®]. MATLAB[®] [94] is one of the most widespread and multi-disciplinary software tools in engineering. It provides tools for programming, data analysis, simulation, deep learning, neural networks, graphics, etc. Thanks to the experience of its users during the years, the base of MATLAB[®] has been expanded with a large number of *Toolboxes*, which increase its applications significantly. Additionally, Simulink[®] [95] is an add-on which currently has as much importance as MATLAB[®]. Simulink[®] provides a new way to model systems, using block language. Simulink[®] has also expanded with the

addition of *Blocksets*, which increase its possibilities (e.g., aerospace, vehicles, control and design...). Finally, it is worth mentioning *SimscapeTM* [96], included into Simulink[®]. *SimscapeTM* is an add-on of Simulink[®] which intends to work with “physical signals”, and not just numbers. The possibilities, flexibility and capacities provided by the three tools led to the development of the generic WT models in this complete environment.

3.1.1. Generic Type 3 model

The generic Type 3 model represents a WT equipped with a Doubly Fed Induction Generator (DFIG). This topology is the most widespread in current power systems. The power converter together with the variable pitch angle allow high controllability. Meanwhile, the fact that the power converter is rated 30-40 % of the nominal power involves relatively low costs. The components of a DFIG WT are shown in Fig. 3.1. The stator is directly connected to the grid, and the rotor is connected via a back-to-back power converter. The DC-link may include a chopper to absorb high currents during faults. Additionally, DFIG WTs may include the crowbar system. This protection system actuates when a voltage dip occurs, short-circuiting the rotor terminals (i.e., turning the DFIG WT into a squirrel cage WT) for a short period of time. This protects the converter to be submitted to high currents originated when a voltage dip occurs [97, 98].

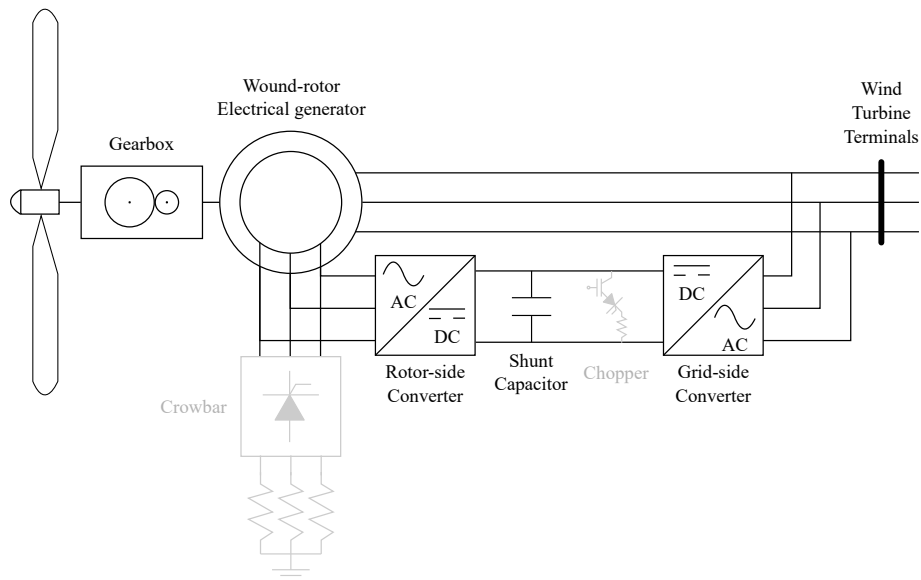


Figure 3.1: Main components of a DFIG WT.

Regarding generic WT models, the Type 3 is the most complex model for both international guidelines. The IEC 61400-27-1 differentiates between Type 3A (not equipped with crowbar system) and Type 3B (equip-

ped with crowbar system). WECC's model does not include this protection system [40]. Since the field measurements used to validate the model were obtained from a WT with crowbar system, the IEC's generic Type 3B model was modeled for the current Doctoral Thesis. The modular structures of the IEC and WECC generic Type 3 models are shown in Fig. 3.4 (See Annex 3.1.3). It is worth mentioning that active and reactive power controllers, as well as current limitation system, are included into 'Control system' without subsystem separation in WECC's guidelines. Nevertheless, in the current Doctoral Thesis these systems have been separated in subsystems for a better comprehension.

For the case of the current Doctoral Thesis, the active and reactive power references ($P_{ref0}/p_{WT,ref}$ and $Q_{ref}/x_{WT,ref}$, respectively)¹ are set manually and constant for most cases. Furthermore, power measurements are obtained directly from the output currents (ip/ip_{WT} and iq/iq_{WT}) using Eq. (3.1). Nevertheless, it is worth noting that generic models are defined to work with reactive power capacitive sign. Thus, the conjugated of the current is not applied in the models in order to correct the reactive power sign.

$$\bar{S} = \bar{U}\bar{I}^* = P + jQ \quad (3.1)$$

Fig. 3.5 (Annex 3.1.3) shows the modular structure of the generic models implemented in Simulink[®]. In Fig. 3.5b, *Pitch Control* is included into *Control model*. Structurally, both models are very similar. Nevertheless, there are two main differences which can be observed. On the one hand, the control modes of the two models differ. Table 3.1 summarizes WECC control modes and Table 3.2 summarizes IEC control modes. Regarding both systems, the differences between the two models are as follows:

Reactive power Both models can follow the same control strategies. However, the WECC model works with 3 different flags, while the IEC model works with the parameter Mq_G only. The relationships between the flags and Mq_G can be found in [99].

Current limitation system During faults, the parameters $PQFlag$ and Mq_{pri} have the same effect, allowing the selection of either active or reactive current priority. However, in steady-state, the IEC model works with active power priority (Mq_{pri} works during faults only). Additionally, the IEC model allows to limit the total current or the stator current. WECC's model does not consider this control. Further-

¹Hereinafter, when the same parameter, signal or system is defined in both WECC and IEC guidelines, but with different name, it will be mentioned as ($name_{WECC}/name_{IEC}$). For example, $P_{ref0}/p_{WT,ref}$ indicate the active power reference signal for WECC (P_{ref0}) and IEC ($p_{WT,ref}$), respectively.

more, the IEC 61400-27-1 considers the over-voltage reactive current limitation.

Active power WECC's guidelines allow to work with either active power or electromagnetic torque control in active power controller. The IEC 61400-27-1 considers torque control only.

Torque control WECC's guidelines allow to work with either active power or speed error in torque controller. The IEC 61400-27-1 considers speed error control only.

Under voltage ride through The IEC 61400-27-1 allows to select between the three different fault behaviors depicted in Table 3.2. WECC's guidelines directly implement the most complex one, leaving the control selection to the parameters definition (e.g., if the post-fault reactive current values 0, the WECC's model works as the IEC with $M_{QUVRT} = 1$). Additionally, the mode $M_{QUVRT} = 0$ does not consider the pre-fault reactive current, and the WECC's model considers it for all cases.

System	Parameter	Function
Reactive power	$PfFlag$	<i>Power factor control</i>
		1 – Power factor control, 0 – Q control
	$VFlag$	<i>Voltage control</i>
1 – Q control 0 – Voltage control		
	$QFlag$	<i>Reactive power control flag</i>
		1 – Voltage/Q control, 0 – Constant pf or Q control
Current limitation	$PQFlag$	<i>P/Q priority</i>
		0 – Q Priority 1 – P priority
Active power	$PFlag$	<i>Power/Torque control</i>
		0 – Torque control, 1 – Active power control
Torque control	$TFlag$	<i>Power/Speed error</i>
		1 – Power error 0 – Speed error

Table 3.1: WECC control flags.

On the other hand, it is worth mentioning an issue regarding voltage. The voltage input of the models are the profiles of voltage magnitude (u_{WT})

System	Parameter	Function
Reactive Power	M_{qG}	<i>Reactive power control mode</i>
		0 – Voltage control
		1 – Reactive power control
		2 – Open loop reactive power control
		3 – Power factor control
		4 – Open loop power factor control
Under Voltage Ride Through	M_{qUVRT}	<i>UVRT control mode</i>
		0 – Current proportional to fault depth
		1 – Pre-fault current plus current proportional to fault depth
		2 – Pre-fault current plus current proportional to fault depth , plus a constant post-fault current
Current Limitation	M_{qpri}	<i>Current priority during fault period</i>
		0 – Active current priority
	$M_{DFS,lim}$	1 – Reactive current priority
		<i>Limitation of Type 3 stator current</i>
		0 – Total current limitation
		1 – Stator current limitation

Table 3.2: IEC control parameters.

and angle. For theoretical simulations, voltage was defined as a sum of steps and ramps, to emulate the desired profile (e.g., the required profiles from the Spanish grid code [100]). In case of validation purposes, the voltage profile of a real voltage dip was introduced as a timeseries. Then, the voltage at the terminals of the WT transformer (V_t) is calculated. The IEC 61400-27-1 uses the equation corresponding to a RL circuit, while the WECC's guidelines do not indicate the methodology. Thus, in the current Doctoral Thesis it is calculated with the IEC methodology. The point is that, in the control systems, the IEC model uses the voltage input (u_{WT}), while the WECC model uses the voltage at the terminals of the WT transformer (V_t). During the fault, due to the injection of reactive power and the low active power consumption/generation, $V_t > u_{WT}$. Thus, this issue must be considered at the parametrization of the models, since with the exact same parameters, the response differs. More information can be found in [99].

Beyond those differences, both guidelines use the same model for two systems:

- The mechanical two mass model, which is used to emulate the interaction between the high and the low speed shafts [101].

- The aerodynamic model, which relates the pitch angle with the mechanical power extracted from the wind.

The rest of the systems are implemented differently for both models. All the systems which compose the WECC and IEC generic Type 3 WT models are shown in the Annex 3.1.3. Figures showing the different systems which compose the Type 3 models are summarized in Table 3.3. The description of the operation of each system, as well as the comparison between the WECC and IEC Type 3 models, are detailed in Section 4. Additionally, these topics are pointed in the following references from the author of the Doctoral Thesis:

- [99] describes and compares the systems which most differ between both guidelines. This work intensively analyzes the consequences of the different points of view from WECC and IEC.
- [102] conducts a parameter analysis of the IEC Type 3 model. This work focuses on those systems which affect to the active power response.
- [103] describes the operation of the active and the reactive power controls of the IEC generic Type 3 model.
- [104] assesses the theoretical analysis of a DFIG, which leads to the electrical generator system of the IEC generic Type 3 model. Additionally, it compares the response from that model developed in Simulink[®] and in DIgSILENT-PowerFactory.

System	WECC	IEC
Control models	Fig. 3.6a	Fig. 3.6b
Two mass model	Fig. 3.7	
Aerodynamic model	Fig. 3.8	
Active power control	Fig. 3.9a	Fig. 3.9b
Torque Proportional-Integral (PI) controller	Fig. 3.10a	Fig. 3.10b
Pitch controller	Fig. 3.11a	Fig. 3.11b
Reactive power control	Fig. 3.12a	Fig. 3.12b
Current limitation system	Fig. 3.13a	Fig. 3.13b
Electrical generator system	Fig. 3.14a	Fig. 3.14b
Reference frame rotational model	X	Fig. 3.15
Reactive power limitation system	X	Fig. 3.16

Table 3.3: Generic Type 3 figures' reference.

3.1.2. Generic Type 4 model

Full-Converter (FC) WTs, also known as Type 4, are more and more important in current power systems. Specially, offshore WPPs use this type of WTs to improve their performance. In Europe, more than 80 % of the offshore WPPs used this topology at the end of 2015, while more than 50 % of the onshore technology was FC as well [11]. In this technology, the WT is completely connected to the grid via a power converter. This converter should be rated at the nominal power of the WT. The use of power electronics allows high flexibility and controllability. Furthermore, this connection has additional advantages:

- Either asynchronous or synchronous generator can be used. Permanent magnet synchronous generator, electrically excited synchronous generator or squirrel-cage induction generator are common technologies.
- The use of a gearbox is not required. The power electronics may assume the frequency control. This allows to retire one of the most critical and heaviest components of the WT.

There are also some drawbacks. The power converter rated at nominal power is an expensive component, and failure rates of electronics can be as harmful as those from the gearbox [105]. Nevertheless, despite these inconveniences, Type 4 WTs are more and more used nowadays. The main components of a Type 4 WT are shown in Fig. 3.2.

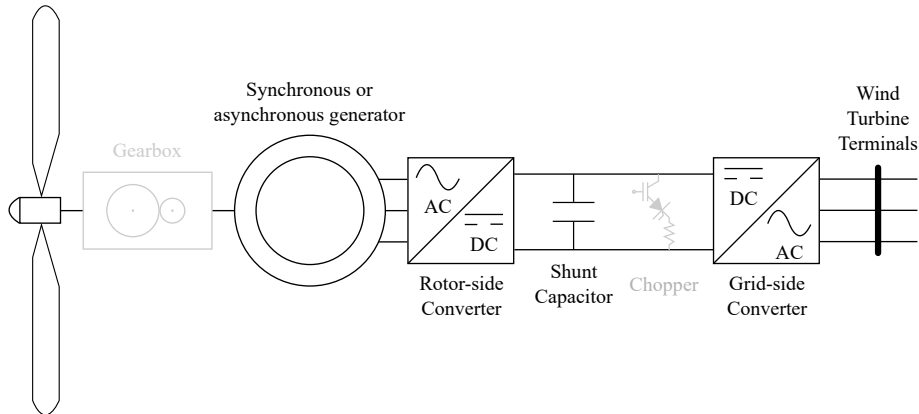


Figure 3.2: Main components of a FC WT.

Regarding the generic Type 4 WT models, they are simpler than the Type 3 models. First, the WECC and IEC structures are shown in Fig. 3.17 (Annex 3.1.3). Additionally, the general structure of the models implemented in Simulink[®] is shown in Fig. 3.18 (Annex 3.1.3). It is worth mentioning that the IEC 61400-27-1 and the WECC “*Second Generation of Generic*

"*Wind Turbine Models*" consider two subtypes of Type 4 models: Type 4A considering the mechanical oscillations, and Type 4B neglecting them. For the current Doctoral Thesis, the Type 4B was modeled. This decision was taken at the time of validating the generic Type 4 models with the field data provided by the WT manufacturer. The field data was obtained from a WT equipped with a brake chopper, which absorbs the excess of power during the fault. Thus, no mechanical oscillations occur. Hence, neither torque PI controller, nor pitch control, nor aerodynamic model, nor mechanical model are modeled. Further information can be found in [106]. With these elements, the WECC and the IEC took two different approaches.

On the one hand, the WECC's model use exactly the same control subsystems as the Type 3 model. The active power reference, which is input to the active power control system (Fig. 3.9a, Annex 3.1.3), is set manually. Additionally, $PFlag$ must take the value of 1 (Table 3.1), since the rotational speed is considered equal to 1 *pu*. $TFlag$ is unused. On the other hand, the IEC Type 4 model does include two new systems: the active power control and the electrical generator system.

- The active power control is a much simpler model than that from Type 3. Basically consists of a first order filter applied to the active power reference, which is divided by the voltage to obtain the command active current.
- The IEC 61400-27-1 allows to choose between a specific generator system designed for Type 4 or that obtained for Type 3A. The Type 4 generator model is simple, very similar to that from the WECC's guidelines (it only includes the coordination with the grid in addition). Nevertheless, aiming for a more complete behavior, the Standard allows to use the Type 3A electrical generator system. This system, as previously explained, is deducted from the behavior of a real DFIG. Thus, it is more complex but allows higher control possibilities. In order to obtain an accurate response, the Type 3A electrical generator system was modeled in the present Doctoral Thesis.

Finally, it is worth mentioning an issue regarding active power control in these models. The simplified control developed in the two guidelines involves that it is not possible to emulate some behaviors from real WTs. For the case of the current Doctoral Thesis, the real WT from which field data was extracted had a particular control of active current during the fault. It keeps constant the pre-fault active current command during the fault and the next 500 ms. This, in addition to the reactive current priority during the fault, produces a step in the active power response during and after the fault. This behavior cannot be emulated by either of the generic Type 4 WT models. In order to conduct the validation of the model, a system which modifies the active power reference during the fault and the following 500 ms

was developed for this work. This system is shown in Fig. 3.3. The inputs are the active power reference (p_WT_ref), the voltage magnitude filtered (u_filt) and the signal F_UVRT . This signal values 0 before the fault, 1 during the fault and 2 during the next 500 ms. The system adds, or subtracts, a value proportional to voltage to the manual reference during the fault. Additionally, it memorizes the lowest voltage value, in order to calculate the proportional value with which to modify the manual reference after the fault. This system is applied to both, WECC and IEC, models in order to conduct their validation. Further information can be found in [106].

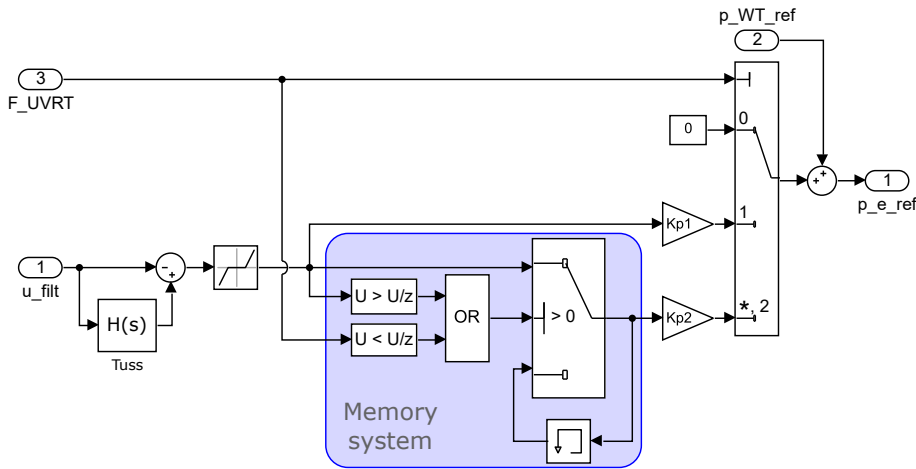


Figure 3.3: Type 4 system that modifies the active power reference during and after the fault.

With all these elements, the generic Type 4 WT model defined by the WECC and the IEC can be completed. All the systems, which compose the WECC and IEC generic Type 4 WT models, are shown in the Annex 3.1.3. Table 3.4 summarizes the figures of the systems with which to build the generic Type 4 models.

System	WECC	IEC
Active power control	Fig. 3.9a	Fig. 3.19
Reactive power control	Fig. 3.12a	Fig. 3.12b
Current limitation system	Fig. 3.13a	Fig. 3.13b
Electrical generator system	Fig. 3.14a	Fig. 3.20
Reference frame rotational model	X	Fig. 3.15
Reactive power limitation system	X	Fig. 3.16

Table 3.4: Generic Type 4 figures' reference.

3.1.3. Annex – Generic models schemes

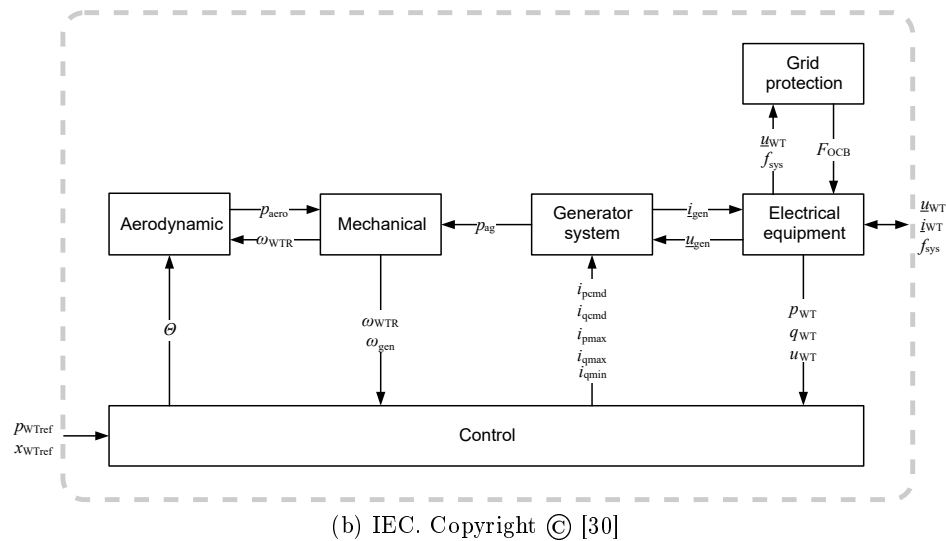
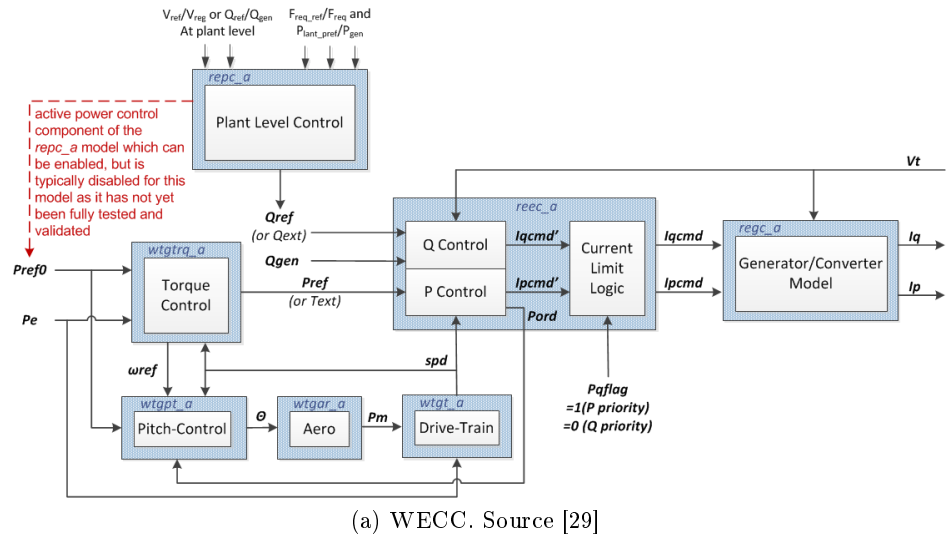


Figure 3.4: Modular structures of generic Type 3 models.

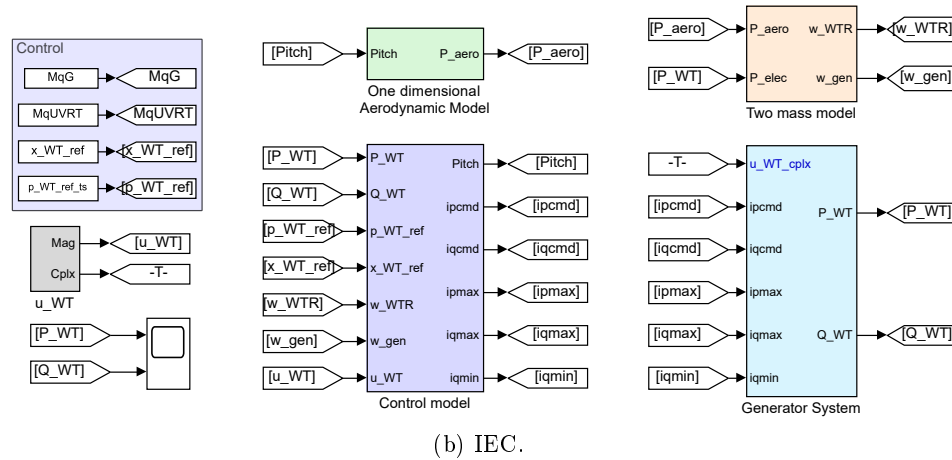
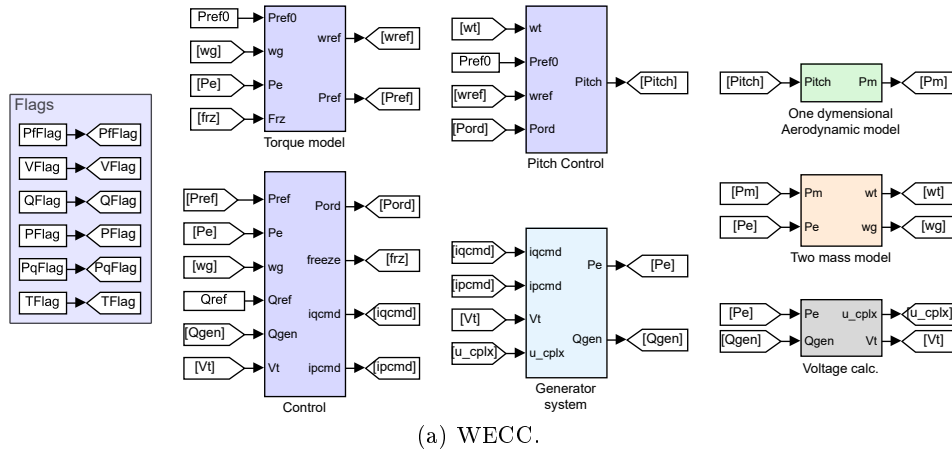
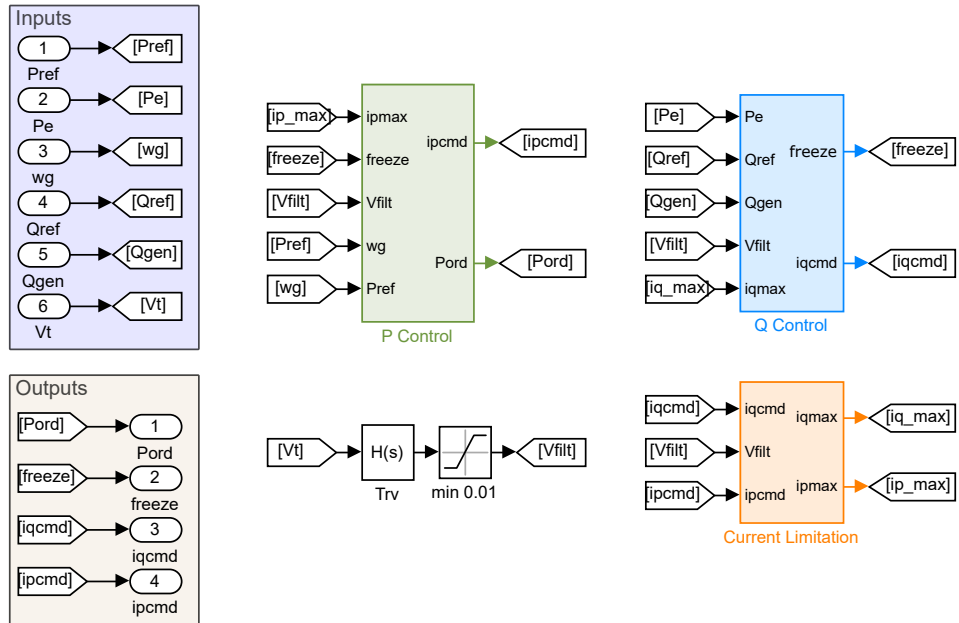
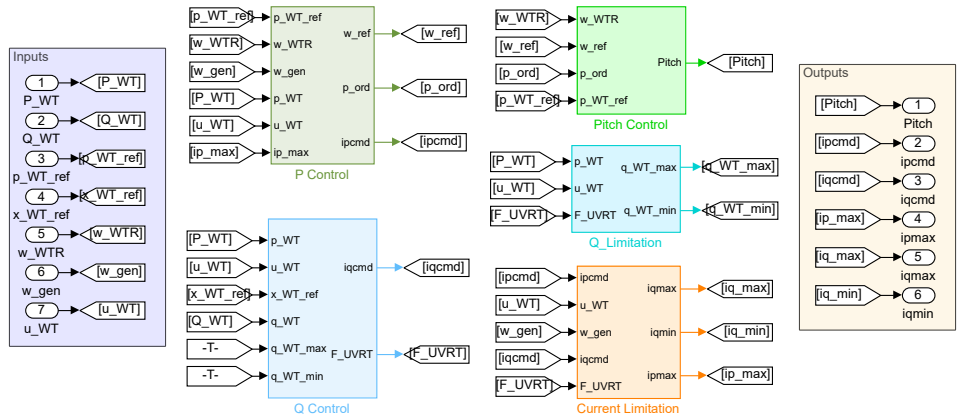


Figure 3.5: General structure of generic Type 3 models implemented in Simulink®.



(a) WECC.



(b) IEC.

Figure 3.6: Control systems of generic Type 3 models implemented in Simulink®.

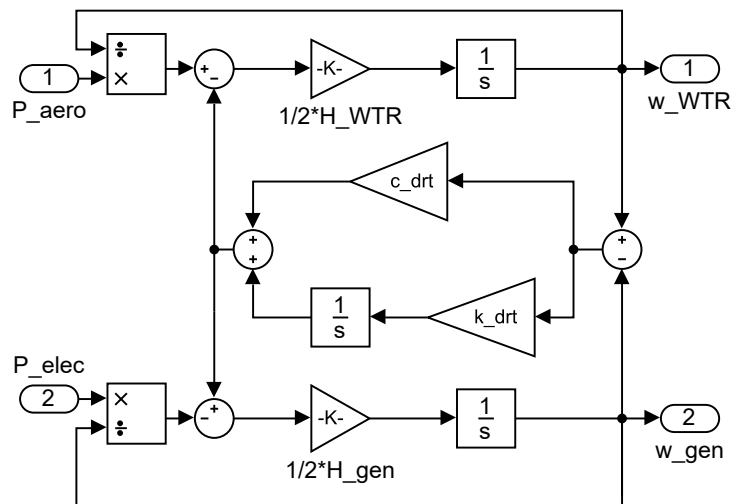


Figure 3.7: Mechanical two mass model implemented in Simulink[®].

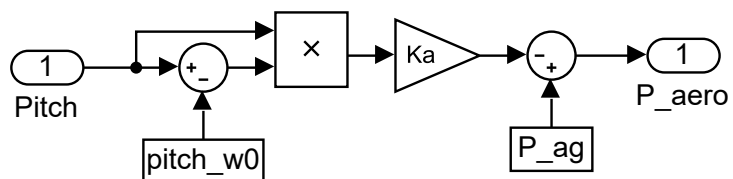


Figure 3.8: One dimensional aerodynamic model implemented in Simulink[®].

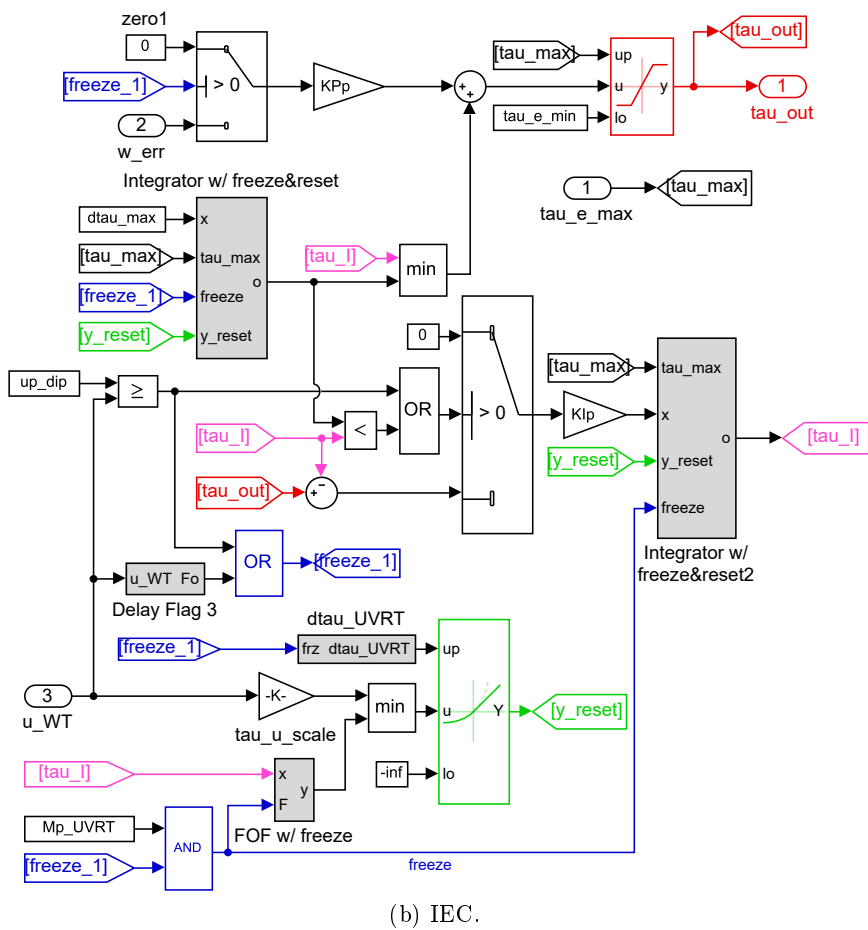
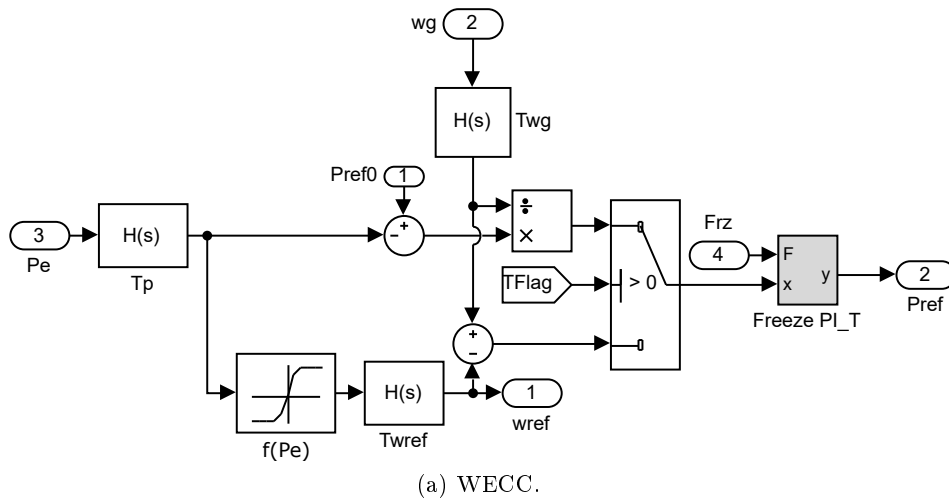
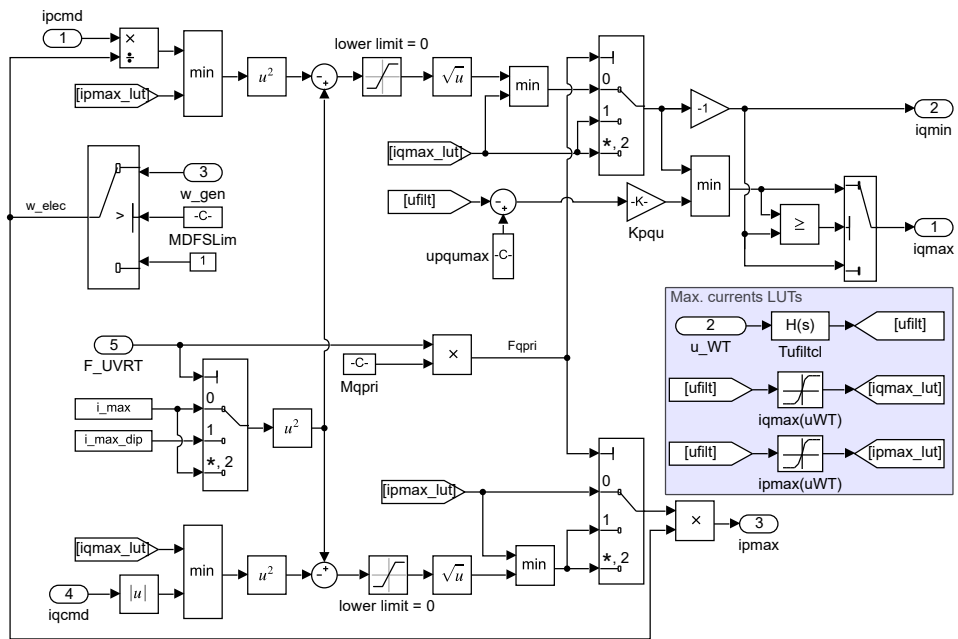


Figure 3.10: Torque PI control models implemented in Simulink®.


```

%% MATLAB code for CLS
if Pqflag==0 %Q priority
    iqmax=min(VDL1,Imax)
    ipmax=min(VDL2,sqrt(Imax^2-iqcmd^2))
else %P priority
    iqmax=min(VDL1,sqrt(Imax^2-iqcmd^2))
    ipmax=min(VDL2,Imax)
end
iqmin=-iqmax
ipmin=0

```

(a) WECC (MATLAB[®] code).

(b) IEC.

Figure 3.13: Current limitation system models implemented in Simulink[®].

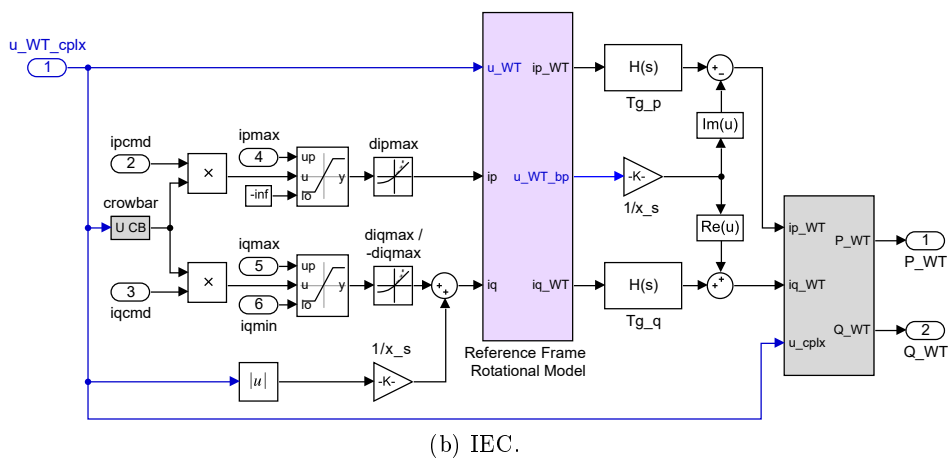
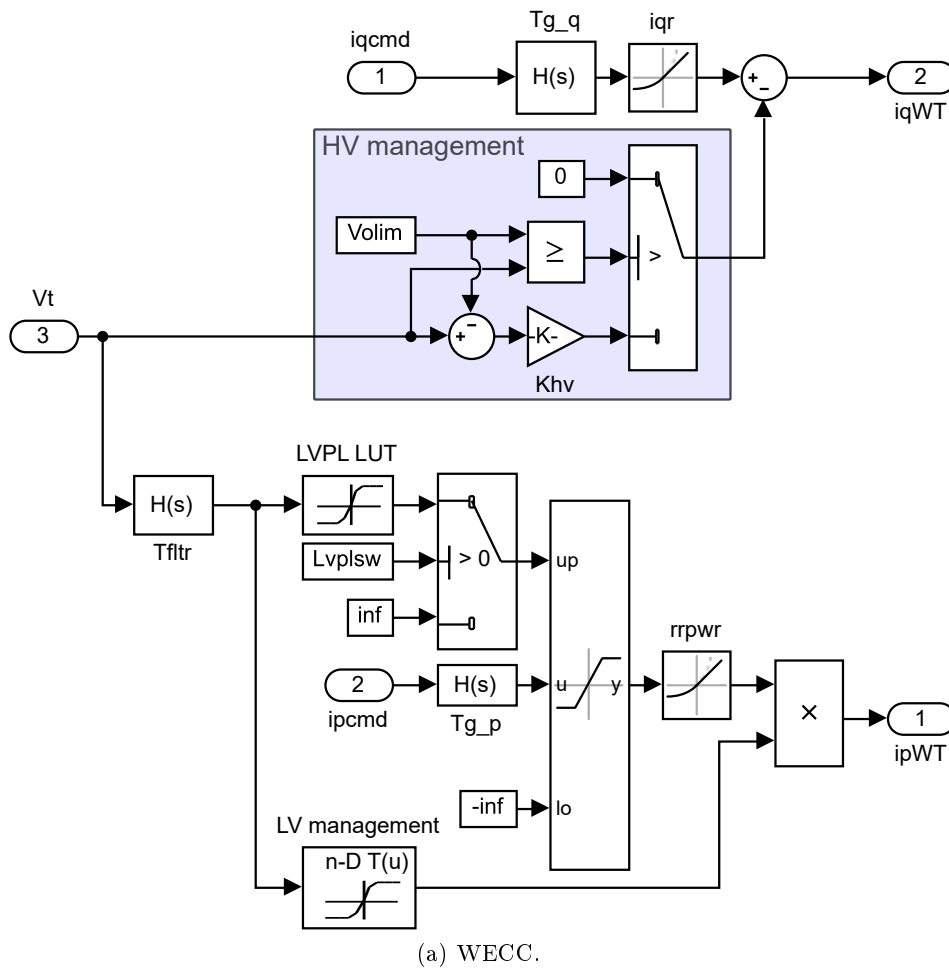


Figure 3.14: Type 3 - Electrical generator models implemented in Simulink®.

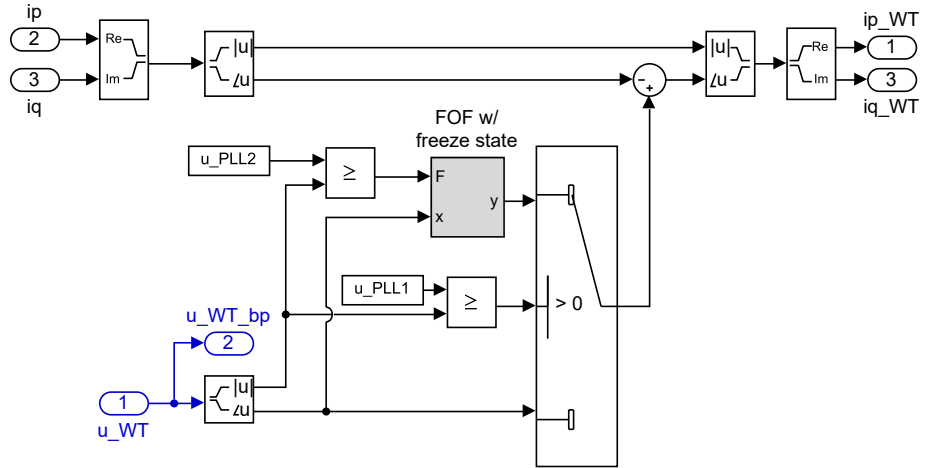


Figure 3.15: IEC 61400-27-1 reference frame rotational model model implemented in Simulink[®].

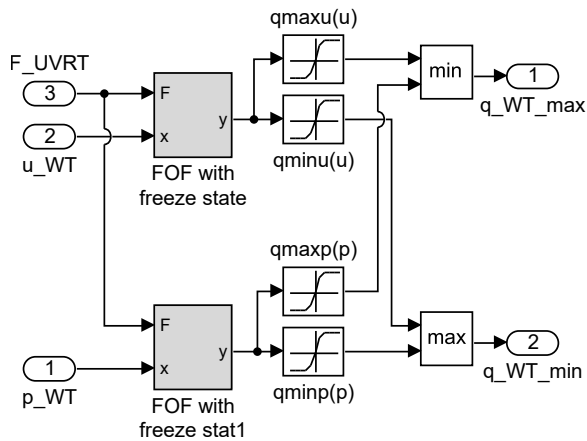
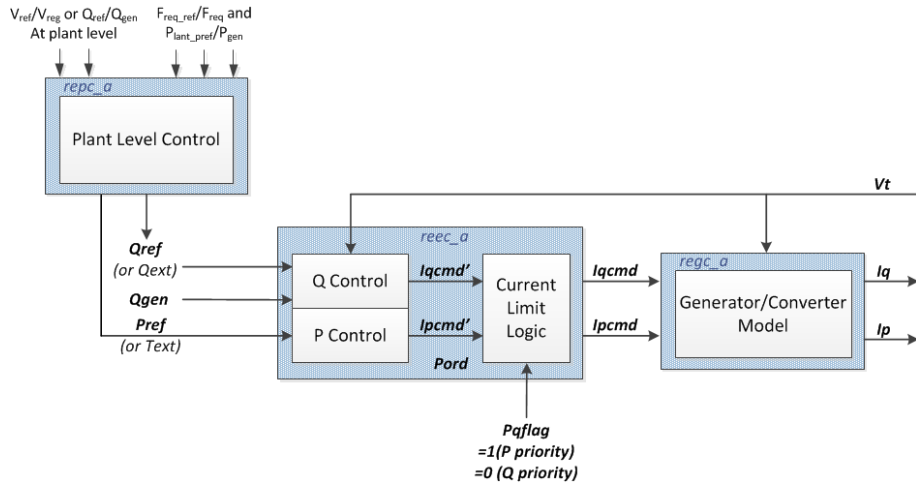
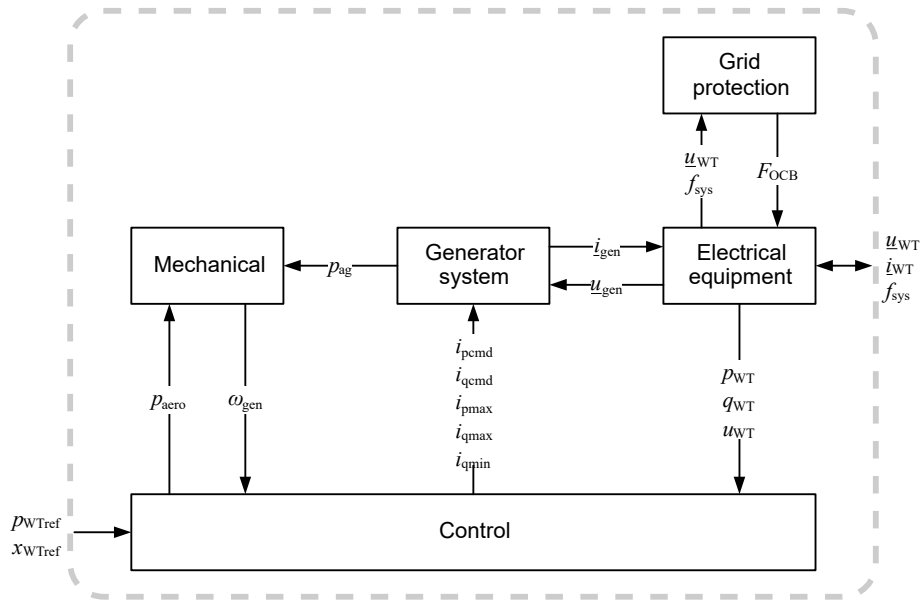


Figure 3.16: IEC 61400-27-1 reactive power limitation model implemented in Simulink[®].

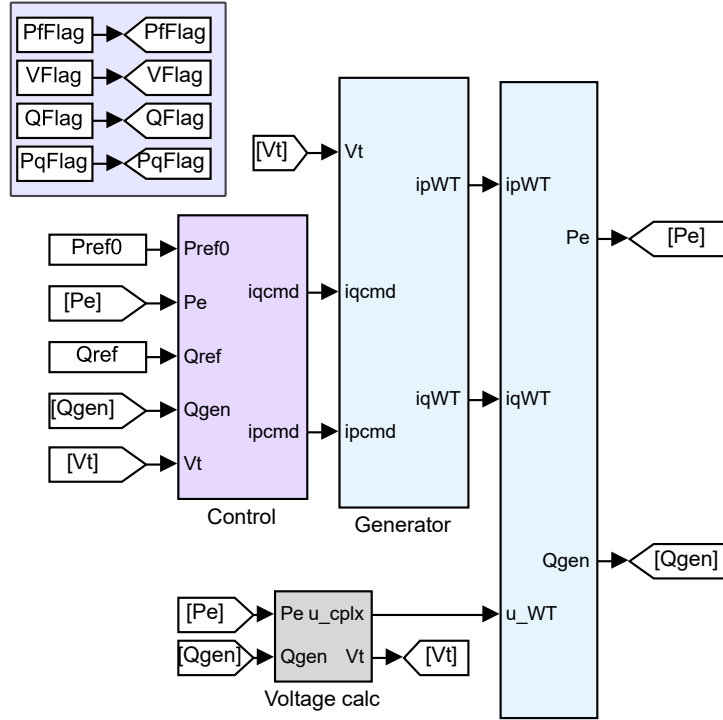


(a) WECC. Source [29]

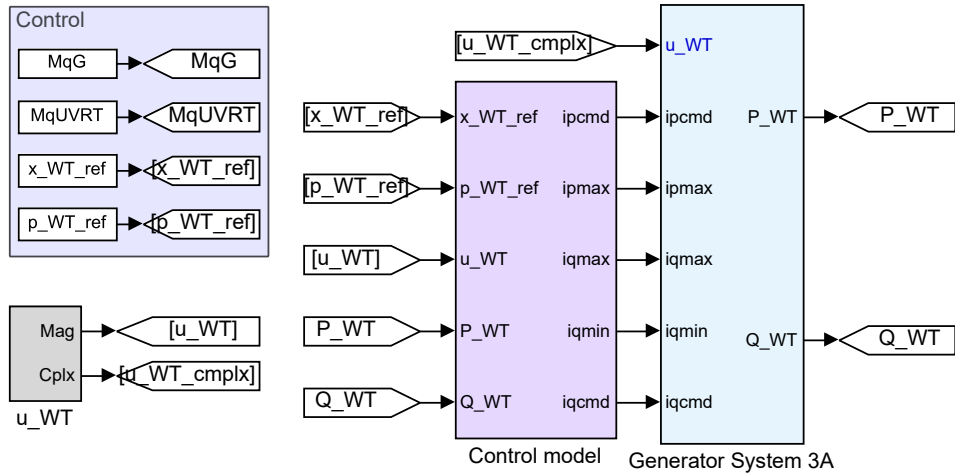


(b) IEC. Copyright © [30]

Figure 3.17: Modular structures of generic Type 4 models.



(a) WECC.



(b) IEC.

Figure 3.18: General structure of generic Type 4 models implemented in Simulink®.

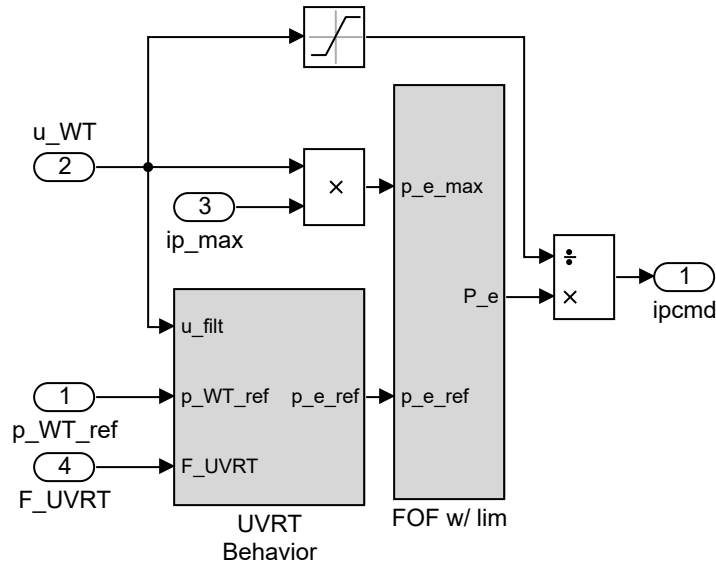


Figure 3.19: IEC 61400-27-1 Type 4 Active power control model implemented in Simulink®.

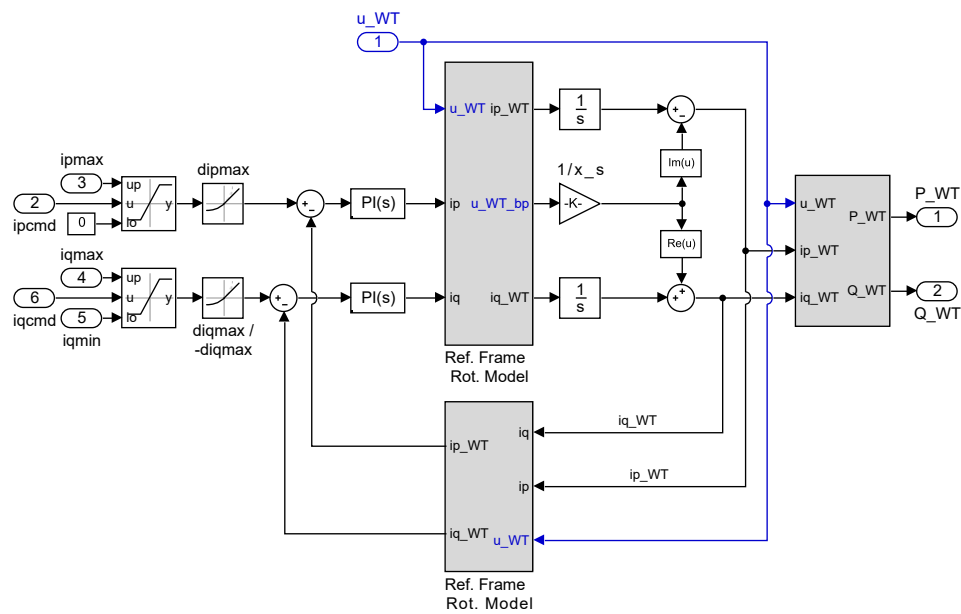


Figure 3.20: IEC 61400-27-1 Type 3A electrical generator model implemented in Simulink®.

3.2. IEC 61400-27-1 Validation Methodology

In order to test the accuracy of the generic WT models, the IEC Committee developed its own validation methodology. Currently, it is briefly depicted in Section 6 of the IEC 61400-27-1 [30]. However, its detailed version will be finally published in the 1st Edition of the IEC 61400-27-2, which is intended to be published in 2020. The validation procedure can be applied between the generic WT models and field data, as well as previously validated fundamental frequency models. It is worth mentioning that, currently, the validation methodology does not indicate any validation threshold. Thus, nowadays, it is not possible to get a passed or failed test, but to simply provide the error magnitude values. Hence, the users should decide whether the results are valid or not.

In order to conduct the validation, it is important to define the measurement point (high or low voltage side of the transformer). Additionally, the measurements should be obtained following the IEC 61400-21 guidelines [107]. Moreover, the IEC 61400-27-1 describes two different validation methods:

Play-back The voltage profile is measured in the WT terminals, following the above mentioned considerations. The timeseries of this measurement is used as input to the model, and the simulation is conducted. Therefore, the grid is not modeled and the generic model works standalone.

Full grid The real grid from which the measurements are obtained is modeled. Then, the voltage dips are conducted via a short-circuit with the adequate impedance characteristics to emulate the real fault.

During the simulation, the active and reactive currents and powers are calculated by the model. Then, both the model and the field responses have to be treated properly. First, if the sample frequency of the field data and the model differs, both signals must be coordinated. Then, the signals must go through a second order critically damped filter, with a cut frequency of 15 Hz, in order to adequate the signals to the bandwidth of the generic models. Remember that these signals are the Root Mean Square (RMS) profiles, not the sinusoidal signals. Finally, the validation procedure is applied between the field data and the model response.

The validation procedure consists of calculating three different magnitudes based on the error between each couple of signals (e.g., measured and simulated active/reactive power). The error (ε_x) is calculated using Eq. (3.3), where x_1 and x_2 are each couple of signals.

$$\varepsilon_x = x_1 - x_2 \quad (3.3)$$

Then, three different magnitudes are calculated:

Mean Error (ME) - Eq. (3.4)

$$x_{ME} = \frac{\sum \varepsilon_x}{N} \quad (3.4)$$

Mean Absolute Error (MAE) - Eq. (3.5)

$$x_{MAE} = \frac{\sum |\varepsilon_x|}{N} \quad (3.5)$$

Maximum Absolute Error (MXE) - Eq. (3.6)

$$x_{MXE} = \max(|\varepsilon_x|) \quad (3.6)$$

Where N is the number of samples for each measurement.

These magnitudes should be calculated in pre-fault, fault and post-fault periods. However, the IEC 61400-27-1 is conscious about the limitations of the generic models. The assumptions with which they are designed make them unable to emulate certain transient behaviors. This especially occurs at the times when the fault begins and ends (sub-transient periods). At the beginning of the fault, the model is unable to emulate the DC-component of the generator flux. At the end, the non-linear aerodynamic effects, as well as wind speed fluctuations affect to active power, while the dynamics of the transformer affect to the reactive power response. To cover these issues, the IEC 61400-27-1 describes different time windows in which errors should be calculated. These windows are referred to as Quasi Steady State (QSS), and dismiss the first 140 ms after the occurrence of the fault and 500 ms when it ends. Fig. 3.21 summarizes the time windows defined by the IEC 61400-27-1. Additionally, Table 3.5 depicts the periods in which each error magnitude should be calculated.

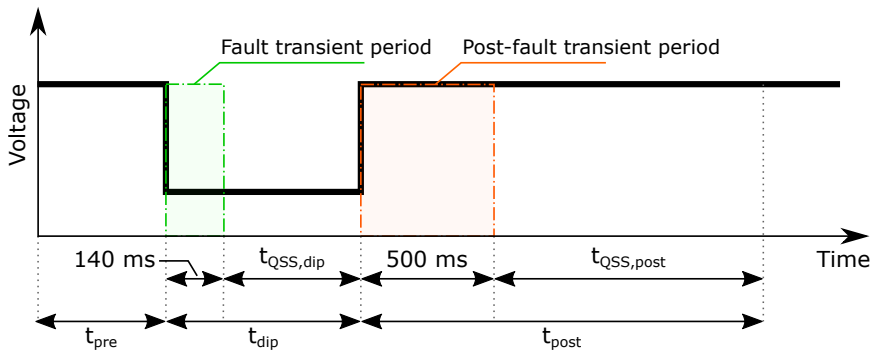


Figure 3.21: IEC 61400-27-1 Validation methodology time windows.

- t_{pre} represents the pre-fault time window (usually 1 s)
- t_{dip} represents the fault time window
- $t_{QSS,dip}$ represents the QSS fault window and is calculated as $t_{dip} - 140 \text{ ms}$
- t_{post} represents the post-fault time window (usually 5 s)
- $t_{QSS,post}$ represents the QSS post-fault window and is calculated as $t_{post} - 500 \text{ ms}$

Period	x_{ME}	x_{MAE}	x_{MXE}
Pre-Fault	t_{pre}	t_{pre}	t_{pre}
Fault	t_{dip}	$t_{QSS,dip}$	$t_{QSS,dip}$
Post-fault	t_{post}	t_{post}	$t_{QSS,post}$

Table 3.5: Time windows for error calculations.

Some limitations have been identified during the development of the current Doctoral Thesis. First, the appliance of the validation methodology during the pre-fault period does not provide practical information. The real WT is working in steady-state, and with that information, the generic model is initialized. Active and reactive power responses should be constant during these periods. Hence, if the model initialization is well conducted, the error should be negligible. Additionally, the mean error (Eq. (3.4)) is a magnitude which provides limited information. Since it is sign-dependent, an error which oscillates between positive and negative values may be erroneously neglected. This fact is not strange with generic WT models. For example, in Type 3, the active power usually oscillates after the fault. If the model does not emulate these oscillations but provides a constant response, the real magnitude would oscillate above and below the model response. Thus, the positive and negative errors would canceled each other, and the ME would be close to zero. A theoretical approach to this issue is shown in Fig. 3.22. In this case, applying Eq. (3.4), $x_{ME} = 3,40\%$. Nevertheless, if MAE, which is independent from the error sign, is calculated using Eq. (3.5), $x_{MAE} = 27,32\%$ is obtained. Thus, the current Doctoral Thesis has dismissed the ME calculation for validation purposes, opting for the MAE.

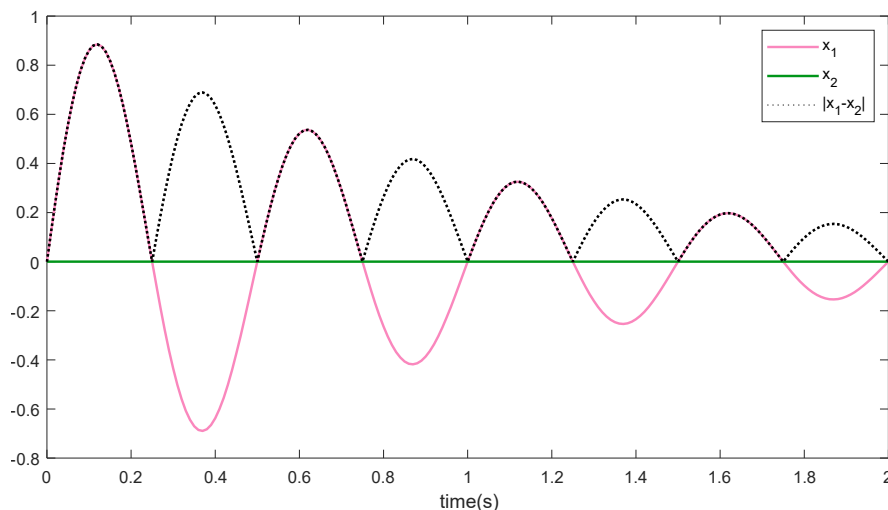


Figure 3.22: Limitation of ME against MAE.

Finally, it is worth mentioning the study of transient response during sub-transient periods. As previously stated, the generic WT models are not supposed to accurately emulate sub-transient response. For this reason, most error magnitudes are calculated during QSS (see Table 3.5). However, the models provide a response during those periods (whether accurate or not). Furthermore, in the current Doctoral Thesis, it has been proved that the IEC's models are more precise than the WECC's ones [99, 106]. Nevertheless, most of these differences occur during sub-transient periods (especially for Type 3 model). When it comes to demonstrating this fact, it was realized that applying the IEC 61400-27-1 validation methodology does not provide enough information to demonstrate the profits of the more complex models depicted in the IEC 61400-27-1. The current Doctoral Thesis proposes to calculate, at least informatively, the MAE and the MXE during these sub-transient periods, instead of completely disregard them. More information can be found in Section 4.2.

3.3. *Simulink*[®] *Design Optimization*TM tool

After the modeling, the parametrization of the generic WT models is the most important process. Establishing the dozens of parameters which define the behavior of the model is not an easy task. For Types 1 and 2, this process may be simpler. Both guidelines point that the electrical generator system should be a software built-it one, which is usually defined by real parameters (e.g., stator and rotor resistances and reactances, mutual reactance, inertia, etc.). These parameters may be obtained from the real generator. Furthermore, the control systems for these models are very simple and defined by a small number of parameters. In contrast, Types 3 and 4 are far more complex.

As shown in Section 3.1, these types are composed of several control systems which do not correspond to those of real WTs. Thus, not even with the parameters of the real WT could the parameters of the simplified model be easily obtained. For the current Doctoral Thesis, the parameters which appear in the literature were used as a first approximation, in order to obtain a model that provides a logical response. Parameters can be found in literature in [36, 44, 91], or even in the WECC's guidelines [29]. It is worth noting the few papers which provide parameters' values. With this first approach, the generic WT models were initially developed. Later, manually, the parameters were varied, trying to determine how every parameter affects to the response of the model. As the conclusion of that comprehensive work, [102] was published. However, despite relatively good results can be obtained adjusting the parameters manually, it is not the best option. In order to obtain the best models performance, the *Simulink*[®] *Design Optimization*TM tool [108] was used.

This tool allows to finely adjust a set of parameters to obtain the required response. Time and frequency domain requirements can be selected.

Time domain requirements: Step response envelopment, signal bound, signal property, custom requirement...

Frequency domain requirements: Gain and phase margin, bode magnitude, closed loop peak gain, damping ratio...

For the case of the current Doctoral Thesis, the most usual requirement is the ‘Signal tracking’. In this requirement, a reference signal is used as input (e.g., either active or reactive power). Then, the signal from the model that should be adjusted to the reference is selected. Additionally, the optimization options (e.g., method, algorithm, tolerance...) can be set. Finally, the set of variables that the user wants to adjust is chosen. For each variable, the maximum and minimum values between which it will vary can be set, as well as the scale that the algorithm will use in these variations. An example of this is shown in Fig. 3.23. Furthermore, it is possible to set a custom requirement to conduct the validation. Thus, the MAE and MXE criteria during the fault and the post-fault periods can be defined and followed during the optimization. Nevertheless, it is hard to set the priorities between them, and since the MXE usually has larger values than the MAE, the tool prioritizes it, which may not be the most adequate requirement. Hence, the error of the full response has been used for this Doctoral Thesis.

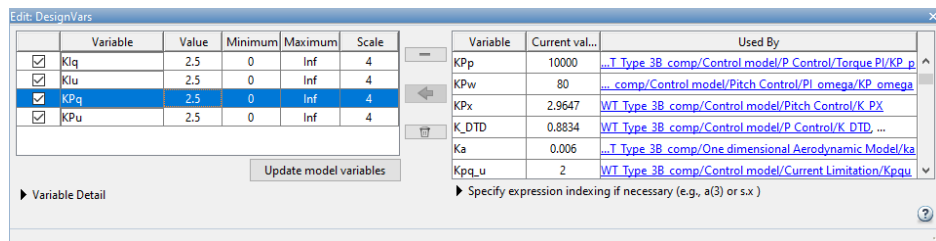


Figure 3.23: *Simulink*[®] *Design Optimization*TM variables set.

Once the requirement and the variables are set, the optimization process can start. The tool automatically conducts simulations varying the selected variables, until it obtains a better response than the previous one. When the selected tolerance is achieved, the optimization process ends. An example of the optimization of the parameters from the PI controllers of the reactive power control system is shown in Fig. 3.24. In the left window, the response of each iteration is shown, as well as the values of the variables and their evolution. For this example case, the initial value was set randomly. In the right window, the number of iterations, as well as how many simulations were conducted in each iteration (F-count) are shown. Finally, the error obtained

on each iteration is shown. The sum of absolute errors or the sum of square errors can be used as requirement.

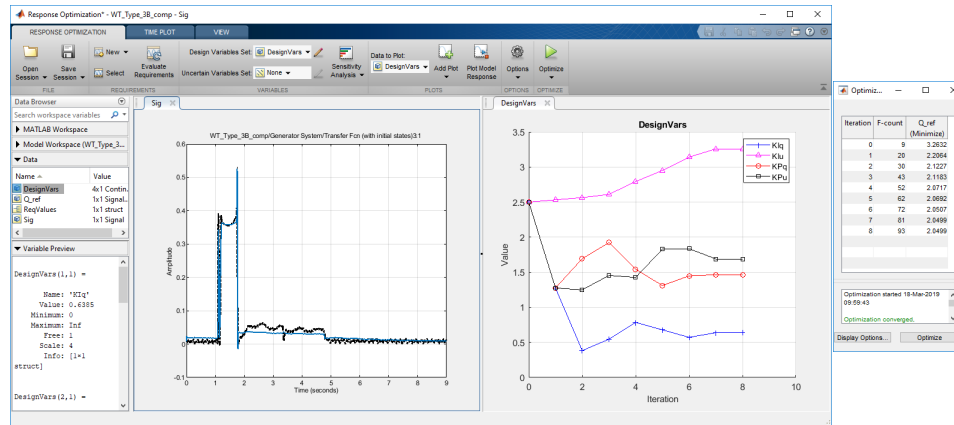


Figure 3.24: Simulink[®] Design OptimizationTM example.

Additionally, several requirements can be set at a time. For example, for those validation studies which include multiple cases, a model for each case is included into a Simulink[®] model. Then, each model is fed with its voltage input, and the requirement for each one is defined in the same optimization session. Then, the values obtained are those which involve the best approximation for all cases at a time. This is especially interesting for variables that cannot be exactly adjusted, since the real performance is different from the generic model response. As an example, DFIG WTs inject a reactive current proportional to the voltage during a fault. In the models, this proportion is modeled by a constant gain. However, in real WTs, this current is defined by a detailed curve dependent on the dip depth. Thus, the response obtained from the generic models cannot be the same as that from the real WT. For these cases, counting on a tool that adjusts the parameters automatically to find the minimum error is extremely useful. An example showing the session used to adjust the reactive power controller for 6 simulation cases at a time of the WECC's generic Type 3 model is shown in Fig. 3.25. For these type of complex cases, the process parallelization allowed by MATLAB[®] is recommended to reduce the optimization time.

Finally, it is worth mentioning that, despite this tool is highly helpful when conducting the parametrization of a model, its use does not prevent the user from having a deep knowledge of the model operation. The most complex models are composed of hundreds of blocks and dozens of parameters. It is not recommended to include all the variables in the tool and let it work. The more variables selected, the higher the optimization time and the lower the accuracy obtained. Thus, selecting the right variables, with a logic initial value and scale is vital for a good performance of the tool. As it happens in the majority of occasions working with software, the merit does not consist

of clicking the execution button, but in knowing in a precise manner all the steps to be taken until getting to that point.

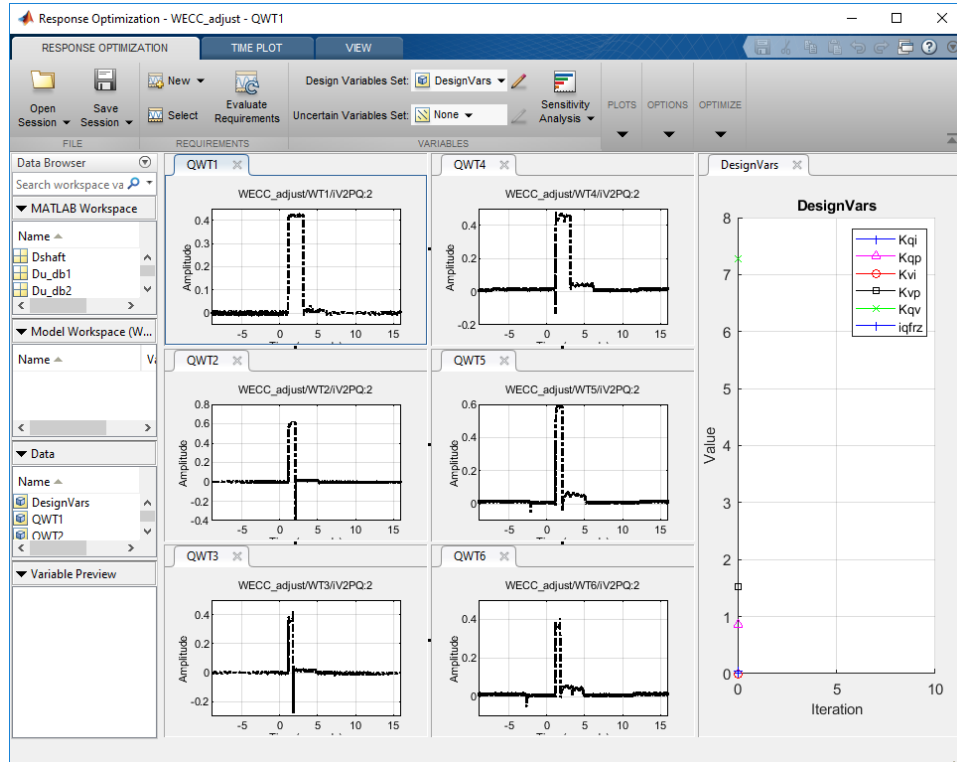


Figure 3.25: *Simulink[®] Design OptimizationTM* with 6 cases at a time.

The results obtained during the development of the current Doctoral Thesis are shown in this Chapter. Three journal papers, published in Journal Citation Report (JCR) indexed Journals are presented. Therefore, this work satisfies the criteria of a thesis dissertation by *Compendium of Publications* according to the Management Committee of the International Doctoral School (EID) of the University of Castilla – La Mancha (UCLM). Additionally, a fourth paper which has been submitted (but still not published) to another indexed journal is included in Section 4.2.

4.1. Published results

The need for development and validation studies regarding generic WT models by the part of TSOs and DSOs has been deeply discussed in Chapters 1 and 2. First, it is vital for stakeholders to have an in-depth knowledge of the internal operation of these generic models, since their proper parametrization depends on this understanding. Paper I (Section 4.1.1) presents a detailed study and a parameter analysis regarding the operation of those systems related to the active power response of an IEC generic Type 3 WT model.

Regarding the comparison of the IEC and WECC guidelines, Paper II (Section 4.1.2) performs an extensive work analyzing the operation and behavior of the systems differently implemented by each entity for a generic Type 3 model. Additionally, an IEC and WECC generic Type 4 model validation study using field data from 10 different test cases is conducted for Paper III (Section 4.1.3). Lastly, an analysis regarding the transient response of a generic Type 3 model for both guidelines is presented in Section 4.2.

4.1.1. Paper I - IEC Type 3 parameter analysis

Paper I presents an in-depth analysis of the operation of the systems related to the active power response of an IEC generic Type 3 model. These systems are the *Two mass model*, the *Active power control (Torque PI controller included)* and the *Pitch Control*. The most relevant parameters for each system are modified, and the impact on the active power response and the rotational speed of the Wind Turbine Rotor (WTR) is analyzed. Additionally, this paper depicts two of the issues identified in the IEC 61400-27-1, both included in the *Pitch Control* system. Finally, an analysis of the influence of the depth and the duration of the voltage dip on the response of the model is conducted.

The main objective of Paper I was to provide users with the necessary information to model and parametrize the IEC generic Type 3 model, assessing the influence of more than 10 different parameters in the model response.




The journal metrics are summarised in Table 4.1, and the full paper as published is included below.

Table 4.1: Journal Metrics – Paper I.

Journal Name	Energies
Impact Factor (2017)	2.676
Category	Energy & Fuels
Quartile in category	Q2
Position in category	48/97
ISSN	1996-1073

Article

Generic Type 3 Wind Turbine Model Based on IEC 61400-27-1: Parameter Analysis and Transient Response under Voltage Dips

Alberto Lorenzo-Bonache ^{1,*}, Andrés Honrubia-Escribano ¹ , Francisco Jiménez-Buendía ², Ángel Molina-García ³  and Emilio Gómez-Lázaro ¹ 

¹ Renewable Energy Research Institute and DIEEAC-EDII-AB, Universidad de Castilla-La Mancha, 02071 Albacete, Spain; andres.honrubia@uclm.es (A.H.-E.); emilio.gomez@uclm.es (E.G.-L.)

² Siemens Gamesa Renewable Energy, S.A., 31621 Pamplona, Spain; fjimenez@gamesacorp.com

³ Department of Electrical Engineering, Universidad Politécnica de Cartagena, 30202 Cartagena, Spain; angel.molina@upct.es

* Correspondence: alberto.lorenzo@uclm.es; Tel.: +34-967-599-200 (ext. 96259)

Received: 31 July 2017; Accepted: 14 September 2017; Published: 19 September 2017

Abstract: This paper analyzes the response under voltage dips of a Type 3 wind turbine topology based on IEC 61400-27-1. The evolution of both active power and rotational speed is discussed in detail when some of the most relevant control parameters, included in the mechanical, active power and pitch control models, are modified. Extensive results are also included to explore the influence of these parameters on the model dynamic response. This work thus provides an extensive analysis of the generic Type 3 wind turbine model and provides an estimation of parameters not previously discussed in the specific literature. Indeed, the International Standard IEC 61400-27-1, recently published in February 2015, defines these generic dynamic simulation models for wind turbines, but does not provide values for the parameters to simulate the response of these models. Thus, there is a pressing need to establish correlations between IEC generic models and specific wind turbine manufacturer models to estimate suitable parameters for simulation purposes. Extensive results and simulations are also included in the paper.

Keywords: DFIG; generic model; IEC 61400-27; model validation; study of sensitivity; standard model; wind turbine

1. Introduction

During the last decade, the integration of renewables into power systems has increased considerably, mainly due to successful policies and substantial investments. Indeed, according to [1], renewables are essential to achieve long-term climate targets; reaching a 30% share by 2030 should be sufficient to prevent global temperatures from rising more than 2 °C above pre-industrial levels. Currently, of the different technologies, wind and solar Photovoltaics (PV) are, globally, the fastest-growing sources of electricity and offer technologically-mature and economically-affordable solutions [2]. In this scenario, the International Energy Agency (IEA) roadmap targets a 15–18% share of global electricity from wind power by 2050, a notable increase of the 12% aimed for in 2009 [3]. This increasing share of wind power has created the need for wind turbine (WT) and wind power plant (WPP) models to be used in power system stability analysis. However, conventional electromagnetic transients simulation (EMTS) models proposed by wind turbine manufacturers fail to satisfy the current needs demanded by Transmission System Operators (TSO) for these power system stability analyses; mainly due to the models being complex, highly detailed and generally confidential. In fact, these manufacturer models usually simulate the behavior of all of the internal components of the wind turbine, and hence, a large

number of parameters is required to achieve accurate simulations, as well as high computational time costs or even specific software for their simulations [4,5]. Therefore, it would be desirable to propose efficient and flexible simulation models that respond to TSO requirements [5,6].

To solve this issue, international institutions worldwide are developing new generic models, also known as standard or simplified models, defined by a limited number of parameters [7,8]. These models are available for any specific simulation software to simulate wind turbines integrated in the grid. The International Electrotechnical Commission published the first version of the Standard IEC 61400-27-1 [9] in February 2015, where these generic wind turbine models were initially defined. This standard classifies the different topologies of wind turbines into four types, representing the majority of wind turbines installed in power systems. The four types of wind turbine generators, which are mainly differentiated by the generator, are: (Type 1) wind turbines equipped with an asynchronous generator directly connected to the grid (usually squirrel-cage) [10]; (Type 2) wind turbines equipped with an asynchronous generator with a variable rotor resistance, directly connected to the grid; (Type 3) wind turbines equipped with a Doubly-Fed Induction Generator (DFIG), with the stator directly connected to the grid and the rotor connected through a back-to-back power converter; (Type 4) wind turbines connected to the grid through a Full-Scale power Converter (FSC) [11].

These dynamic models are suitable to be tested even under transients, such as switching of power lines, loss of generation or loads, balanced faults, voltage dips, etc. [12,13]. In this work, the generic Type 3 WT model facing a three-phase voltage dip will be tested. These balanced faults are not the most common, but they represent the worst-case dimensional scenario. However, the study of unbalanced faults also constitutes a very interesting case for DFIG and FSC wind turbines (Types 3 and 4, respectively), but currently, the wind turbine models specified in IEC 61400-27-1 are only for fundamental frequency positive sequence response. In [14], field measurements from a 52-MW wind power plant are used to validate an IEC Type 3 wind turbine model with a wind turbine level voltage controller and with a wind power plant level power factor controller. Nevertheless, in the specific literature, there are few studies on the values of parameters to be used for simulation purposes [15,16]. Moreover, the recent publication of the standard, as well as the constraints of the wind turbine manufacturers [17] have led to the need to conduct studies that provide parameter values and simulation results [18], thus allowing the adjustment of the generic wind turbine and wind power plant models by both researchers and institutions [19,20]. Finally, the contributions of the authors presented in the present work may be considered by the International Electrotechnical Commission for inclusion in Edition 2 of IEC 61400-27-1, which is currently under development and is intended for publication in 2018.

Considering previous works and current TSO requirements, this paper describes a generic Type 3 wind turbine model developed in MATLAB/Simulink based on the IEC 61400-27-1 standard. The parameters of the model have been estimated to provide a dynamic response under voltage dips. Additionally, the results have been compared to those of other studies and simulations by manufacturers [21–23]. Extensive simulations have been conducted, modifying the parameters and discussing their effects on the wind turbine response in terms of active power and rotational speed. The contributions of the current paper focus on: (i) providing public parameter values and simulation results of a generic Type 3 wind turbine model; (ii) analyzing the influence of the parameter variations on the dynamic wind turbine response under voltage dips and describing the process of model tuning; (iii) contributing to the development of Edition 2 of IEC 61400-27-1.

The rest of the paper is structured as follows: Section 2 introduces the main characteristics of the DFIG wind turbine topology, the details of its implementation in MATLAB/Simulink and describes the methodology. Section 3 discusses the simulation results related to the mechanical two-mass model, and the influence of the control system parameters is studied in Section 4. Section 5 analyzes the effects of varying the parameters of voltage dips on the model's response. Finally, Section 6 presents conclusions.

2. IEC 61400-27-1 Type 3 Wind Turbine Model

According to the classification presented in the previous section, Type 3 is currently the most widely-used topology. Indeed, around 45% of the wind turbines installed in Europe are of this type [24]. Type 4 wind turbines are increasingly being integrated into new wind power plants, mainly due to their control and stability advantages, as well as the reduction in electronic component cost. Thus, both types of WTs constitute an interesting field of study. In this sense, due to the benefits of using a full power converter, from the TSO point of view, the performance of Type 4 is simpler than Type 3. In fact, the standard Type 4 WT model can be considered a simplified Type 3 model. Consequently, this paper focuses on a Type 3 wind turbine generic model from a more general perspective.

2.1. MATLAB/Simulink Implementation of the Type 3 WT Model

Figure 1 shows the general structure of the generic Type 3 WT model implemented in MATLAB/Simulink (The MathWorks, Inc, Natick, MA, USA). This model has been developed following the guidelines provided by IEC 61400-27-1 [9] and represents one of the first implementations in MATLAB/Simulink in the scientific literature. The dynamic performance depends on both active and reactive power references, $p_{WT,ref}$ and $x_{WT,ref}$, respectively, as well as two further control parameters setting the reactive power control mode (MqG) and the response under voltage dips ($MqUVRT$). A two-mass model is used to simulate the mechanical interactions between high and low speed shafts. The wind turbine rotor (along with the blades) and the electrical generator are modeled by their inertia parameters. They are coupled by a spring with a certain stiffness and a damper with a damping coefficient. These parameters have a significant effect on the active power (P_{WT}) and generator rotational speed (ω_{WTR}). Further information can be found in Section 3.

With regard to the electrical generator model, Type 1 and Type 2 use an electrical generator model derived from the simulation software. However, and in line with IEC 61400-27-1, the generic Type 3 model is composed of a conventional block diagram. The voltage input is considered as a balanced three-phase voltage input, defined by both magnitude and phase, instead of using a three-phase source, as can be seen in the lower left side of Figure 1 ($u_{WT,Mag}$ and $u_{WT,Phase}$)

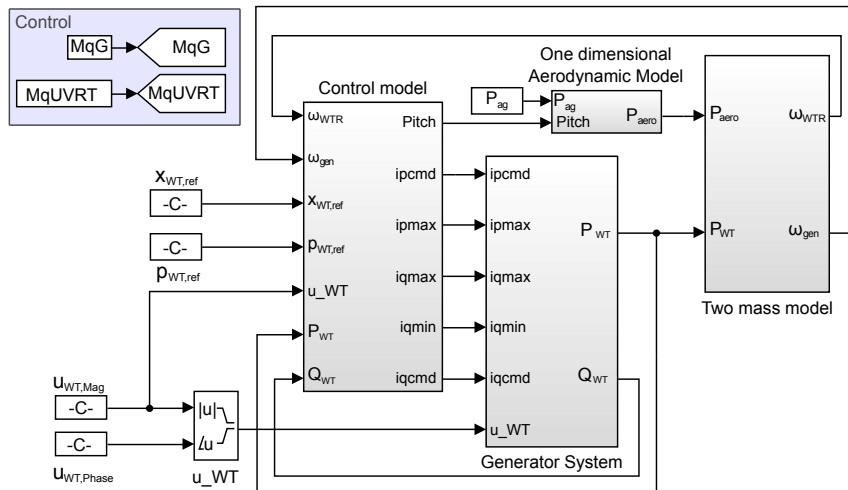


Figure 1. Generic Type 3 WT model: MATLAB/Simulink implementation.

The electrical generator system is a simplification based on [25,26], including the power converter dynamics; see Figure 2. It is mainly commanded by an active and a reactive current signal provided

by the control system. Moreover, the corresponding IEC Standard divides the Type 3 generic model into two types depending on the Fault Ride-Through (FRT) solution adopted [5]: (i) Type 3A, with no protection system to avoid the disconnection of the wind turbine under voltage dips [27]; (ii) Type 3B, including a crowbar protection system to avoid over-currents under voltage dips, thus preventing power converter damage. In the generic Type 3B model, this crowbar system multiplies the current references of the generator by zero for a certain period of time, when the variation of the voltage goes beyond a certain limit [18]. Taking into account that this protection system is commonly used by wind turbine manufacturers to meet the mandatory grid codes in Europe [28], the model implemented in this paper is Type 3B.

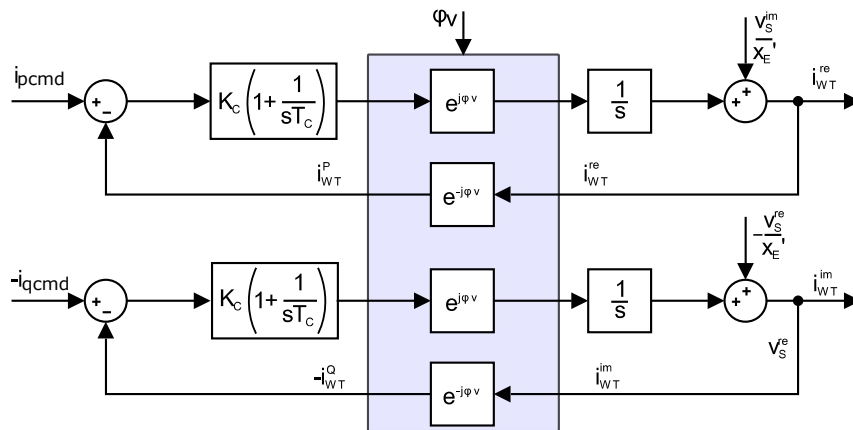


Figure 2. Generic Type 3 WT model: electrical generator system.

Figure 3 shows the control system, also included in Figure 1. The control system of the generic Type 3 WT model does not represent the actual controller of the WT, which sets the references to the Rotor-Side Converter (RSC) and the Grid-Side Converter (GSC), but provides the current command signals to obtain an accurate response of active and reactive power, observed from the grid side. This control system is composed of five control subsystems. Active power and pitch control systems are discussed in detail due to their influence on P_{WT} and ω_{WTR} , which are the main variables analyzed in this work. The reactive power control system (Q control) provides the reactive current reference (i_{qcmd}), used as an input to the electrical generator system according to reference $x_{WT,ref}$ and the reactive power control mode (voltage control, reactive power control or power factor control). Both the current and reactive power limitation control subsystems set the maximum and minimum currents and reactive power values that the wind turbine is able to provide, according to parameters such as voltage or active power.

Finally, the influence of the pitch blade angle on the wind power absorbed by the wind turbine is modeled by the aerodynamic model; see Figure 4. It is a one-dimensional model where P_{ag} is the active wind power (in pu) modeled by a constant parameter (P_{ag} in Figure 1). This parameter, in accordance with IEC 61400-27-1 [9], is kept constant during the simulation.

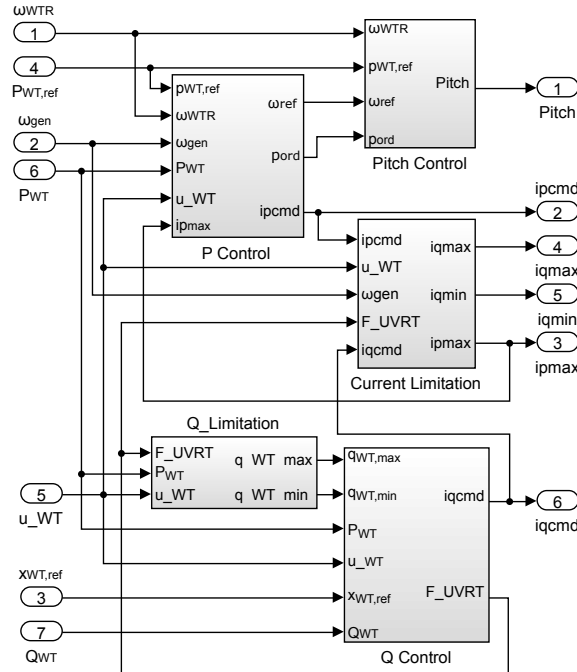


Figure 3. Generic Type 3 WT model: control system.

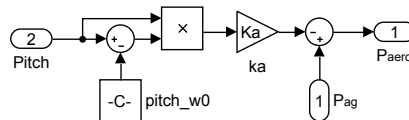


Figure 4. One-dimensional aerodynamic model.

2.2. Simulations Conducted for the Parameter and Transient Response Analysis

This paper aims to analyze the active power (P_{WT}) and the rotational speed of the wind turbine rotor (ω_{WTR}) submitted to voltage dips when the IEC 61400-27-1 Type 3 model parameters are modified. Specifically, the mechanical two-mass model and the active power control and the pitch control systems have been modified, and their corresponding responses have been analyzed. Parameter values and variations are summarized in Table 1. A reference value for each parameter has been defined in order to obtain a benchmark system. Subsequently, each parameter can be set to a lower and a higher value than the corresponding reference. The Type 3 WT model’s responses under voltage dips for the different parameter values are depicted in the same axis to compare the influence of these variations on the active power and rotational speed evolution along the transient. The values of these parameters do not follow a physically-based pattern. They have been selected to clearly represent different performances in order to provide guidelines for Type 3 model adjustment under certain simulation conditions. For example, conventional values of H_{WTR} are usually from 5 s to 15 s.

The simulations carried out by the authors are based on a balanced three-phase voltage dip, with a duration of 0.2 s and a residual voltage of 0.1 pu. This voltage dip has been considered in order to follow the guidelines provided by IEC 61400-21 [29], which consider a three-phase voltage dip with a residual voltage of 0.2 ± 0.05 pu with a duration of 0.2 s. Moreover, the voltage dip considered is

more severe than this reference in order to be included within the guidelines of the recently-published Commission Regulation (EU) 2016/631 [28], which considers the minimum voltage of 0.05–0.30 pu with a duration of 0.14–0.25 s for the most restrictive conditions.

Steady-state conditions are considered before these transients. An additional 1-s time interval before the dip is also shown in the simulations to represent the previous steady-state values. As a preliminary finding, the benchmark response of the initial system values is shown in Figure 5. This response represents the dynamic response of the Type 3 WT model under the voltage dip. Parameters from the initial benchmark system have been adjusted to be in line with the results published in previous works [18,22].

Table 1. Parameter values of Type 3 WT: references and variations.

System	Parameter	Ref. Value	Var.Range
Two mass model	H_{WTR} -Inertia constant of WT rotor (s)	10	[5 10 25]
	H_{gen} -Inertia constant of generator (s)	1	[0.3 1 3]
	k_{drt} -Drive train stiffness (pu)	100	[20 100 500]
	c_{drt} -Drive train damping (pu)	0.5	[0.2 0.5 1]
Active power control	KP_p -PI controller proportional gain	6	[0.5 6 10]
	KI_p -PI controller integration parameter	3	[0.3 3 24]
	K_{DTD} -Gain for active drive train damping	0.5	[0 0.5 3]
Pitch control	KI_ω -Speed PI controller integration gain	50	[10 50 500]
	KP_ω -Speed PI controller proportional gain	200	-
	KI_c -Power PI controller integration gain	10	[1 10 40]
	KP_c -Power PI controller proportional gain	10	-
	KP_X -Pitch cross coupling gain	0	[0 0.1]

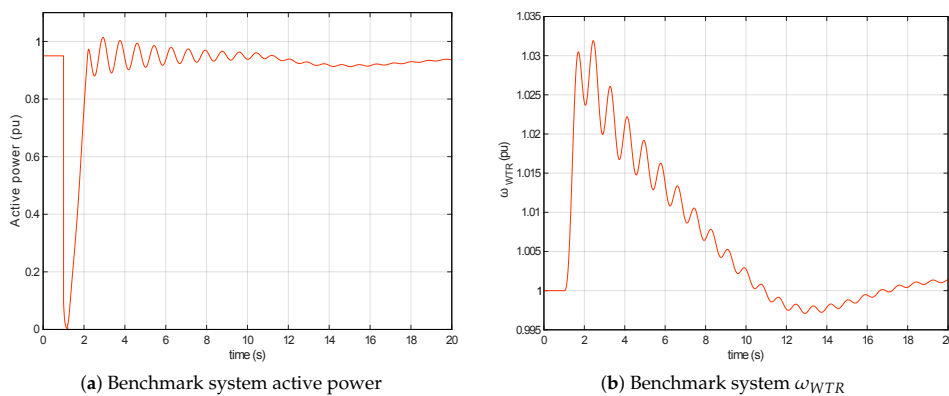


Figure 5. Benchmark response of Type 3 WT: reference parameters.

3. Mechanical Parameter Analysis under Voltage Dips of the Type 3 WT Model

Standard IEC 61400-27-1 establishes a mechanical two mass model to simulate the interaction between high and low speed shafts [30]. Both shafts are coupled by a spring with a certain stiffness

(k_{drt}) and a damper with a certain damping coefficient (c_{drt}). The wind turbine rotor and the electrical generator are represented by their inertia coefficients (H_{WTR} and H_{gen} , respectively). A representation of this relationship is shown in Figure 6. Both shafts rotate with a certain speed (ω_{WTR} and ω_{gen}) and are subjected to a torque. The wind turbine rotor torque (T_{WTR}) represents the mechanical aerodynamic torque of the wind. The electrical generator torque (T_{gen}) represents the electromagnetic torque. The expressions to describe system performance are the following [31]:

$$2H_{WTR} \cdot \frac{d\omega_{WTR}}{dt} = T_{WTR} - k_{drt} \cdot (\theta_{gen} - \theta_{WTR}) - c_{drt} \cdot (\omega_{WTR} - \omega_{gen}), \tag{1}$$

$$2H_{gen} \cdot \frac{d\omega_{gen}}{dt} = -T_{gen} + k_{drt} \cdot (\theta_{gen} - \theta_{WTR}) + c_{drt} \cdot (\omega_{WTR} - \omega_{gen}). \tag{2}$$

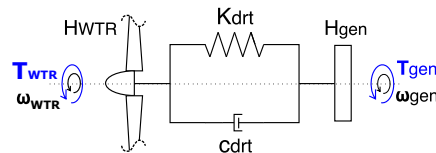


Figure 6. Physical representation of the two mass model.

Figure 7 shows the mechanical system implemented in MATLAB/Simulink. Mechanical wind power ($P_{aero} = \omega_{WTR} \cdot T_{WTR}$) obtained from the aerodynamic model and electrical active power ($P_{elec} = \omega_{gen} \cdot T_{gen}$) obtained from the generator system are considered as the inputs of the system. The variation of the four parameters that define this system (H_{WTR} , H_{gen} , k_{drt} and c_{drt}) modifies the response of the overall system in terms of P_{WT} and ω_{WTR} response. Subsequently, the influence of these parameter variations on the Type 3 WT response under voltage dips is analyzed during the transient, considering the parameter values given in Table 1.

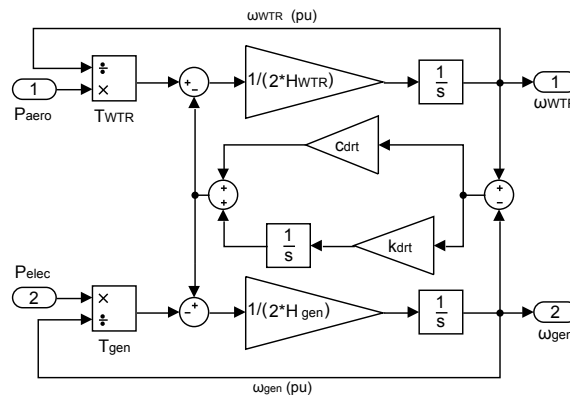


Figure 7. Two mass model implemented in MATLAB/Simulink.

Figure 8 shows the P_{WT} and ω_{WTR} dynamic response under a voltage dip when H_{WTR} is modified according to Table 1. H_{WTR} variations do not have a significant influence on the active power response (see Figure 8a), reducing the oscillation frequency and the over-response before the new steady-state conditions. As can be seen in Figure 8b, ω_{WTR} oscillations are clearly affected by the H_{WTR} parameter variation, presenting an inverse relation with ω_{WTR} frequency and oscillations.

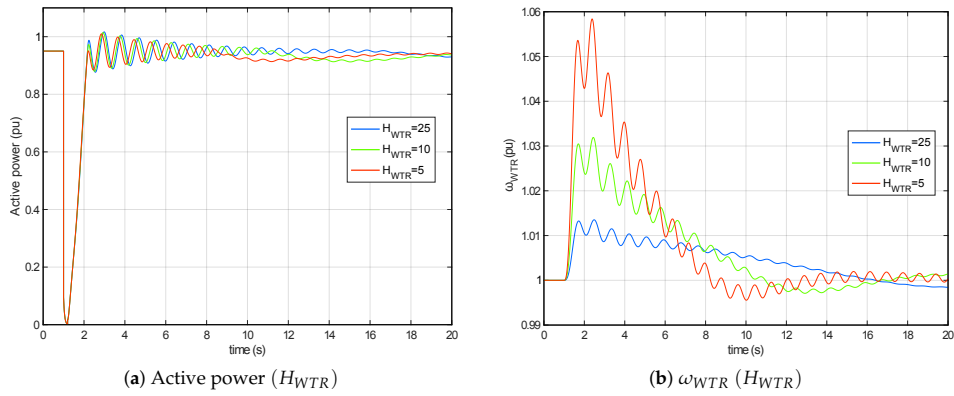


Figure 8. H_{WTR} parameter analysis: P_{WT} and ω_{WTR} evolution under a voltage dip.

The transient response of the system when the H_{gen} parameter is modified is shown in Figure 9. The increase in this parameter makes a considerable contribution to the oscillations of both P_{WT} and ω_{WTR} ; see Figure 9a,b. The oscillation frequency is inversely proportional to the value of H_{gen} . However, the oscillation amplitude proportionally increases with the H_{gen} parameter value. This increasing H_{gen} also has an effect that is inversely proportional to the oscillation damping.

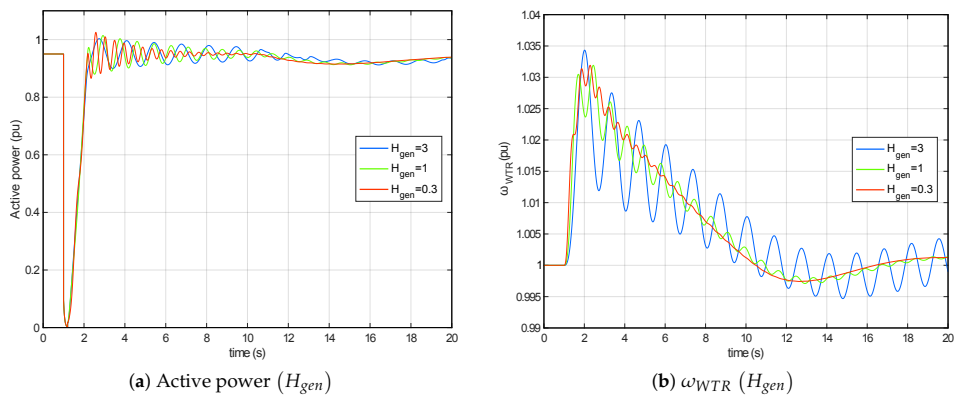


Figure 9. H_{gen} parameter analysis: P_{WT} and ω_{WTR} evolution under a voltage dip.

The frequency of these oscillations (ω_{osc}) can be determined by the following expression [32],

$$\omega_{osc} = \sqrt{k_{drt} \cdot \left(\frac{1}{2 \cdot H_{WTR}} + \frac{1}{2 \cdot H_{gen}} \right)}. \quad (3)$$

An interval from 1-5 Hz produces usual values for commercial Type 3 wind turbines. These oscillations are proportional to k_{drt} values and inversely proportional to both H_{WTR} and H_{gen} parameters. However, and considering that the value of H_{WTR} is usually much higher than one, its influence can be considered as almost negligible; see Figure 8. In contrast, H_{gen} variations clearly have a notable influence on the transient response, as shown in Figure 9.

According to Equation (3), the increase in the spring’s stiffness (k_{drt}) proportionally affects the frequency of the response oscillations; see Figure 10. This parameter has an important influence on the active power oscillation amplitude (Figure 10a). Moreover, the k_{drt} parameter has a much greater effect than any other parameter under voltage dips. The ω_{WTR} oscillation amplitude is lower than k_{drt} variations, in an inverse relation with the increasing H_{gen} (Figure 10b). Finally, the damping coefficient variations (c_{drt}) have no influence on the oscillations, beyond the rate at which they are damped. Figure 11 shows the active power and rotational speed responses under c_{drt} variations. The c_{drt} parameter can be artificially increased in wind turbines to emulate active damping performed by real control by means of this ‘passive damping coefficient’ [33].

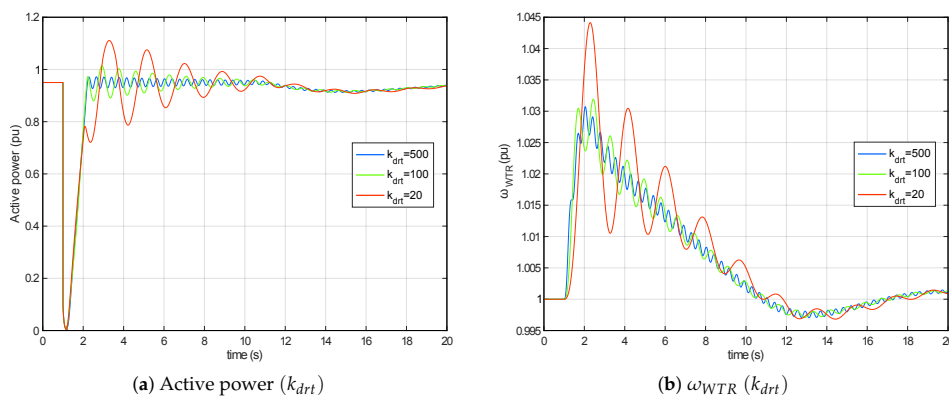


Figure 10. k_{drt} parameter analysis: P_{WT} and ω_{WTR} evolution under a voltage dip.

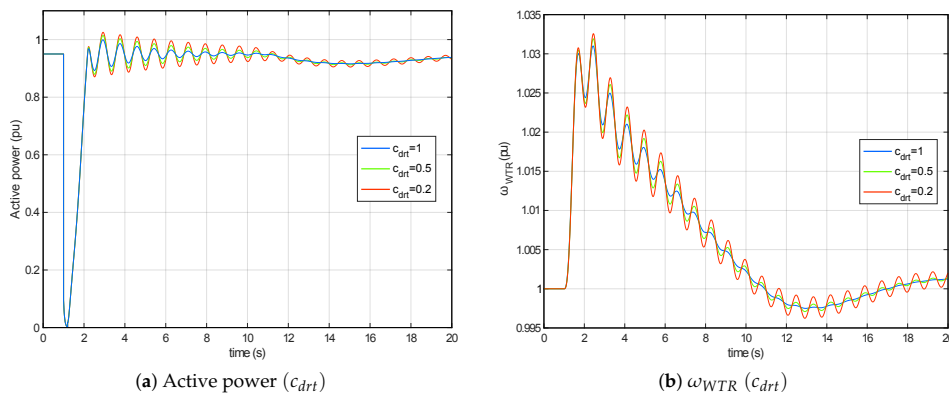


Figure 11. c_{drt} parameter analysis: P_{WT} and ω_{WTR} evolution under a voltage dip.

4. Control Parameter Analysis under Voltage Dips of the Type 3 WT Model

4.1. Active Power Control Model

Active power control is included in the control system of the wind turbine. Figure 12 shows the block diagram of the active power control model implemented in MATLAB/Simulink. The inputs of the system are the following:

- ω_{WTR} and ω_{gen} : rotational speed values from the two mass model discussed in Section 3.

- $p_{WT,ref}$: active power reference to be injected into the grid by the WT (manually adjusted).
- P_{WT} : active power obtained from the electrical generator system.
- u_{WT} : voltage reference from the electrical generator system.
- $i_{p,max}$: maximum active current able to be injected into the grid by the WT as determined by the current limitation system.

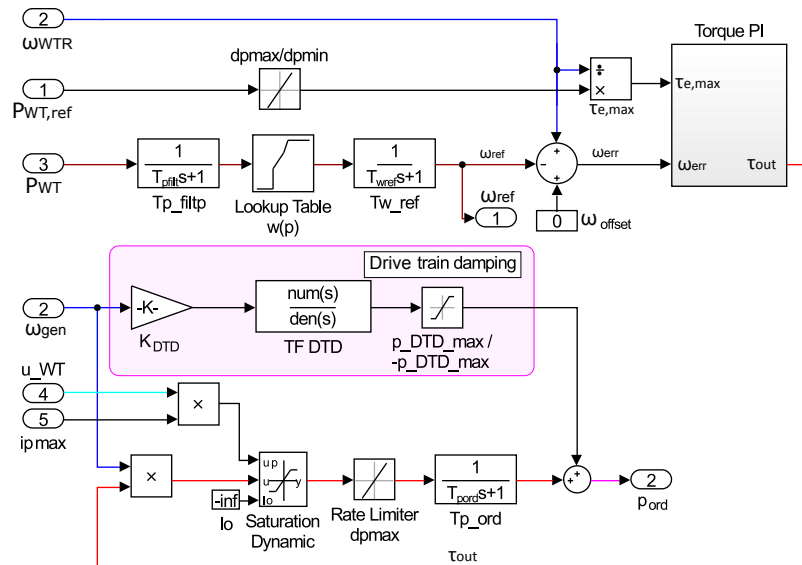


Figure 12. Active power control system implemented in MATLAB/Simulink.

The WT active power is filtered by using T_p_filt . This filter avoids sudden changes in the reference speed. Moreover, if this constant is set to an extremely high value, it allows keeping a fixed reference rotational speed during the entire simulation, representing a specific operational model. This filtered active power reference goes through a look-up table, which represents the rotational speed at which the generator must rotate when providing a certain active power value. A common look-up table for this system is shown in Figure 13, as well as a table with conventional values [34]. This table summarizes four operation zones for a Type 3 wind turbine:

- Zone 1, where the minimum rotational speed has been reached (ω_{1-2}) and consequently cannot decrease further due to component limits, mainly converter maximum slip.
- Zone 2, this operation mode covers the minimum rotational speed (ω_{1-2}) to the rated rotational speed, where the wind turbine operates at its maximum power tracking.
- Zone 3, operation mode maintaining a fixed rated speed (ω_{3-4}) and below the rated active power. In some cases, instead of a fixed rated rotational speed, there is a linear rotational speed variation to achieve the rated rotational speed at the rated active power [35].
- Zone 4, this last operation mode is set at the rated rotational speed (ω_{3-4}) and the rated active power. Dotted lines included in Figure 13a imply that, under simulation conditions, the active power reference presents a certain slope, simplifying the model and offering more stable simulations; although under real control conditions, this look-up table has the two vertical lines originally indicated.

These reference look-up tables are conventionally defined by the wind turbine generator torque [36]. However, the corresponding IEC uses an active power reference. For this reason, the values provided in this work are related to P_{WT} .

The rotational speed reference ω_{ref} is filtered by the $T\omega_{ref}$, which can present a similar function to the active power filter (Tp_{filt}). Differences between ω_{WTR} and ω_{ref} are determined, and then, a rotational speed error is estimated. In order to model real wind turbine controller filters, the IEC 61400-27-1 allows using a first order filter $T\omega_{gen}$ for ω_{gen} . Considering that these models of a real wind turbine only have the drive train resonant frequency as perturbation, this filter is intended to filter these oscillations. However, the simplicity of a first-order filter as the low pass filter does not efficiently meet the drive train perturbations. As a contribution of the authors to the future IEC version to be published in 2018, the new version will include an option to choose between ω_{WTR} and ω_{gen} as an input to the proportional-integral (PI) torque controller. Therefore, ω_{WTR} is chosen as a simplified way to determine a ω_{gen} filtered value. It is usually associated with the application of drive train damping. However, ω_{gen} is used if the drive train damping function is achieved using the torque PI itself, instead of the drive train damping function $K_{DTD} = 0$. This ω_{WTR} or ω_{gen} is then considered as the main input to the torque PI subsystem, as shown in the upper right region of Figure 12. The other input to the torque PI subsystem is the maximum electromagnetic torque ($\tau_{e,max}$) to be provided by the WT. It is determined by the relation between $p_{WT,ref}$ and ω_{WTR} . As an additional contribution of the authors, the future version of Standard IEC 61400-27-1 [9] to be published in 2018 will also define the use of ω_{WTR} or ω_{ref} going through a filter. However, the oscillations of ω_{WTR} are much smaller, and hence, the performance of the system is more accurate. Taking into account that Standard IEC 61400-27-1 has been developed recently, very few model implementations can be found in the specific literature, and thus, the current work contributes significantly to the IEC improvements.

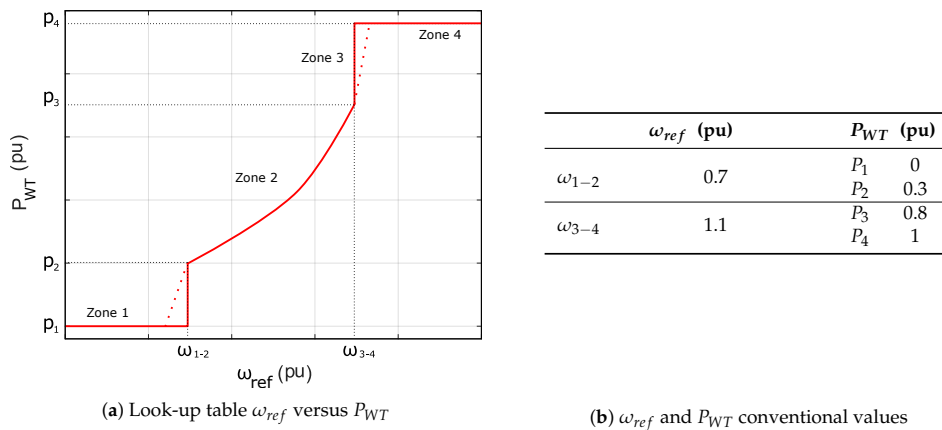


Figure 13. Look-up table ω_{ref} vs. P_{WT} and conventional values.

Figure 14 shows the torque PI subsystem. This control system gives an output proportional to the rotational speed error by adding the minimum between:

- A ramp with a constant slope defined by the parameter $dtau_max$. This ramp function is only used under voltage dip conditions.
- The torque output filtered by an integral controller with a constant estimated as KI_p/KP_p .

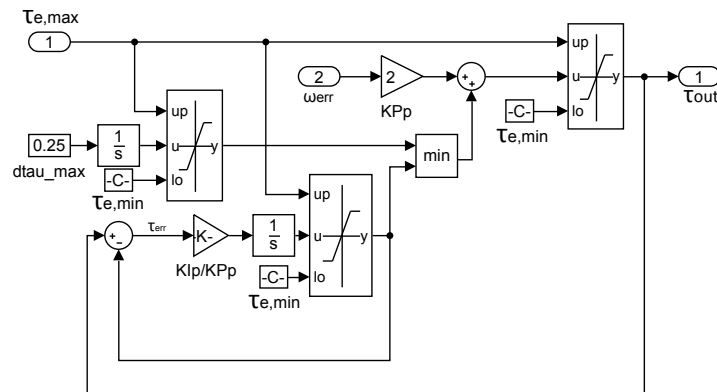


Figure 14. Torque PI system implemented in MATLAB/Simulink.

The τ_{out} output is saturated between $\tau_{e,max}/\tau_{e,min}$, returning to the main control system. This torque is multiplied by the generation rotational speed, obtaining an active power signal. The rate active power and the value of this signal is saturated and filtered, and then, the active power command signal, which is used by the rest of the control systems, is obtained [37]. An additional signal from the Drive Train Damping (DTD) system is added to the estimated output [32]. This control system provides an electrical torque accounting for the natural damping by considering speed differences between both low and high speed shafts. It is modeled through a second-order transfer function as follows,

$$TF_{DTD} = \frac{2 \cdot \zeta \cdot \omega_{DTD} \cdot s}{s^2 + 2 \cdot \zeta \cdot \omega_{DTD} \cdot s + \omega_{DTD}^2}, \quad (4)$$

where ω_{DTD} is determined as the frequency of the two mass model oscillations; see Equation (3). This system thus compensates the mechanical oscillations by adding an oscillating electrical power and then producing a highly efficient damping effect.

Figure 15 shows the effects of the KP_p parameter of the torque PI controller. The decrease in this proportional parameter involves a more under-damped behavior with higher overshoot. This behavior increases due to the inverse influence of KP_p in the integral gain of the controller. The responses of the system when parameter KI_p is modified are shown in Figure 16. Increasing KI_p produces a more oscillating response. The overshoot in ω_{WTR} is decreased for higher KI_p values, although the active power response is oscillating much more.

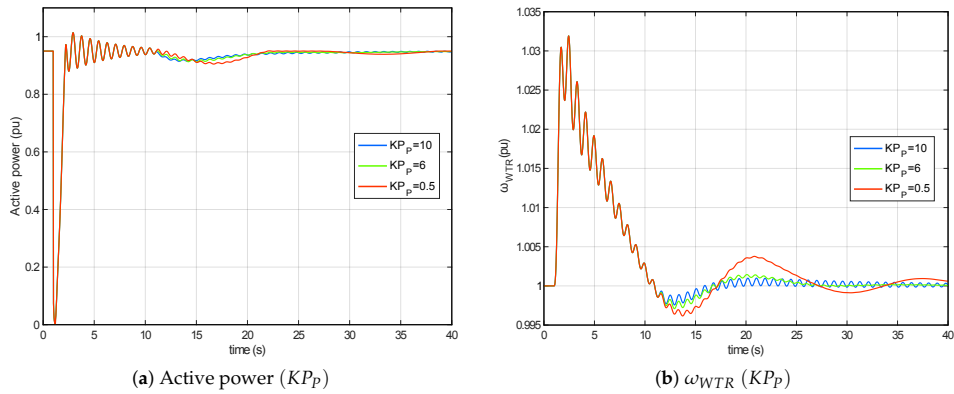


Figure 15. K_{Pp} parameter analysis: P_{WT} and ω_{WTR} evolution under a voltage dip.

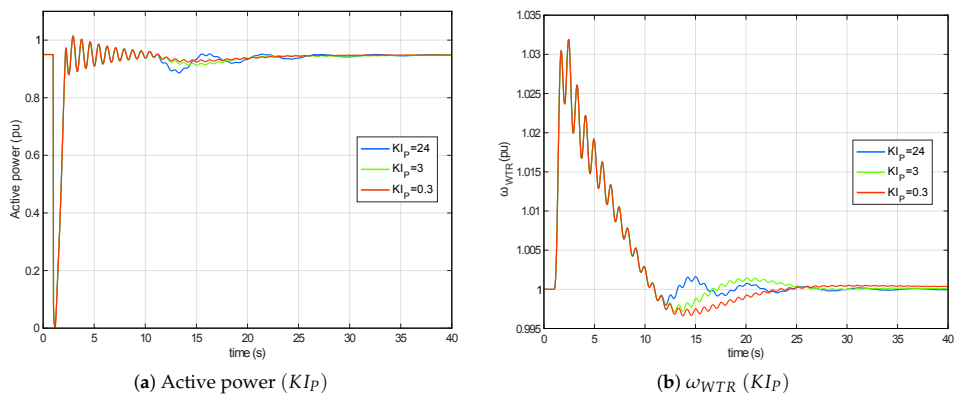


Figure 16. K_{I_p} parameter analysis: P_{WT} and ω_{WTR} evolution under a voltage dip.

Figure 17 shows the active power and ω_{WTR} responses when the DTD system is not considered ($K_{DTD} = 0$). The influence of the DTD system can be easily observed, damping the oscillations at a high rate. The second-order transfer function used to model this subsystem constitutes a band-pass filter, the tuning frequency of which is the natural frequency of the mechanical system. The addition of an oscillating active power with this frequency dampens the natural oscillations caused by the interaction between high and low speed shafts. Figure 18a shows a Bode Diagram of this transfer function for the original system parameters, which involves a natural frequency $\omega_{DTD} = 7.4162$ rad/s. As the input to the transfer function is ω_{gen} itself, the harmonic components of this frequency are almost negligible, and thus, the TF damping coefficient is not of great importance in the response of this system. This absence of harmonic components also implies that, in the case of a bad tuning in the frequency of the TF, the filter will not allow the oscillation to pass through, and hence, the effect will be equivalent to reducing K_{DTD} to zero, thus deactivating the system. Figure 18b shows $(\omega_{gen} - 1)$; the mean value of 1 pu is subtracted in order to compare between the DTD system output and the output from the band pass filter. Both signals have the same frequency, and the band pass filter also dampens the acceleration due to the voltage dip. Under steady-state operation conditions, the

output of this subsystem is considered as zero. The filter output is saturated and directly considered as an active power signal added to the active power obtained from the torque PI subsystem output.

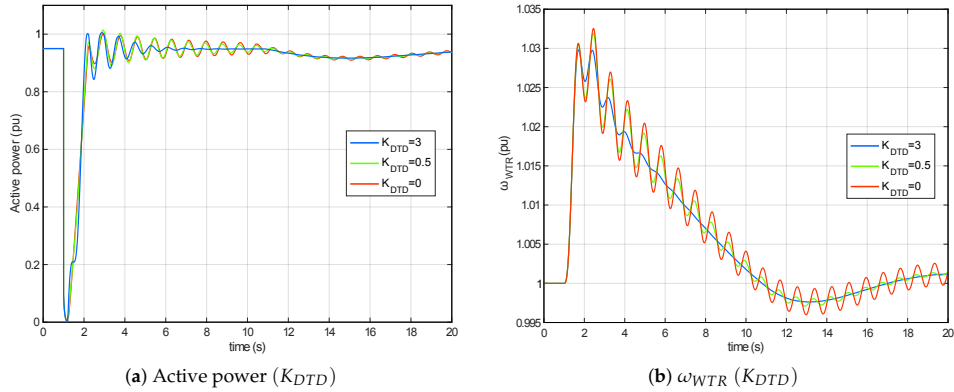


Figure 17. K_{DTD} parameter analysis: P_{WT} and ω_{WTR} evolution under a voltage dip.

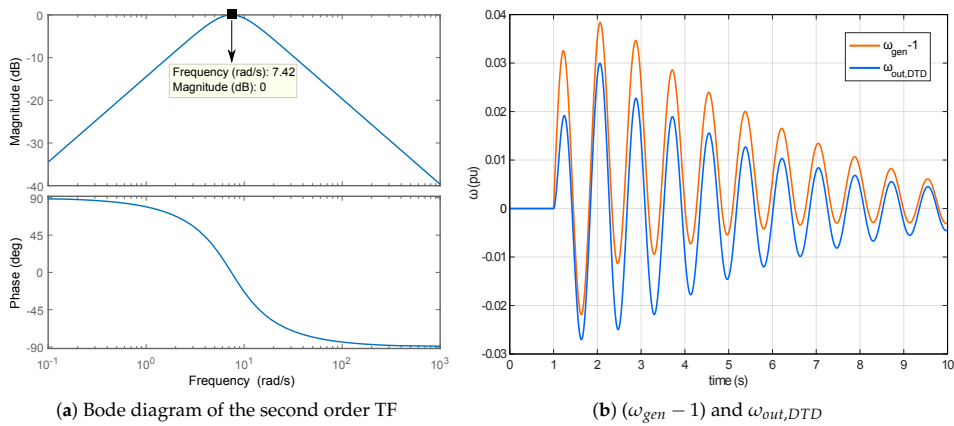


Figure 18. Bode diagram. DTD system response.

This active power constitutes the main output of the P_{Ctrl} system (p_{ord}). The active current input to the electrical generator system is then estimated by dividing p_{ord} by the voltage signal. An alternative method can be considered using ω_{gen} instead of ω_{WTR} as torque PI input, and with $K_{DTD} = 0$. However, this option has some drawbacks:

- The oscillation amplitude is larger since K_{IP} is significantly higher than K_{DTD} , and thus, the system may become unstable.
- The drive train oscillation is delayed by the T_{p_ord} filter, which models the converter time response. The addition of this phase to the system means the drive train damping is less efficient than if the drive train damper function injects after T_{p_ord} .

4.2. Pitch Control Model

The pitch control model is mainly formed by the addition of two PI controllers, usually depending on the WT rotor rotational speed and the active power reference provided by the active power control

model [38,39], w_{WTR} and p_{ord} respectively in Figure 19. A cross-coupling between both controllers is considered as a proportional gain KP_x commonly included by manufacturers to obtain more robust WT control.

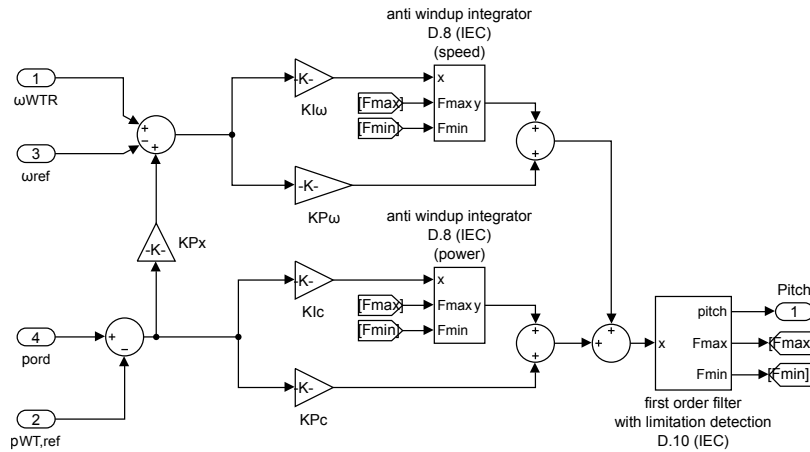


Figure 19. Pitch control model implemented in MATLAB/Simulink.

Figure 20 shows the first order filter with limitation detection (D.10) system. Highlighted relational operator blocks represent two comparison blocks. According to IEC 61400-27-1 [9], these comparison blocks are \geq . However, if the equal sign is kept in the blocks, the anti wind-up protection system will be active under normal operation, due to the pitch rate limit not actuating, and hence, its inputs and outputs will be equal. When the anti wind-up protection system performs properly, the signals F_{max} and F_{min} are activated either when the pitch rate is too high or too low, respectively, or when the pitch value itself is higher or lower than the maximum and minimum WT pitch. This modification proposed by the authors is currently under study to be included in the second edition of IEC 61400-27-1, which is expected to be issued in February 2018.

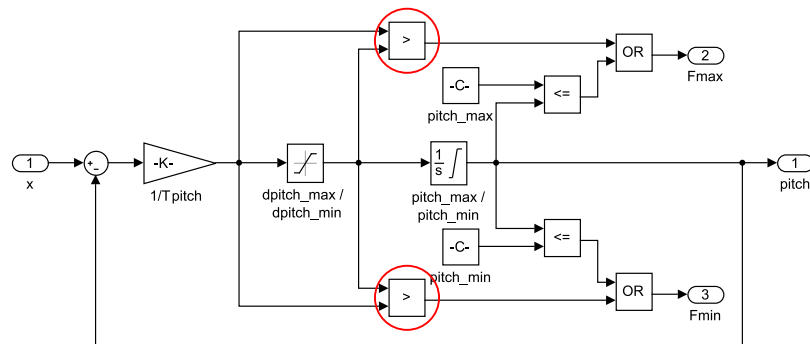


Figure 20. First order filter with limitation detection (D.10) implemented in MATLAB/Simulink.

The F_{max} and F_{min} signals are inputs to the anti wind-up integrator system, as can be seen in Figure 21. They disable the integral actuation by the action of saturator blocks, limiting the error signal to zero. Standard IEC 61400-27-1 [9] indicates that the integrator included in this system may be saturated in order to control the output of each controller. However, for the current work, these outputs

will not be saturated (limits are set to infinite) in order to allow the maximum interaction between both controllers.

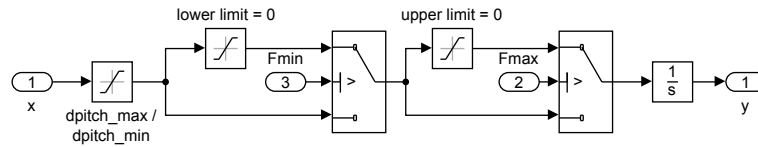


Figure 21. Anti wind-up integrator implemented in MATLAB/Simulink.

Table 1 summarizes the analyzed parameters under voltage dips. For the pitch control system, when the proportional gains of the controllers are increased keeping the rest of the gains constant, the model's response is faster than the response with lower proportional gain (unless these gains are too large and the system becomes unstable). Consequently, these performances have not been included in the paper. However, changes in the controller integral gains have a considerable effect shown in the following figures. Figure 22 depicts the responses when the parameter KI_ω is changed. When considering the different KI_ω values, the ω_{WTR} evolution along the disturbance is predictable, because the higher the integral gain is, the more under-damped it is, thus being faster and with a higher over-shoot. However, the active power response is detrimental to ω_{WTR} , being much slower and unstable when KI_ω rises.

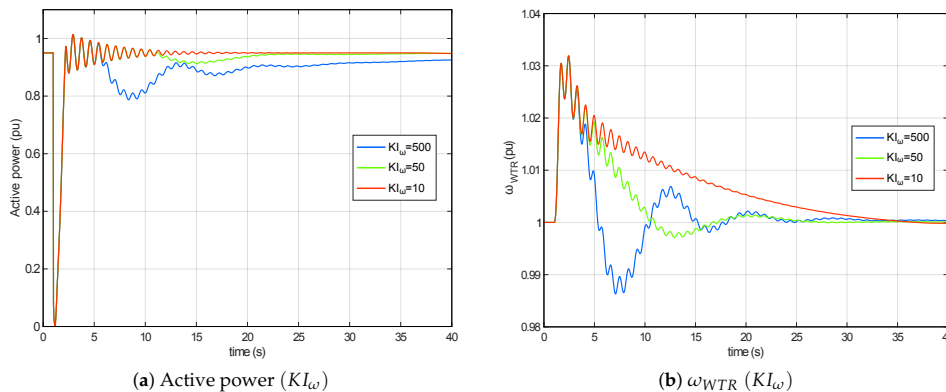


Figure 22. KI_ω parameter analysis: P_{WT} and ω_{WTR} evolution under a voltage dip.

By contrast, an adverse reaction to the response of ω_{WTR} occurs when the active power controller integral gain KI_c is modified, as shown in Figure 23. The active power response is then faster when KI_c is increased, detrimentally affecting the response of ω_{WTR} . It is worth noting this interaction as the systems depend on different error signals. Moreover, under the $KP_x = 0$ condition corresponding to the simulations in this paper, these systems are completely independent. Therefore, neither controller can be adjusted separately, due to the behavior of one having a considerable impact on the other as a consequence of the multiple dependences with the rest of control systems.

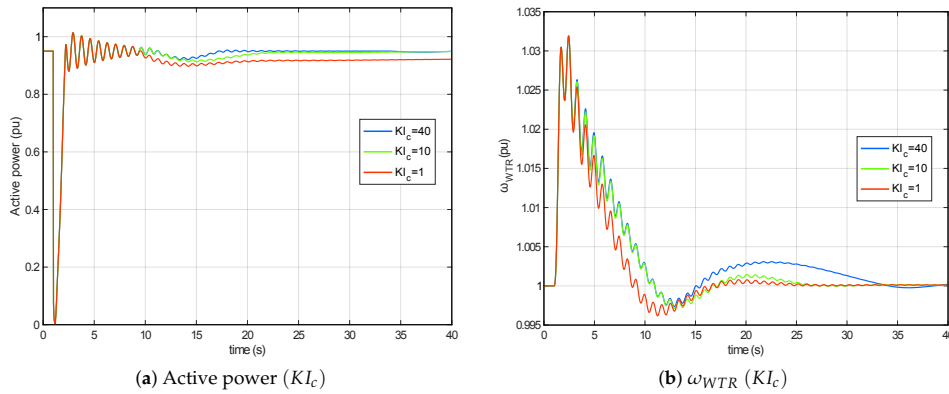


Figure 23. KI_c parameter analysis: P_{WT} and ω_{WTR} evolution under a voltage dip.

Finally, we have also studied the influence of the use of both PI controllers as compared to the use of the cross-coupling parameter KP_x . Theoretically, and according to the block models shown in Figure 19, if the following condition is fulfilled,

$$\frac{KI_c}{s} + KP_c = KP_x \cdot \left(\frac{KI_\omega}{s} + KP_\omega \right), \quad (5)$$

the behavior of both topologies should be equal. However, as shown in Figure 24, the two responses are not the same. This is due to the presence of the ramp limiters (and possibly value saturators) in the anti wind-up integrator systems; see Figure 21. If each error signal goes through its own controller, the possibility of reaching the saturation value is lower than if both signals are added and then the value goes through just one controller. This case is depicted in the example in Figure 24, in which the addition of both errors results in a high value, which is saturated if the cross-coupling method is used. However, if both controllers are used, the signals of each one fail to reach the ramp limiters, or even the value saturators if they are used. These considerations involve slight differences between the systems.

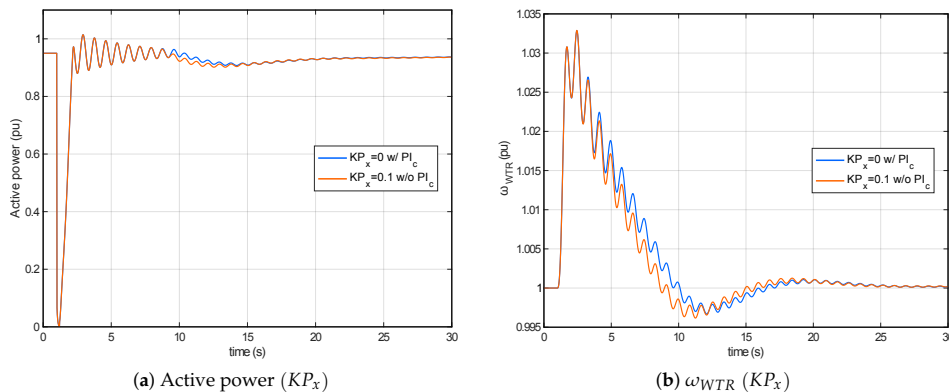


Figure 24. KP_x parameter analysis: P_{WT} and ω_{WTR} evolution under a voltage dip.

As previously mentioned, the cross-coupling gain is commonly used by manufacturers to obtain stable control of the wind turbine. The addition of two PI controllers may cause coordination issues in

some situations, which have been detected by the authors. For example, if the wind turbine is working in Zone 4, as in Figure 13, an active power increase is set by the control (still remaining in Zone 4), the PI_{ω} controller will not actuate since the ω_{ref} reference would be the same in both situations, but PI_C will decrease its output. However, if this output was originally close to zero, it can become a negative value, and if the saturations of the standard are considered, the pitch angle would never reach its reference. Figure 25 shows this performance. In $t = 20$ s, the active power reference changes from 0.6 pu to 1 pu; the PI_{ω} output keeps constant under steady-state conditions, but the PI_C output decreases the pitch angle to achieve the new active power reference (1 pu). As shown in Figure 25a, if the controller is saturated, the final P_{aero} of 1 pu is not achieved, and then, the wind turbine response is incorrect. This problem is solved by the use of KP_x , because only PI_{ω} is working, and subsequently, these coordination problems disappear.

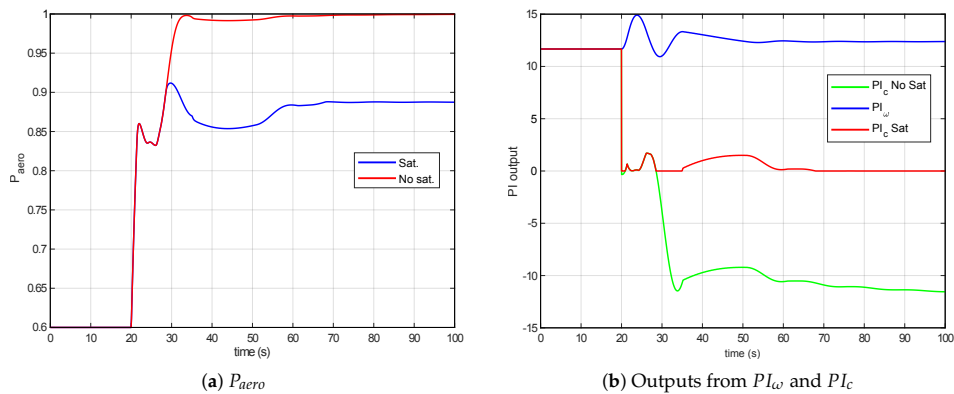


Figure 25. Problems with saturators in IEC 61400-27-1 pitch control.

5. Influence of Voltage Dip Characteristics: Depth and Duration

According to [40], a voltage dip is a temporary reduction of the root-mean-square (rms) voltage at a point in the electrical system below a given threshold. It is mainly characterized by two parameters: (i) depth, defined as the difference between the rms-voltage reference and the minimum rms-voltage achieved during the event and generally expressed as a percentage of the rms-voltage reference; (ii) and duration, which is the time between the rms-voltage dropping below the threshold given by the corresponding grid-code and the rms-voltage being recovered above the threshold. In this section, the effects of the variation in depth and duration of the voltage dip on the WT response are discussed in detail. The ranges of variation for depth and duration are summarized in Table 2.

Table 2. Voltage dip parameter variations.

Parameter	Original Value	Variation Range
Depth (d_{dip})	90%	[0.9 0.5 0.2]
Duration (t_{dip})	0.2 s	[0.05 0.2 0.8]

The depth variations of the voltage dip have a slight influence on the response of the model, as shown in Figure 26. For a certain depth, the variation in the response of the active power may seem predictable; however, and according to Figure 26a, there is no linear relation between the depth of the voltage dip and the minimum value of the active power provided by the WT (for example, with a $d_{dip} = 0.2$, the minimum active power value is lower than 0.4 pu), due to the dynamics of the

different control systems, as well as to the operation of the crowbar system. An increase in the depth also involves a higher acceleration; see Figure 26b. However, this parameter does not have as much influence as the duration of the dip.

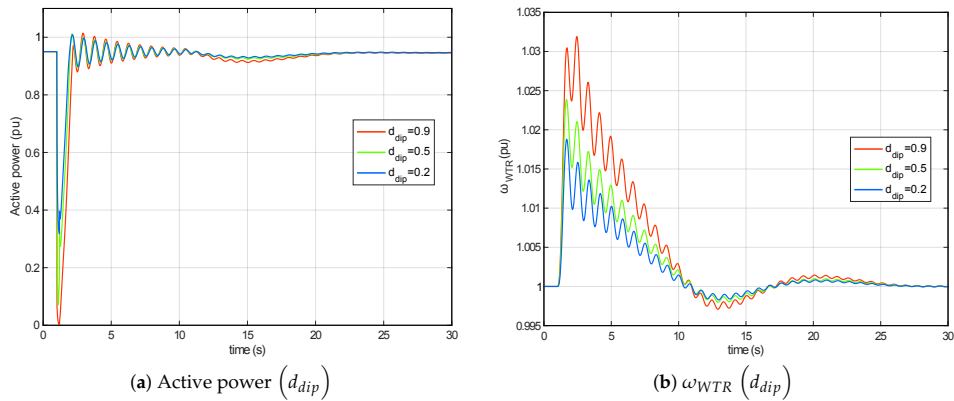


Figure 26. P_{WT} and ω_{WTR} responses under different voltage dip depths.

Figure 27 shows the different responses when t_{dip} is increased. The longer the voltage dip, the higher is the value reached by ω_{WTR} , because of the lack of electromagnetic torque that counteracts the mechanical torque produced by the wind. This maintained acceleration involves the actuation of PI_{ω} from the pitch control system, increasing the pitch angle in order to limit this acceleration; see Figure 28. This response involves a higher overshoot in rotational speed, which creates an active power reduction when $\omega_{WTR} < 0$. Then, if we wish to control this response, the values to be changed correspond to the PI_{ω} controller from pitch control, varying the performance during the transient, as was previously discussed in the simulations.

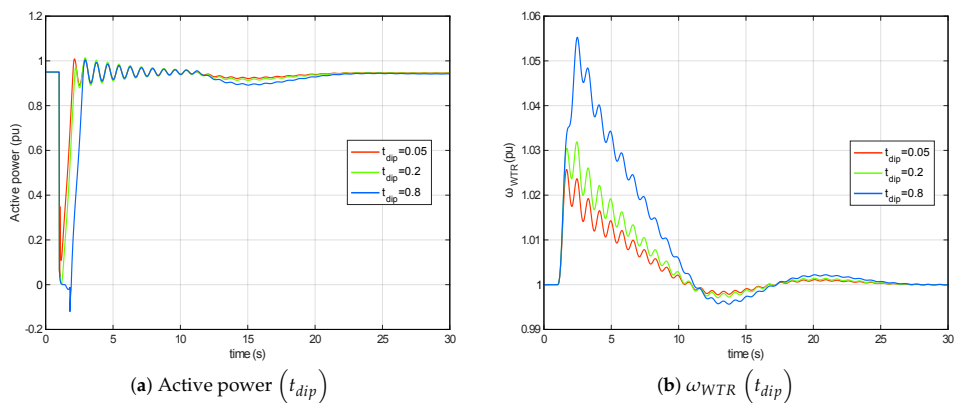


Figure 27. P_{WT} and ω_{WTR} responses under different voltage dip durations.

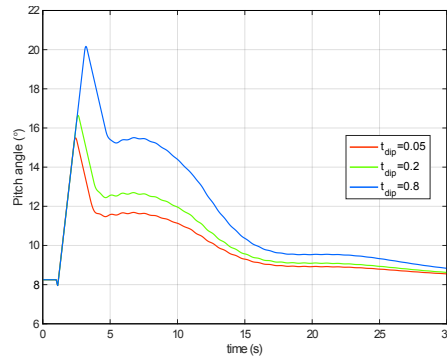


Figure 28. Pitch angle under different voltage dip durations.

6. Conclusions

A Type 3 WT model previously tested by the authors is adjusted and analyzed to give a complete benchmark response under voltage dips. Values and possible modifications of the parameters are also included in the paper, offering a notable reference for future studies. Parameters corresponding to the mechanical two mass model, the active power control and the pitch angle control models have been widely described, and their influence on the model's response is analyzed in terms of active power and rotational speed evolution during the disturbance. Extensive simulations have been carried out by the authors and included in the paper, and the different responses have also been compared. Furthermore, the model's responses have been discussed in detail, aiming to provide a better understanding of these recent complex generic models based on IEC 61400-27-1.

The two mass model parameters affect the physical response of the system, varying the frequency and amplitude of the oscillations of both active power and rotational speed under disturbances. For the active power control system, the response of the model can be adjusted by the PI parameter selection. Key results are obtained from the drive train damping system, which allows a significant damping effect by the injection of an oscillating active power with the same frequency as the mechanical oscillations. Regarding the pitch control model, the influence of the increase in the integral gain of the controllers also yields significant results, since the improvement in the behavior of one influences the proper response of the signal controlled by the other. The effect of a cross-coupling gain is also included in this analysis. In this way, and although theoretically there should be no difference, the behavior varies slightly between the two simulations due to the limiters included in the model.

This paper thus provides practical and complete parameters and simulations for a Type 3 WT model based on IEC 61400-27-1 submitted to voltage dips. Results and parameters are of significant interest to researchers and wind turbine manufacturers currently working on the definition and adjustment of this type of model.

Acknowledgments: This work was supported by the "Ministerio de Economía y Competitividad" and European Union FEDER, which supported this work under Project ENE2016-78214-C2-1-R. Furthermore, the authors would like to express their appreciation to the wind turbine manufacturer Siemens Gamesa Renewable Energy for the technical support received.

Author Contributions: Alberto Lorenzo-Bonache, Andrés Honrubia-Escribano and Emilio Gómez-Lázaro conceived of the paper, wrote the manuscript and analyzed the results. Francisco Jiménez-Buendía checked the results with the manufacturer generic wind turbine models. Ángel Molina-García supervised the research and the manuscript.

Conflicts of Interest: The authors declare no conflict of interest.

Abbreviations

The following abbreviations are used in this manuscript:

DFIG	Doubly-Fed Induction Generator
DSO	Distribution System Operator
DTD	Drive Train Damping
EMT	Electro-Magnetic Transient
EU	European Union
FRT	Fault Ride-Through
FSC	Full-Scale Converter
GSC	Grid-Side Converter
IEA	International Energy Agency
IEC	International Electrotechnical Commission
PV	Solar Photovoltaics
rms	root mean square
RSC	Rotor-Side Converter
TF	Transfer Function
TSO	Transmission System Operator
WECC	Western Electricity Coordinating Council
WT	Wind Turbine

References

1. Amin, A. *REmap: Roadmap for a Renewable Energy Future*; Technical Report; International Renewable Energy Agency (IRENA): Abu Dhabi, UAE, 2016.
2. Mueller, S. *Next Generation Wind and Solar Power*; Technical Report; International Energy Agency (IEA): Paris, France, 2016.
3. Philibert, C.; Holttinen, H. *Technology Roadmap Wind Energy*; Technical Report; International Energy Agency (IEA): Paris, France, 2013.
4. Honrubia-Escribano, A.; Jiménez-Buendía, F.; Molina-García, A.; Fuentes-Moreno, J.; Muljadi, E.; Gómez-Lázaro, E. Analysis of Wind Turbine Simulation Models: Assessment of Simplified versus Complete Methodologies. In Proceedings of the XVII International Symposium on Electromagnetic Fields in Mechatronics, Electrical and Electronic Engineering, Valencia, Spain, 10–12 September 2015; p. 8.
5. Honrubia Escribano, A.; Gomez-Lazaro, E.; Fortmann, J.; Sørensen, P.; Martín-Martínez, S. Generic dynamic wind turbine models for power system stability analysis: A comprehensive review. *Renew. Sustain. Energy Rev.* **2017**, in press.
6. Liu, Y.J.; Chen, P.A.; Lan, P.H.; Chang, Y.T. Dynamic simulation and analysis of connecting a 5 MW wind turbine to the distribution system feeder that serves to a wind turbine testing site. In Proceedings of the 2017 IEEE 3rd International Future Energy Electronics Conference and ECCE Asia (IFEEC 2017-ECCE Asia), Kaohsiung, Taiwan, 3–7 June 2017; pp. 2031–2035.
7. Asmine, M.; Brochu, J.; Fortmann, J.; Gagnon, R.; Kazachkov, Y.; Langlois, C.E.; Larose, C.; Muljadi, E.; MacDowell, J.; Pourbeik, P.; et al. Model Validation for Wind Turbine Generator Models. *IEEE Trans. Power Syst.* **2011**, *26*, 1769–1782.
8. Fortmann, J.; Engelhardt, S.; Kretschmann, J.; Feltes, C.; Erlich, I. New Generic Model of DFG-Based Wind Turbines for RMS-Type Simulation. *IEEE Trans. Energy Convers.* **2014**, *29*, 110–118.
9. International Electrotechnical Commission. *IEC 61400-27-1: Electrical Simulation Models for Wind Power Generation—Wind Turbines*; International Electrotechnical Commission: Geneva, Switzerland, 2015.
10. Villena-Ruiz, R.; Lorenzo-Bonache, A.; Honrubia-Escribano, A.; Gómez-Lázaro, E. Implementation of a generic Type 1 wind turbine generator for power system stability studies. In Proceedings of the International Conference on Renewable Energies and Power Quality, Malaga, Spain, 4–6 April 2017.
11. Das, K.; Hansen, A.; Sørensen, P. Understanding IEC standard wind turbine models using SimPowerSystems. *Wind Eng.* **2016**, *40*, 212–227.
12. Sørensen, P. *IEC 61400-27. Electrical Simulation Models for Wind Power Generation*; European Energy Research Alliance (EERA): Brussels, Belgium, 2012.

13. Honrubia-Escribano, A.; Gómez-Lázaro, E.; Jiménez-Buendía, F.; Muljadi, E. Comparison of Standard Wind Turbine Models with Vendor Models for Power System Stability Analysis. In Proceedings of the 15th International Workshop on Large-Scale Integration of Wind Power into Power Systems as well as on Transmission Networks for Offshore Wind Power Plants, Vienna, Austria, 15–17 November 2016.
14. Göksu, O.; Altin, M.; Fortmann, J.; Sorensen, P. Field Validation of IEC 61400-27-1 Wind Generation Type 3 Model with Plant Power Factor Controller. *IEEE Trans. Energy Convers.* **2016**, *31*, 1170–1178.
15. Honrubia-Escribano, A.; Gómez-Lázaro, E.; Viguera-Rodríguez, A.; Molina-García, A.; Fuentes, J.A.; Muljadi, E. Assessment of DFIG simplified model parameters using field test data. In Proceedings of the IEEE Symposium on Power Electronics & Machines for Wind Application, Denver, CO, USA, 16–18 July 2012; pp. 1–7.
16. Sørensen, P.; Andersen, B.; Bech, J.; Fortmann, J.; Pourbeik, P. Progress in IEC 61400-27. Electrical Simulation Models for Wind Power Generation. In Proceedings of the 11th International Workshop on Large-Scale Integration of Wind Power into Power Systems as well as on Transmission Networks for Offshore Wind Power Plants, Lisbon, Portugal, 13–15 November 2012; p. 7.
17. Bech, J. Siemens Experience with Validation of Different Types of Wind Turbine Models. In Proceedings of the IEEE Power and Energy Society General Meeting, Washington, DC, USA, 27–31 July 2014.
18. Jiménez-Buendía, F.; Barrasa Gordo, B. Generic Simplified Simulation Model for DFIG with Active Crowbar. In Proceedings of the 11th International Workshop on Large-Scale Integration of Wind Power into Power Systems as well as on Transmission Networks for Offshore Wind Power Plants, Lisbon, Portugal, 13–15 November 2012; p. 6.
19. Honrubia-Escribano, A.; Jiménez-Buendía, F.; Gómez-Lázaro, E.; Fortmann, J. Field Validation of a Standard Type 3 Wind Turbine Model for Power System Stability, According to the Requirements Imposed by IEC 61400-27-1. *IEEE Trans. Energy Convers.* **2017**, doi:10.1109/TEC.2017.2737703
20. Zeni, L.; Gevorgian, V.; Wallen, R.; Bech, J.; Sørensen, P.E.; Hesselbæk, B. Utilisation of real-scale renewable energy test facility for validation of generic wind turbine and wind power plant controller models. *IET Renew. Power Gener.* **2016**, *10*, 1123–1131.
21. Lorenzo-Bonache, A.; Villena-Ruiz, R.; Honrubia-Escribano, A.; Gómez-Lázaro, E. Real time simulation applied to the implementation of generic wind turbine models. In Proceedings of the International Conference on Renewable Energies and Power Quality, Malaga, Spain, 4–6 April 2017.
22. Honrubia-Escribano, A.; Jiménez-Buendía, F.; Gómez-Lázaro, E.; Fortmann, J. Validation of Generic Models for Variable Speed Operation Wind Turbines Following the Recent Guidelines Issued by IEC 61400-27. *Energies* **2016**, *9*, 1048.
23. Göksu, O.; Sorensen, P.; Morales, A.; Weigel, S.; Fortmann, J.; Pourbeik, P. Compatibility of IEC 61400-27-1 Ed 1 and WECC 2nd Generation Wind Turbine Models. In Proceedings of the 15th Wind Integration Workshop, Vienna, Austria, 15–17 November 2016.
24. Hernández, C.V.; Telsnig, T.; Pradas, A.V. *JRC Wind Energy Status Report 2016 Edition*; Market, Technology and Regulatory Aspects of Wind Energy; JRC Science for Policy Report; European Commission: Brussels, Belgium, 2017.
25. Fortmann, J.; Engelhardt, S.; Kretschmann, J.; Janben, M.; Neumann, T.; Erlich, I. Generic Simulation Model for DFIG and Full Size Converter based Wind Turbines. In Proceedings of the 9th International Workshop on Large-Scale Integration of Wind Power into Power Systems as well as on Transmission Networks for Offshore Wind Plants, Quebec, QC, Canada, 18–19 October 2010; p. 8.
26. Lorenzo-Bonache, A.; Villena-Ruiz, R.; Honrubia-Escribano, A.; Gómez-Lázaro, E. Comparison of a Standard Type 3B WT Model with a Commercial Build-in Model. In Proceedings of the IEEE International Electric Machines & Drives Conference, Miami, FL, USA, 21–24 May 2017.
27. Subramanian, C.; Casadei, D.; Tani, A.; Sorensen, P.; Blaabjerg, F.; McKeever, P. Implementation of Electrical Simulation Model for IEC Standard Type-3A Generator. In Proceedings of the 2013 European Modelling Symposium (EMS), Manchester, UK, 20–22 November 2013; pp. 426–431.
28. European Commission. *EU 2016/631 of 14 April 2016 Establishing a Network Code on Requirements for Grid Connection of Generators*; European Commission: Brussels, Belgium, 2016.
29. Morales, A.; Robe, X.; Maun, J.C. *Wind Turbine Generator Systems. Part 21. Measurement and Assessment of Power Quality Characteristics of Grid Connected Wind Turbines*; IEC/CEI: Geneva, Switzerland, 2001.

30. Muyeen, S.; Ali, M.; Takahashi, R.; Murata, T.; Tamura, J.; Tomaki, Y.; Sakahara, A.; Sasano, E. Comparative study on transient stability analysis of wind turbine generator system using different drive train models. *IET Renew. Power Gener.* **2007**, *1*, 131–141.
31. Perdana, A. Dynamic Models of Wind Turbines. A Contribution towards the Establishment of Standardized Models of Wind Turbines for Power System Stability Studies. Ph.D. Thesis, Chalmers University of Technology, Gothenburg, Sweden, 2008.
32. Fortmann, J. Modeling of Wind Turbines with Doubly Fed Generator System. Ph.D. Thesis, Department for Electrical Power Systems, University of Duisburg-Essen, Duisburg, Germany, 2014.
33. Behnke, M.; Ellis, A.; Kazachkov, Y.; McCoy, T.; Muljadi, E.; Price, W.; Sanchez-Gasca, J. Development and validation of WECC variable speed wind turbine dynamic models for grid integration studies. In Proceedings of the AWEA Wind Power Conference, Los Angeles, CA, USA, 4–7 June 2007; pp. 1–5.
34. Burton, T.; Sharpe, D.; Jenkins, N.; Bossanyi, E. *Wind Energy Handbook*; John Wiley & Sons: Hoboken, NJ, USA, 2001; p. 642.
35. Bossanyi, E.A. The Design of Closed Loop Controllers for Wind Turbines. *Wind Energy* **2000**, *3*, 149–163.
36. Wright, A.D.; Fingersh, L.J. *Advanced Control Design for Wind Turbines. Part I: Control Design, Implementation, and Initial Tests*; Technical Report; NREL: Golden, CO, USA, 2008.
37. Lorenzo-Bonache, A.; Villena-Ruiz, R.; Honrubia-Escribano, A.; Gómez-Lázaro, E. Operation of Active and Reactive Control Systems of a Generic Type 3 WT Model. In Proceedings of the IEEE International Conference on Compatibility, Power Electronics and Power Engineering, Cadiz, Spain, 4–6 April 2017.
38. Lin, L.; Zhang, J.; Yang, Y. Comparison of Pitch Angle Control Models of Wind Farm for Power System Analysis. In Proceedings of the IEEE Power Energy Society General Meeting, Calgary, AB, Canada, 26–30 July 2009; pp. 1–7.
39. Muljadi, E.; Butterfield, C.P. Pitch-controlled variable-speed wind turbine generation. *IEEE Trans. Ind. Appl.* **2001**, *37*, 240–246.
40. Institute of Electrical and Electronics Engineers (IEEE). *1564-2014—IEEE Guide for Voltage Sag Indices*; IEEE: New York, NY, USA, 2014; pp. 1–59.



© 2017 by the authors. Licensee MDPI, Basel, Switzerland. This article is an open access article distributed under the terms and conditions of the Creative Commons Attribution (CC BY) license (<http://creativecommons.org/licenses/by/4.0/>).

4.1.2. Paper II - IEC and WECC Type 3 comparison

Paper II presents a detailed comparison of the IEC and WECC modeling approaches regarding the most complex generic model: Type 3 (see Section 3.1.1). This paper deeply describes those systems which most differ between the two guidelines: *Active power control*, *Reactive power control*, *Current limitation system* and *Electrical generator system*. The impact of the additional complexity of the IEC model is assessed from two different points of view: the controllability of the active and reactive power responses, and the simulation time.

The objectives of this paper were to provide stakeholders with enough information to choose which model better fits their purpose depending on their needs: accuracy (IEC) versus simplicity (WECC).

Table 4.2 summarizes the metrics of the journal in which the paper was published. The full paper is included below, as published.

Table 4.2: Journal Metrics – Paper II.

Journal Name	IET Renewable Power Generation
Impact Factor (2017)	3.488
Category	Engineering, Electrical & Electronic
Quartile in category	Q1
Position in category	50/260
ISSN	1752-141

Generic Type 3 WT models: comparison between IEC and WECC approaches

ISSN 1752-1416
 Received on 5th November 2018
 Revised 15th January 2019
 Accepted on 6th February 2019
 doi: 10.1049/iet-rpg.2018.6098
 www.ietdl.org

Alberto Lorenzo-Bonache¹ ✉, Andres Honrubia-Escribano¹, Jens Fortmann², Emilio Gómez-Lázaro¹

¹Wind Energy and Power Systems Department, Renewable Energy Research Institute, Universidad de Castilla-La Mancha, Albacete, Spain

²HTW Berlin-University of Applied Sciences, Berlin, Germany

✉ E-mail: alberto.lorenzo@uclm.es

Abstract: The widespread use of renewable energies around the world has generated the need for new tools and resources to allow them to be properly integrated into current power systems. Power system operators need new dynamic generic models of wind turbines and wind farms adaptable to any vendor topology and which permit transient stability analysis of their networks with the required accuracy. Under this framework, the International Electrotechnical Commission (IEC) and the Western Electricity Coordinating Council (WECC) have developed their own generic dynamic models of wind turbines for stability analysis. Although these entities work in conjunction, the focus of each is slightly different. The WECC models attempt to minimise the complexity and number of parameters needed, while the IEC approach aims to optimise comparison with real turbine measurements. This study presents a detailed comparison between these two different approaches for modeling a Type 3 (i.e., DFIG) wind turbine in MATLAB/Simulink. Finally, several simulations are conducted, with which the consequences of the different approaches are evaluated. The results of this paper are of interest to power system operators as well as wind turbine manufacturers who require further assistance in adapting their specific models to the simplified versions provided by the International Committees.

Nomenclature

P control	active power control
Q control	reactive power control
Q limitation	reactive current limitation

1 Introduction

The current needs of power systems around the world have resulted in the development of new tools and resources that permit the integration of the increasingly important renewable energy sources. Power system operators such as transmission system operators (TSOs) or distribution system operators (DSOs) need to perform transient stability analysis in order to react to dynamic grid events such as voltage dips, loss of loads or generation, and switching of lines [1]. However, there is a lack of universal, standardised, publicly available and validated wind turbine (WT) models that allow these analyses to be conducted. For example, conventional vendor models only represent one specific WT model. Furthermore, since vendor models are intended to simulate the behaviour of specific components and controls of the WT [2, 3], they are complex, and require many parameters and specific simulation software [4].

To meet the needs of TSOs and DSOs, international organisations such as the International Electrotechnical Commission (IEC) and the Western Electricity Coordinating Council (WECC) have been working in recent years on the development of generic WT and wind farm models for power system stability analysis [5, 6]. These generic models can represent the behaviour of any vendor's WT model. Their aim is to provide sufficiently accurate results without the need for a large number of parameters, and with sufficient documentation for them to be implemented in any simulation software. In February 2015, the IEC published the first edition of the Standard IEC 61400-27-1 [7]. The second edition of this standard is currently under development, and is expected to be published in 2019. In January 2014, the WECC published their report entitled 'WECC Second Generation Wind Turbine Models' [8], the first generation of which was published in 2010 [9]. These two documents classify the different topologies of WTs into four types [10], depending mainly on their

electrical generator. Type 3, which is studied in this paper, represents a WT equipped with a doubly fed induction generator (DFIG)/asynchronous generator, in which the stator is directly connected to the grid and the rotor is connected through an alternating current (AC)/direct current (DC)/AC power converter [11]. Worldwide, this is the most commonly installed topology of WT [12]. In addition, the Type 3 simulation model is the most complex of the four types for both International Committees.

WT manufacturers are the most important stakeholders involved in the development of these generic models, providing field data and values of the parameters that define their behaviour. The first generation WECC models were developed primarily by one manufacturer, while development of the second generation coincided with that of the IEC, with the involvement of manufacturers such as GE, Siemens, ABB, REpower/Senvion, and to a limited extent Vestas and Gamesa, who contributed to both models. The IEC model was later extended, based mainly on data provided by Gamesa, Senvion, and Vestas. The debate on IEC and WECC models is based primarily on issues of complexity (number of states), number of parameters and model execution speed (in the focus of WECC [13]), and accuracy during faults close to 90% voltage, as well as unbalanced conditions, in order to fulfil the validation requirements in certain European countries, which is the IEC's main goal. Hence, the comparison of the response provided by both models plays a key role in spreading their use and application in current power systems.

With reference to the existing literature, a number of implementation and validation works regarding IEC and WECC generic models have been published. One of the first published works on generic WT models is [14], which shows the development of the WECC models (the first version of the WECC's guidelines was published in 2010). Concerning the IEC standard, which was published subsequently (2015), the first works focused on modelling can be found in [15–17], which also describe the ongoing work. Furthermore, in 2011 Asmine *et al.* [18] and Keung *et al.* [19] started to investigate validation methodologies for generic WT models. During the following years, contributions focused on the development of the second generation of WECC WT models [20–22], as well as the first edition of the IEC 61400-27-1 [23–25]. Since the publication of the standard, the

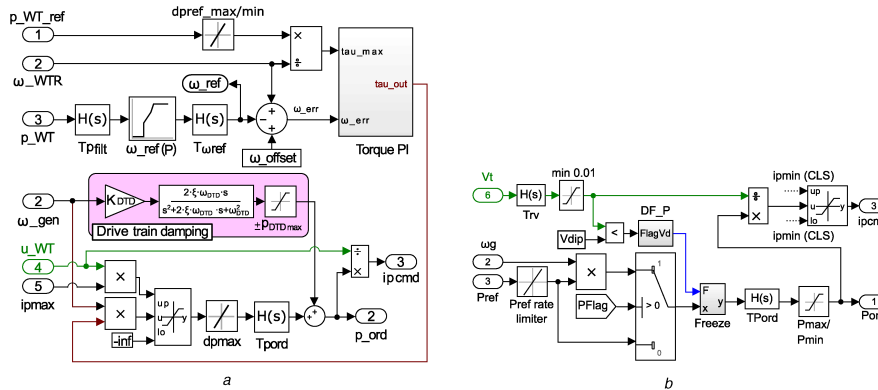


Fig. 2 Simulink implementation of the Type 3 active power control defined by both international guidelines (a) IEC 61400-27-1, (b) WECC second generation

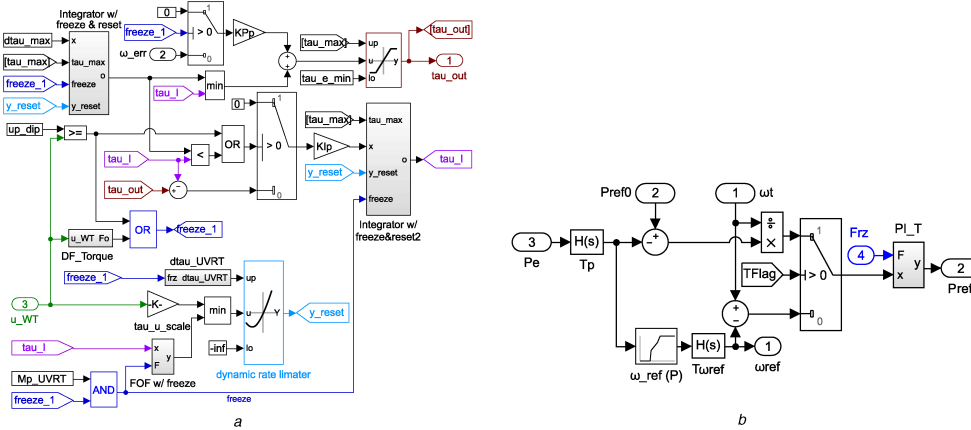


Fig. 3 Simulink implementation of the Type 3 torque PI subsystem defined by both international guidelines (a) IEC 61400-27-1, (b) WECC second generation

CLS systems are included in the control model [29], without subsystem separation, contrary to the IEC model. However, in this work they will be separated in order to facilitate the understanding of the differences between both modelling approaches.

As members of both international working groups have collaborated almost since their inception, some systems have been implemented in the same form for both generic WT models [39]. These systems are the mechanical two-mass model (pink in Fig. 1), the one-dimensional aerodynamic model (green) and the pitch control system. However, the absence of a dynamic reactive power limitation control in the WECC generic Type 3 model constitutes an important difference. In the IEC model, this system allows the reactive power limits to be controlled through look-up tables depending on the voltage or the active power at any time. The WECC model provides systems to control the reactive power, but they are set as fixed values. The remaining systems, as explained hereafter, are not equivalent for IEC and WECC generic models approaches.

3 Systems with different implementations in IEC and WECC

The following sections describe the systems with different interpretations and constructions in IEC 61400-27-1 and WECC second generation.

3.1 Active power control

The active power control systems from IEC 61400-27-1 [7] and WECC ‘Second Generation of WT models’ [8] are shown in Figs. 2a and b, respectively. Moreover, the torque proportional-integral (PI) subsystems, which are part of the active power control, despite being included in the general structure of WECC model, are shown in Figs. 3a and b, for the IEC and WECC approaches, respectively. The nomenclature followed in the diagrams corresponds to the one used by each entity. Furthermore, hereafter, the transfer function blocks indicated as $H(s)$ represent first-order filters which follow (1), in which T_{name} represents the time constant for each filter, shown in the diagrams as the name of the transfer function block.

$$H(s) = \frac{1}{sT_{name} + 1} \quad (1)$$

As can be deduced from Figs. 2 and 3, the Type 3 active power control model defined by the IEC Committee is more complex than that of the WECC. It contains more sophisticated functions for controlling power during grid faults and subsequent voltage recovery. The general behaviour of these systems is governed by the look-up table $\omega_{ref}(P)$ (see Figs. 2a and 3b), which provides the rotational speed at which the WT should be rotating when it is injecting a certain active power. This speed reference is subtracted from the actual rotational speed of the WT rotor (ω_{WTR}/ω_t) (when a parameter or signal is included in both models, but named

differently, it will be referred as $IEC_{parameter}/WECC_{parameter}$ (i.e. ω_{WTR} is the IEC parameter which refers to the rotational speed of the WT rotor, which is called ωt in the WECC guidelines), and the speed error is then the input to a PI controller, providing the electromagnetic torque of the WT (τ_{out}/P_{ref}). On the basis of Göksu *et al.* [36], the parameters of the PI controller are not the same for both models, which is explained by their different behaviour when facing a voltage dip, as explained hereafter. In the present work, they are defined as follows. Additionally, model parameters are depicted in Table 1

- $KP_p = 500/K_{pp} = 0.1$
- $KI_p = 10/K_{ip} = 0.1$

This τ_{out}/P_{ref} is then multiplied by the generator speed (ω_{gen}/ω_g) to obtain the active power of the WT (p_{ord}/P_{ord}). Finally, the active power is divided by the voltage (u_{WT}/V_t) to obtain the active current command signal ($ipcmd$), which is the input to the generator system.

The WECC model allows the selection of different control modes by flags PFlag and TFlag. PFlag establishes whether active

power control is commanded by the electromagnetic torque or the active power. Since the IEC model uses active power for this purpose, in order to obtain similar results, PFlag takes the value of 1 in this work. TFlag is included to choose between using the rotational speed error and the active power error in the torque PI system (Fig. 3b). Since the IEC model actuates according to the rotational speed error only, TFlag is equal to 0 in the present work.

The main differences between the two active power control models are related to the control during and following voltage dip, which is more complex in the IEC model. In the IEC model, the reset (freeze) system can control the torque output rate and value more accurately. When a fault occurs, the signal freeze_1 takes the value of 1, and is maintained during the fault and a certain post-fault period controlled by the delay flag block DF_Torque (Fig. 3a). The proportional component (in the upper side of Fig. 3a) then takes the value of 0. The other part of the controller takes the minimum value between two possible signals: the torque value increasing as a ramp at maximum rate $d\tau_{max}$ (which can be used either to control the mechanical stress or to meet a certain grid code) or the output of the integral part, which actuates according to the error between its own output τ_{I} and the output of the system τ_{out} . When the fault occurs, the output of the first

Table 1 Parameters associated with the generic Type 3 models, both IEC and WECC

IEC	Symbol	Submodel	Description	Value	
				IEC	WECC
	$T_{CW}(du)$	generator	CB duration versus voltage variation	0.05	—
	x_s		electromagnetic transient reactance	[0.2 : 0.4]	—
		LVPL _{0.5}	LVPL gain breakpoint ($V = 0.5$ pu)	—	[0 : 1]
	T_{wo}		time constant for CB washout filter	0.5	—
	di_{pmax}	rrpwr	maximum active current ramp rate	2.75	—
	M_{qG}	reactive power control	reactive power control mode	1	—
		PfFlag	constant Q (0) or power factor (PF) (1) local control	—	0
		Vflag	voltage control (0) or Q control (1)	—	1
		Qflag	bypass (0) or engage (1) inner voltage regulator loop	—	1
	M_{qUVRT}		under voltage ride through (UVRT) reactive power control mode	2	—
	K_{qv}	kqv	voltage scaling factor for UVRT current	0.55	0.60
	i_{qpost}	iqfrz	post-fault reactive current injection	0.5	—
	r_{drop}	Rt	resistive component of voltage drop impedance	0.01	—
	x_{drop}	Xt	inductive component of voltage drop impedance	0.1	—
	T_{qord}	Tqord	time constant in reactive power order lag	0.001	—
	u_{max}	V max	maximum voltage in voltage PI controller integral term	1.1	—
	u_{min}	V min	minimum voltage in voltage PI controller integral term	0.9	—
	u_{qdip}	Vdip	voltage threshold for UVRT detection in Q control	0.9	—
	M_{DFSLim}	current limitation control	limitation of Type 3 stator current	0	—
	M_{qpr1}		prioritisation of reactive power control during UVRT	1	—
	$T_{\omega filtp3}$	active power control	filter time constant for generator speed measurement	1	—
	ω_{offset}		offset to reference value that limits controller action	0.0	—
	K_{DTD}		gain for active DTD	[0 : 1]	—
	T_{pfilt}	Tpt	time constant in power measurement filter	0.001	—
	T_{pord}	Tpord	time constant in power order lag	0.001	—
	T_{ufilt}	Tuord	time constant in voltage measurement filter	0.001	—
	dp_{max}	dprefmax	maximum WT power ramp rate	1	—
	$T_{\omega ref}$	twref	time constant in speed reference filter	200	—
	$d_{tau, UVRT}$	torque PI	limitation of torque rise rate during UVRT	[0 : 1]	—
	τ_{u_scale}		voltage scaling factor of reset torque	[0 : 1]	—
	KPp	Kpp	proportional constant of torque PI controller	500	0.1
	KIp	kip	integral constant of torque PI controller	10	0.1
	Kpx	Kcc	pitch cross-coupling gain	[0 : 0.04]	0.016
	Θ_{max}	Θ max	maximum pitch angle	30	—
	Θ_{min}	Θ min	minimum pitch angle	0	—
	$d\Theta_{max}$	$d\Theta$ max	maximum pitch angle rate	[5 : 10]	—
	$d\Theta_{min}$	$d\Theta$ min	minimum pitch angle rate	[-10 : -5]	—

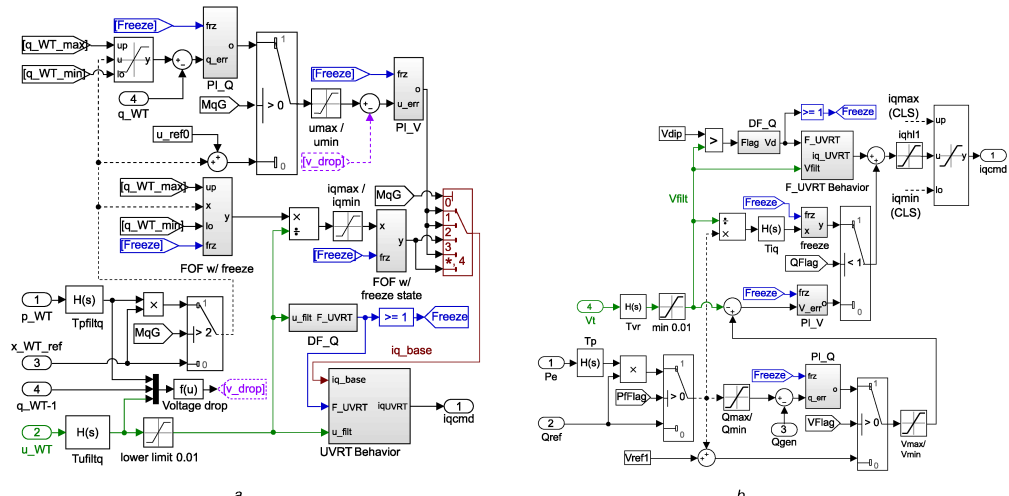


Fig. 4 Simulink implementation of the Type 3 Reactive power control defined by both international guidelines
 (a) IEC 61400-27-1, (b) WECC second generation

Table 2 Correspondence between control flags for reactive power control

IEC MqG	PfFlag	WECC VFlag	QFlag	Control mode
0	0	0	1	voltage control
1	0	1	1	reactive power control
2	0	1	0	open-loop reactive power control
3	1	1	1	power factor control
4	1	0	0	open-loop power factor control

system takes the value y_{reset} , and the second can either continue working according to its input or be forced to value y_{reset} , depending on the parameter Mp_{UVRT} . This value y_{reset} is calculated as the minimum between the residual voltage multiplied by the gain τ_{u_scale} or the value τ_{u_I} . The maximum rate of y_{reset} is also modified during the dip (system $d\tau_{UVRT}$), usually not allowing y_{reset} to increase during the fault. After the post-fault period, the proportional component continues working according to ω_{err} , and the integral part will increase from y_{reset} to the steady-state value, with a maximum rate defined by $d\tau_{u_max}$.

The WECC torque control system is defined as a PI controller working either with the torque or the rotational speed error, depending on TFlag, as previously explained. During the fault, the PI controller is frozen, which means that the proportional part takes the value of 0, as well as the input to the integral part (keeping constant its output). This behaviour constitutes a key difference to the IEC model. The WECC system maintains the steady-state value during the fault, while the IEC approach is able to adjust it by use of the parameters τ_{u_scale} and $d\tau_{UVRT}$. Thus, for the WECC model, the value of the active power during the fault depends only on the dip depth, and its control or adjustment is not possible. The consequences of this different behaviour are discussed in-depth in Section 4.

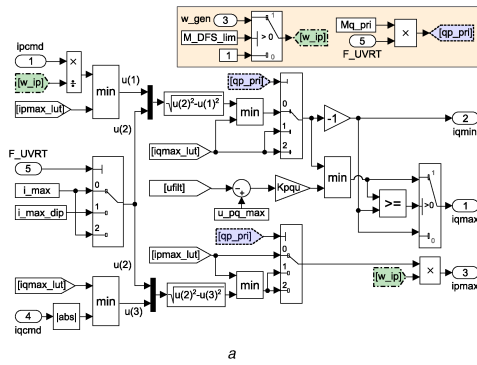
3.2 Reactive power control

The Simulink implementations of the Type 3 reactive power control systems from IEC and WECC are shown in Figs. 4a and b, respectively. Both systems work similarly, using flags to define the path the reference signal must follow. In both cases, the reactive power reference is assumed to come from a plant controller. It can be either a reactive power reference or a voltage reference. A number of switches allow the activation of different control types. In the IEC model, a single flag (MqG, whose value is between 0

and 4) is used, while three flags are needed in the WECC model (PFlag, VFlag, and QFlag, which can be defined as 0 or 1) [40]. The correspondence between the flags is shown in Table 2, where it can be observed that the same control modes are available. Open-loop controls (MqG = 2 and 4) can only be used if the power plant controller is built, which is not the case of this work.

The control mode chosen for the simulations is a closed-loop reactive power control, following the reference x_{WT_ref}/Q_{ref} . The reference signal goes through two PI controllers: one actuating according to the reactive power error and other actuating according to the voltage error. Then, the reactive current command signal (iq_{cmd}), which is the input to the electrical generator system, is obtained.

In terms of the behaviour of the system under a voltage dip, the IEC model is more complex, as it allows a choice between three control modes. For the IEC model, three different control modes can be chosen by adjusting the parameter Mq_{UVRT} . If Mq_{UVRT} takes the value of 0, the reactive current injected during the dip is proportional to the voltage depth; when Mq_{UVRT} is set to 1, the reactive current injected during the dip depends on the current injected prior to the fault plus a value proportional to the voltage depth; finally, if Mq_{UVRT} takes the value of 2, the behaviour is the same as Mq_{UVRT} equal to 1, but adding a constant reactive current component during a certain post-fault period. The WECC model, the transient control system of which is included in the block F_{UVRT} Behavior, directly implements the most complex system. Hence, the WECC transient control system is modelled as the IEC one with Mq_{UVRT} equal to 2. Thus, the behaviour of Mq_{UVRT} can be obtained if $iq_{post} = 0$. However, the mode Mq_{UVRT} equal to 0 is not equivalent between both systems, since the current from the steady-state controller is always added in the WECC model. Furthermore, another difference is that the IEC model uses the steady-state voltage to obtain the depth of the dip (adjusting the time constant of a first-order filter with a large value,



```

%% MATLAB code for CLS
if Pqflag==0 %Q priority
    iqmax=min(VDL1, I_max)
    ipmax=min(VDL2, sqrt(I_max^2-iqcmd^2))
else %P priority
    iqmax=min(VDL1, sqrt(I_max^2-iqcmd^2))
    ipmax=min(VDL2, I_max)
end
iqmin=-iqmax
ipmin=0

```

Fig. 5 Implementation of the Type 3 CLSs defined by both international guidelines (a) IEC 61400-27-1 Simulink implementation, (b) WECC second generation MATLAB code

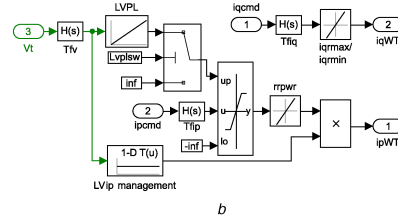
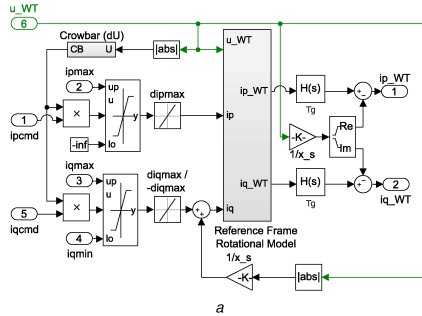


Fig. 6 Simulink implementation of the Type 3 generator systems defined by both international guidelines (a) IEC 61400-27-1, (b) WECC second generation

e.g. 100 s), while the WECC model uses a predefined value (V_{ref0}).

Another important difference regarding the reactive power control system, which also affects the behaviour of active power and CLSs, is that the IEC model uses the voltage profile defined as the input to the system (u_{WT}) in order to calculate, for example, the reactive power injected during the voltage dip. In contrast, the WECC model uses the voltage in the high-voltage (HV) terminal of the transformer (V_t) to conduct these operations. This voltage V_t is calculated as the voltage in a point which is located using the serial impedance from the WT terminal (typically a transformer). This means that, during the dip, due to the reactive power injection and low active power consumption, $V_t > u_{WT}$, and hence, parameters such as K_{qv} (used to calculate the reactive power proportional to the dip depth that should be injected during the fault) have to be adjusted using different values in both models to obtain the same response. For the current work

- $K_{qv, IEC} = 0.55$ pu.
- $K_{qv, WECC} = 0.60$ pu.

Finally, as commented in Section 1, the IEC model implements a dynamic reactive power limitation system. The signals q_{WT_max} and q_{WT_min} , which can be seen in Fig. 4a, are obtained from this limitation system. Both signals are calculated by use of the minimum value between two look-up tables, dependent on the u_{WT}/V_t and the active power provided P_{WT}/P_e . The WECC model uses static limiters, as shown in Fig. 4b.

3.3 Current limitation system

The Simulink implementation of the Type 3 CLS from IEC 61400-27-1 is shown in Fig. 5a, while the logic followed by the WECC guideline is depicted in the MATLAB code shown in

Fig. 5b. The behaviour of both systems regarding the maximum current which can be provided by the WT follows the logic defined in the WECC report [8], shown in Fig. 5b. In the IEC system, parameter Mq_pri is equivalent to flag $PqFlag$; which is used for selecting active or reactive current priority. However, in the IEC model, this priority is only set during faults (Mq_pri is multiplied by F_UVVRT), while in steady state the priority is always set to active power.

During faults, the IEC system allows modification of the maximum current which can be injected by the WT, using the definition of the parameter i_max_dip (during a fault, the maximum current is usually smaller). Moreover, by using parameter M_DFS_lim (found in the highlighted square of Fig. 5a), this model allows the maximum active current ip_max to be multiplied by the rotational speed of the generator ω_gen , which is equivalent to limiting the total current ($M_DFS_lim = 0$) or the stator current ($M_DFS_lim = 1$). Finally, the maximum reactive current can also be defined by the partial derivative of reactive current limit versus voltage $Kpqu$ (i.e. the IEC model allows the maximum reactive current to be controlled depending on the voltage level). These three considerations are not included in the WECC model, and thus, the control of the current injected during the fault can be more accurately adjusted in the IEC model, despite the larger number of parameters used. There can also exist differences because of the use of u_{WT} or V_t as input of the look-up tables, as previously commented in Section 3.2.

3.4 Type 3 generator system

The Simulink implementation of the Type 3 generator systems from IEC and WECC is shown in Figs. 6a and b, respectively. The WECC generator system is a simplification of the IEC system, which is based on [24, 41]. In the WECC approach, the current command signals are only filtered and saturated. However, after

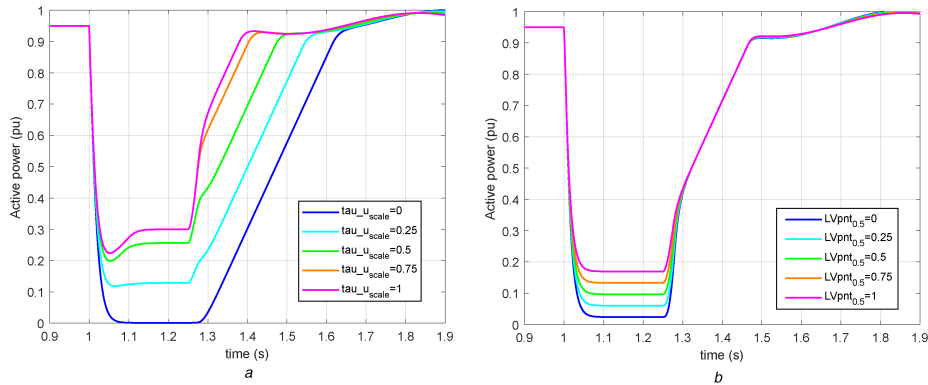


Fig. 7 Active power response during a fault
(a) IEC 61400-27-1 Type 3: τ_{u_scale} variation, **(b)** WECC Type 3: LV_{pmt} variation

these operations in the IEC approach, the voltage terminals are coordinated to the grid (*reference frame rotational model*), and the dynamics of the generator reactance are considered (x_s) [37], describing the impact of the rotor flux derivative. The addition of this component allows a better control of the transient behaviour when the fault occurs. Moreover, the IEC generator system considers the crowbar (CB) protection system, which is a conventional technology used to avoid the disconnection of the WT during the voltage dip [26, 42]. This system actuates when the variation of the voltage is larger than a threshold, and multiplies by 0 the currents over a certain period of time.

The WECC generator system includes transient control systems such as a *low-voltage (LV) active current management*, which has been modelled as a look-up table (*LVip management* in Fig. 6b) or the *LV power logic* (LVPL) system, conventionally used by WTs during faults. Furthermore, the WECC generator system also features HV reactive current management, but since no HV case is considered in this work, it is not included here. These managing systems are detailed in [43]. Finally, the active and the reactive powers injected to the grid are calculated as usual, using the equation below:

$$P_{WT} + jQ_{WT} = (ip_{WT} + j \times iq_{WT})ul_{WT} \quad (2)$$

It is important to emphasise that the reactive power should be considered with capacitive sign convention, and all the systems are modelled following this reference. Reactive currents and reactive power have the same sign convention. It is considered that the reactive current follows the equation below::

$$iq_{WT} = -\text{Im}(\bar{i}_{WT}) \quad (3)$$

4 Generic Type 3 simulation results

Simulations were carried out in order to identify the different features that both generic model approaches offer. First, the differences in the active power response are analysed, which are mainly due to the differences in the control approaches described in Section 3.1. Furthermore, the consequences of the different perspectives in the response of the pitch angle are analysed, as well as the action of the CB protection system. Then, the influences of the different implementations of the electrical generator system are studied for the reactive power behaviour. Finally, the benefits of the WECC perspective regarding simplicity are studied.

4.1 Active power response

First, the consequences of the different torque control behaviours during the fault are shown in Fig. 7. The simulation carried out consisted of a voltage dip with a residual voltage of 0.5 pu and a duration of 200 ms. For the IEC model (Fig. 7a), the active power value during the voltage dip depends on the voltage depth and the

parameter τ_{u_scale} , as described in Section 3.1. Depending on the value of τ_{u_scale} , the output of torque PI system (Fig. 3a) during the fault is calculated. For the cases, in which $\tau_{u_scale} = \{0; 0.25; 0.5\}$, the active power is limited by torque PI system, whereas for the cases $\tau_{u_scale} = \{0.75; 1\}$ the active power is limited by the CLS. For these last two cases, it can be seen that the value of τ_{u_scale} modifies the value from which the active power recovers its steady-state value at nominal rate. The time at which this occurs is the same for all cases, but since the value from which the recovery begins is different, the time needed to reach the steady state varies. The active power control system of the WECC model contains no system that can control the value of torque during the fault (Fig. 7b). Moreover, the torque value during the fault is frozen, and thus does not decrease as for the IEC model. The only way provided by the WECC guidelines to modify the value during the fault is the *LV active current management* system included in the *generator system* (Fig. 6b). However, as shown in Fig. 7b, this system does not provide such complete control as the IEC model, since it only modifies the active power value during the fault, but the recovery is equal for all cases.

Additionally, this electromagnetic torque control involves a different behaviour in the *pitch control* system, shown in Fig. 8. The *pitch control* model is depicted in detail in [27]. It is composed of two PI controllers, which depend on the rotational speed error (ϵ_ω – between ω_{WTR}/ω_r and ω_{ref}) and the active power error (ϵ_c – between p_{ord}/P_{ord} and $p_{WT.ref}/P_{ref0}$). However, both guidelines consider the possibility of using a cross-coupling gain K_{PX}/K_{cc} , which is used to add the active power error to the rotational speed error, and hence uses only one PI controller, which is the case considered in this work. In this sense, the use of only one PI controller avoids certain coordination issues. The difference in the behaviour of the torque controller in both guidelines has an influence on ϵ_c . The signals p_{ord}/P_{ord} , as shown in Fig. 2, are directly calculated by multiplying the torque by the rotational speed of the generator. Hence, for the IEC model, p_{ord} decreases to a value dependent on τ_{u_scale} , whereas P_{ord} (WECC approach) is maintained constant (except for the oscillations after the fault). Then, for the IEC model, ϵ_c is negative during the fault, which causes a decrease in pitch angle. Under the assumption that the WT is working at partial load (i.e. pitch angle is 0°, which means that the electric power is equal to the wind power absorbed by the blades), what is obtained is a delay in the time at which the pitch angle starts to increase. This is shown in Fig. 8a. The simulation conducted consisted of a voltage dip with a residual voltage of 0.5 pu and a duration of 500 ms. The delay can be controlled by adjusting K_{PX} , which controls the proportion of ϵ_c in the input error to the pitch PI controller. This variation of pitch angle has an important influence in the rotational speed of the WT, which needs

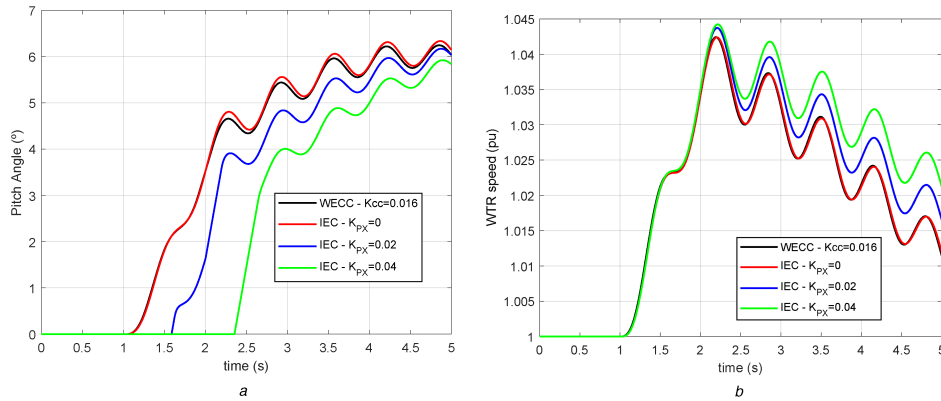


Fig. 8 Influence of torque control implementation in the pitch angle and rotor speed
(a) Modification of pitch response due to torque control, (b) Influence of pitch variation in rotor speed

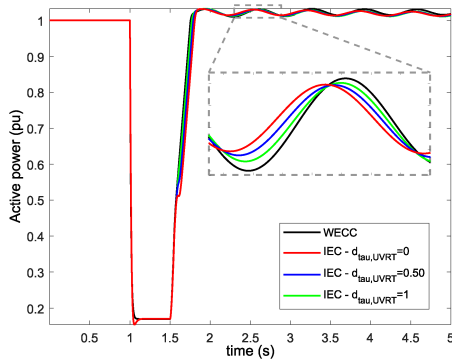


Fig. 9 Voltage post-fault control ($M_p_UVRT = 1$) varying d_{τ_UVRT}

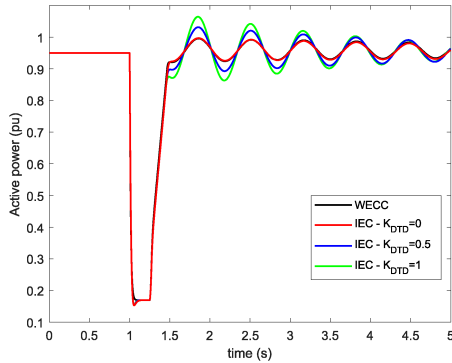


Fig. 10 Control of oscillations by the active DTD system

more time to recover the steady-state condition, as shown in Fig. 8b.

Regarding the control of the active power during the post-fault period, Fig. 9 shows the voltage post-fault control mode provided by the IEC model by adjusting the parameter $M_p_UVRT = 1$. This control mode freezes the output of torque PI control system for a certain time T_{DVS} , set to 0.1 s for this study. During this time, the output of torque PI system takes the value y_reset (Fig. 3a). When the fault is cleared, u_{WT} recovers the value 1 pu, and thus, the value of y_reset tends to increase. During T_{DVS} , this rise will depend on the maximum rate defined by the parameter d_{τ_UVRT} . As shown in Fig. 9, the adjustment of this parameter allows the active power

behaviour to be controlled after the fault. Furthermore, as shown in the zoom included in Fig. 9, with the variation of this parameter, the mechanical oscillations phase can be modified. The frequency of these oscillations is calculated according to (4) [7]. From the value $d_{\tau_UVRT} = 0$ to $d_{\tau_UVRT} = 1$, the phase is modified by 28.45° . WECC system (black colour in Fig. 9) does not provide any similar post-fault control mode, and the active power increases at a constant ramp rate. As d_{τ_UVRT} increases, the behaviour of the IEC model approximates to that of the WECC

$$\omega_{osc} = \sqrt{k_{dt} \times \left(\frac{1}{2H_{WTR}} + \frac{1}{2H_{gen}} \right)} \quad (4)$$

$$= \sqrt{237.7854 \text{ pu} \left(\frac{1}{2 \times 10 \text{ s}} + \frac{1}{2 \times 1.5 \text{ s}} \right)} = 9.5473 \text{ rad/s}$$

Moreover, not only can the oscillation phase be more accurately adjusted by the IEC model, but also its magnitude. For the WECC approach, this behaviour depends only on the dynamics of the two-mass model. However, as explained in Section 3, the *active power control* of the IEC model includes the active drive train damping (DTD) system, which is able to control the amplitude, as shown in Fig. 10 (the black signal – WECC – coincides with the red one – IEC $K_{DTD} = 0$). As a consequence, due to the capability of controlling the phase and the magnitude of the mechanical oscillations during the post-fault period, the IEC model presents further options of flexibility and adaptability.

Finally, Fig. 11 shows the influence of the CB system included in the IEC electrical generator system. The WECC curve coincides with that of the IEC without CB. Since the operation of the CB system consists of multiplying the active current commanded by the control system (i_{p_cmd}) by zero, the active power consequently decreases. The CB system depends on the variation of the voltage, defining the time which is activated by adjusting the positive and negative thresholds (i.e. it is possible to define if it only actuates when the fault occurs and/or is cleared, as well as for how long it is activated). From Fig. 11, it can also be observed that the oscillation phase is also modified by the CB system.

4.2 Reactive power response

Since both (IEC and WECC) reactive power control systems are similar, and the control mode after the fault is defined in the same way, the differences related to reactive power response are mainly due to the electrical generator system.

First, the influence of including the dynamics of the electrical generator reactance (x_s in Fig. 6a) on the reactive power response is studied (Fig. 12). For all the simulation cases conducted in this section, the voltage dip was defined with a depth of 0.5 pu and a duration of 500 ms, and the CB system is deactivated. Moreover, the voltage angle is kept as 0 during the simulation (i.e.

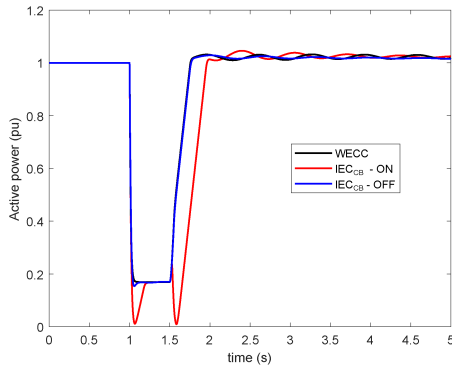


Fig. 11 Influence of the CB system in the active power response

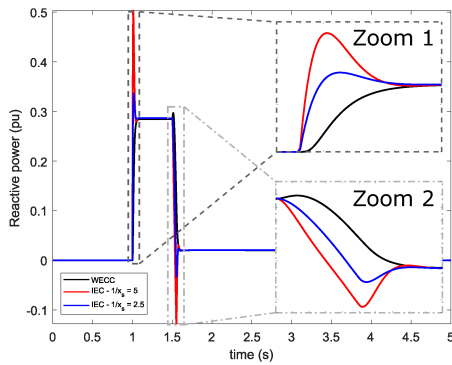


Fig. 12 Influence of the parameter x_s on the reactive power response

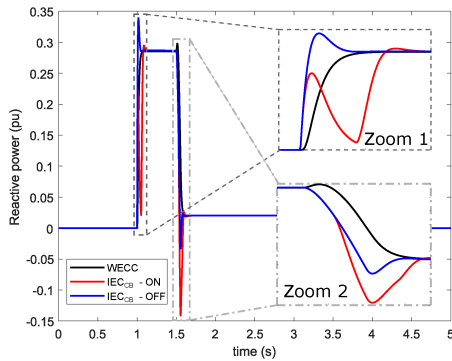


Fig. 13 Influence of the CB system on the reactive power response

$\text{abs}(u_{WT}) = \text{Re}(u_{WT})$). As shown in Fig. 6a, both these magnitudes are multiplied by $1/x_s$ and then added before and after the filter which models the dynamics of the converter. This causes a delay between the two additions, causing the peaks shown in Fig. 12, which are zoomed before and after the fault (Zoom 1 and Zoom 2). The values $x_s = \{0.2, 0.4\}$ are representative of real values of a WT. A method which can be used to estimate this parameter is found in [41].

Additionally, the behaviour of the CB system complements this control of the reactive power peaks. The influence of this protection system is shown in Fig. 13, in which the parameter $1/x_s = 2.5$ for this case. On the one hand, when the fault occurs (Zoom 1), the CB system actuates countering the peak, since it multiplies by zero the commanded reactive current. In fact, the

adjustment of the parameters of the CB system, as well as x_s , allows a flexible control of these peaks, which is not possible with the WECC system. On the other hand, when the fault is cleared (Zoom 2), the negative value of the peak is accentuated by the cancellation of the reactive current command signal. Indeed, the WECC model is unable to model this behaviour, and as shown in Fig. 13, the rise and fall are commanded by the control system, which results in uncontrolled peaks in transient periods. Real WT's reactive power responses do not show the peaks modelled by the WECC model, but they are highly similar to the IEC behaviour [32].

4.3 Complexity and simulation time

As explained in Section 1, IEC and WECC modelling approaches focus on different aspects. While the IEC centres on accuracy and better emulation of transient periods, the WECC guidelines focus on reducing the number of parameters and the simulation time. Since the greater flexibility of the IEC model has been clearly illustrated by the previous results, the authors also tested the advantages of the simplicity of the WECC model.

First, the number of parameters and Simulink blocks were calculated using the MATLAB command `sldiagnostics`. If blocks such as input or 'go to' blocks (which do not contribute to the complexity of the model) are disregarded, the IEC model is defined by ~ 100 parameters and 435 Simulink blocks. The WECC model is defined by ~ 75 parameters and 260 Simulink blocks. Thus, one of the objectives of the WECC model is achieved, since the definition and modelling of its model is simpler than the IEC approach.

Concerning the simulation time, which is highly related to the complexity of the model, the authors ran simulations of 5 s of a voltage dip of 500 ms of duration and 0.5 pu of depth. Two different tests were conducted with each modelling approach (IEC and WECC): (i) 500 simulations of one WT, (ii) 250 simulations of ten WTs. The simulations were carried out using the fixed-step solver `ode4` (Runge-Kutta) and with a step size of 1 ms. The computer used is equipped with an Intel(R) Core(TM) i7-4720HQ central processing unit, working at 2.60 GHz, 8 GB of random access memory, and running in a 64 bits operational system. Box plots are used to summarise the simulation duration results, see Fig. 14. It can be observed in both tests that the time used by the IEC model doubles the time of the WECC model. Hence, this constitutes an important limitation of the IEC model, which needs larger computational resources.

Regarding the extra accuracy provided by the IEC model, the cases, in which it is most important are the transient periods. However, most of the validation methods, and even the IEC validation method itself, disregard these transient periods [44], assuming the inability of the generic models when modelling certain behaviours. When the fault occurs, according to IEC 61400-27-1 [7], the mean absolute error and the maximum error should not be calculated during the first 140 ms. This is due to the limitation of replicating the DC-component of the generator flux by the model. Moreover, when the fault is cleared, the maximum error should not be calculated within the first 500 ms. During this period, the reactive power is affected by the transformer inrush, whereas the active power may be modified by aerodynamic and mechanical fluctuations. Thus, as shown in the simulations, most of the periods, in which the differences between the two international guidelines are larger are dismissed by this validation methodology. Hence, stakeholders should assess their particular needs in order to prioritise the simulation time or the accuracy.

5 Conclusions

This work has provided a better understanding of the generic Type 3 (DFIG) WT models under development by international organisations. In February 2015, the IEC published the Standard IEC 61400-27-1, and in January 2014, the WECC published the WECC Second Generation WT Models. Both of these documents define generic WT models, which can be adapted to any specific vendor model by adjusting a limited number of parameters.

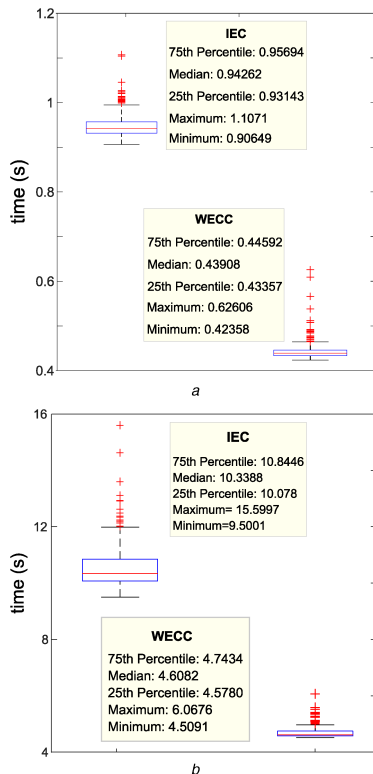


Fig. 14 Comparison of simulation times
(a) Boxplot of simulation times for test 1, (b) Boxplot of simulation times for test 2

Although both international guidelines were developed in conjunction, as they focus on different aspects (simplicity versus exact representation of faults), the implementations differ. Type 3 represents what is currently the most conventional technology, and this model is the most complex of the four types in both organisations. In this work, the generic Type 3 models, developed following the guidelines provided by both Committees, were implemented in MATLAB/Simulink, and adjusted in order to provide the most similar response. First, the general structure of both models is described, highlighting the main similarities and differences. Then, the systems that most differ between both modelling approaches are analysed. The active power control system is one of the most different models, with the IEC being more flexible in the modelling of fault and post-fault responses. Regarding the reactive power control, the main differences are a result of the different control logics of the models. The behaviour of the CLS is similar during the voltage dip. However, the IEC system includes more conditions when providing the maximum and minimum current. Finally, the generator system described by WECC is modelled by first-order filters and saturation blocks, while the IEC system is more complex and includes the dynamics of the electrical generator reactance, as well as the grid voltage coordination. However, the WECC model includes LVPL and active current management systems, providing some flexibility as well.

As a consequence, on the one hand, the generic IEC 61400-27-1 Type 3 model is more complex than the WECC model. It includes systems such as the active DTD in active power control, the CB protection system in the generator model and even a dynamic reactive power limiter control system, which result in a more accurate response when compared with the field response of real WTs, due to the higher transient response control. Moreover, the IEC approach represents the WT model in a more open manner,

without being linked to any specific software (such as GE PSLF™ and Siemens PTI PSS®E). On the other hand, the WECC model needs fewer parameters and blocks for its definition and modelling than the IEC model. This leads to the simulation time of the WECC model being approximately more than 50% smaller than that of the IEC model.

Finally, while the IEC model can adapt its response to that of the WECC by the adjustment of its parameters, conversely it is impossible for the WECC system to emulate certain behaviours. Nevertheless, the need to include specific systems such as that previously mentioned, has been rejected by the WECC committee, because they consider they do not significantly affect the behaviour of the WT response, and complicate the model unnecessarily. Additionally, most of the differences in the model response occur during the transient periods, which may be dismissed for some studies (e.g. the IEC validation methodology itself disregards some time windows during transient periods). Thus, as both committees decided to set a different focus, the stakeholders (researchers, WT manufacturers, DSOs, TSOs, ...) implementing these models should decide about their highest concern: accuracy or simplicity.

In summary, this paper has shown the differences between the generic Type 3 WT models developed by IEC and WECC, as well as the consequences of the different focus of each guideline. It has been shown that both these models can provide comparable responses of active and reactive powers, and hence, projects which have used different models can be coordinated to obtain similar results. However, depending on the study to be conducted, the more flexible control systems provided by the IEC model may be necessary. For cases that do not require modelling transient periods, the simplicity of the WECC model can be used in advance since lower computational resources are needed. Finally, the different focus of each entity constitutes a clear advantage for stakeholders, who can choose the model that best fits their needs.

6 Acknowledgments

This work was supported by the 'Ministerio de Economía y Competitividad' and European Union FEDER, which supported this work under project ENE2016-78214-C2-1-R. This work has received funding from the Agreement signed between the UCLM and the Council of Albacete to foster the Research in the Campus of Albacete

7 References

- [1] Basit, A., Hansen, A.D., Altin, M., *et al.*: 'Wind power integration into the automatic generation control of power systems with large-scale wind power', *J. Eng.*, 2014, **2014**, (10), pp. 538-545. Available at: <http://digital-library.theiet.org/content/journals/10.1049/joe.2014.0222>, accessed 21 February 2019
- [2] Hu, J., Huang, Y., Wang, D., *et al.*: 'Modeling of grid-connected DFIG-based wind turbines for dc-link voltage stability analysis', *IEEE Trans. Sustain. Energy*, 2015, **6**, (4), pp. 1325-1336
- [3] Prajapat, G.P., Senroy, N., Kar, I.N.: 'Wind turbine structural modeling consideration for dynamic studies of DFIG based system', *IEEE Trans. Sustain. Energy*, 2017, **8**, (4), pp. 1463-1472
- [4] Hu, Y.L., Wu, Y.K.: 'Comparative analysis of generic and complex models of the type-3 wind turbine'. 2016 IEEE PES Asia-Pacific Power and Energy Engineering Conf. (APPEEC), Xi'an, China, 2016, pp. 392-396
- [5] Honrubia-Escribano, A., Jiménez-Buendía, F., Molina-García, A., *et al.*: 'Analysis of wind turbine simulation models: assessment of simplified versus complete methodologies'. XVII Int. Symp. Electromagnetic Fields in Mechatronics, Electrical and Electronic Engineering, Valencia, Spain, 2015, p. 8
- [6] Aziz, A., Amanullah, M., Vinayagam, A., *et al.*: 'Modelling and comparison of generic type 4 WTG with EMT type 4 WTG model'. 2015 Annual IEEE India Conf. (INDICON), New Delhi, India, 2015, pp. 1-6
- [7] International Electrotechnical Commission: 'IEC 61400-27-1: electrical simulation models for wind power generation - wind turbines', 2015
- [8] WECC REMTF: 'WECC second generation of wind turbine models' (WECC, USA, 2014)
- [9] WECC: 'WECC first generation of wind turbine models' (WECC, USA, 2010)
- [10] Sørensen, P.: 'Introduction to IEC 61400-27. Electrical simulation models for wind power generation'. EERA Workshop on Generic Electric Models for Wind Power, Amsterdam, Netherlands, 2012
- [11] Honrubia-Escribano, A., Gómez-Lázaro, E., Viguera-Rodríguez, A., *et al.*: 'Assessment of DFIG simplified model parameters using field test data'. IEEE Symp. Power Electronics & Machines for Wind Application, Denver, USA, 2012, pp. 1-7

- [12] Cristina-Vázquez-Hernández, T.T., Pradas, A.V.: 'JRC wind energy status report 2016 edition'. Market, technology and regulatory aspects of wind energy. JRC Science for policy report, 2017
- [13] Pourbeik, P.: 'Proposed changes to the WECC WT3 generic model for type 3 wind turbine generators' (Electric Power Research Institute, USA, 2014)
- [14] Behnke, M., Ellis, A., Kazachkov, Y., et al.: 'Development and validation of WECC variable speed wind turbine dynamic models for grid integration studies'. AWEA WindPower Conf., Los Angeles, USA, 2007, p. 5
- [15] Fortmann, J., Sørensen, P.: 'IEC work on modelling – generic model development. IEC 61400-27 – expected outcome', 2011
- [16] Sørensen, P., Andersen, B., Fortmann, J., et al.: 'Overview, status and outline of the new IEC 61400-27 – electrical simulation models for wind power generation'. Tenth Int. Workshop on Large-Scale Integration of Wind Power into Power Systems as well as on Transmission Networks for Offshore Wind Power Farms, Aarhus, Denmark, 2011, p. 6
- [17] Sørensen, P., Andersen, B., Bech, J., et al.: 'Progress in IEC 61400 – 27. Electrical simulation models for wind power generation'. 11th Int. Workshop on Large-Scale Integration of Wind Power into Power Systems as well as on Transmission Networks for Offshore Wind Power Farms, Lisbon, Portugal, 2012, p. 7
- [18] Asmine, M., Brochu, J., Fortmann, J., et al.: 'Model validation for wind turbine generator models', *IEEE Trans. Power Syst.*, 2011, **26**, (3), pp. 1769–1782
- [19] Keung, P.K., Kazachkov, Y., Senthil, J.: 'Generic models of wind turbines for power system stability studies'. IET Conf. Proc., London, UK, 2009, pp. 128–128(1). Available at: <http://digital-library.theiet.org/content/conferences/10.1049/cp.2009.1785>, accessed 21 February 2019
- [20] Ellis, A., Kazachkov, Y., Muljadi, E., et al.: 'Description and technical specifications for generic WTG models – a status report'. IEEE/PES Power Systems Conf. Exposition (PSC), Phoenix, USA, 2011, pp. 1–8
- [21] Pourbeik, P.: 'Proposed changes to the WECC WT3 generic model for type 3 wind turbine generators' (Electric Power Research Institute, USA, 2012)
- [22] Pourbeik, P., Ellis, A., Sanchez-Gasca, J., et al.: 'Generic stability models for types 3 & 4 wind turbine generators for WECC'. IEEE Power and Energy Society General Meeting, Vancouver, Canada, 2013, pp. 1–5
- [23] Sørensen, P., Andresen, B., Fortmann, J., et al.: 'Modular structure of wind turbine models in IEC 61400-27-1'. IEEE Power and Energy Society General Meeting, Vancouver, Canada, 2013, pp. 1–5
- [24] Fortmann, J., Engelhardt, S., Kretschmann, J., et al.: 'New generic model of DFIG-based wind turbines for RMS-type simulation', *IEEE Trans. Energy Convers.*, 2014, **29**, (1), pp. 110–118
- [25] Sørensen, P., Fortmann, J., Jiménez-Buendía, F., et al.: 'Final draft international standard IEC 61400-27-1. Electrical simulation models of wind turbines'. 13th Wind Integration Workshop, Berlin, Germany, 2014, p. 5
- [26] Honrubia-Escribano, A., Gómez-Lázaro, E., Fortmann, J., et al.: 'Generic dynamic wind turbine models for power system stability analysis: a comprehensive review', *Renew. Sustain. Energy Rev.*, 2018, **81**, pp. 1939–1952
- [27] Lorenzo-Bonache, A., Honrubia-Escribano, A., Jiménez-Buendía, F., et al.: 'Generic type 3 wind turbine model based on IEC 61400-27-1: parameter analysis and transient response under voltage dips', *Energies*, 2017, **10**, (9), p. 23
- [28] Lorenzo-Bonache, A., Villena-Ruiz, R., Honrubia-Escribano, A., et al.: 'Operation of active and reactive control systems of a generic Type 3 WT model'. IEEE Int. Conf. Compatibility, Power Electronics and Power Engineering, Cádiz, Spain, 2017
- [29] Ellis, A., Pourbeik, P., Sanchez-Gasca, J.J., et al.: 'Generic wind turbine generator models for WECC – a second status report'. IEEE Power and Energy Society General Meeting, Denver, USA, 2015, pp. 1–5
- [30] Richwine, M.P., Sanchez-Gasca, J.J., Miller, N.W.: 'Validation of a second generation type 3 generic wind model'. IEEE Power Energy Society General Meeting, Washington DC, USA, 2014, pp. 1–4
- [31] Honrubia-Escribano, A., Jiménez-Buendía, F., Gómez-Lázaro, E., et al.: 'Validation of generic models for variable speed operation wind turbines following the recent guidelines issued by IEC 61400-27', *Energies*, 2016, **9**
- [32] Honrubia-Escribano, A., Jiménez-Buendía, F., Gomez-Lázaro, E., et al.: 'Field validation of a standard type 3 wind turbine model for power system stability, according to the requirements imposed by IEC 61400-27-1', *IEEE Trans. Energy Convers.*, 2017, **PP**, (99), p. 1
- [33] Lorenzo-Bonache, A., Honrubia-Escribano, A., Jimenez, F., et al.: 'Field validation of generic type 4 wind turbine models based on IEC and WECC guidelines', *IEEE Trans. Energy Convers.*, 2018, p. 1
- [34] Göksu, Ö., Altin, M., Fortmann, J., et al.: 'Field validation of IEC 61400-27-1 wind generation type 3 model with plant power factor controller', *IEEE Trans. Energy Convers.*, 2016, **31**, (99), pp. 1170–1178
- [35] Pourbeik, P., Etzel, N., Wang, S.: 'Model validation of large wind power plants through field testing', *IEEE Trans. Sustain. Energy*, 2017, **9**, pp. 1212–1219
- [36] Göksu, Ö., Sørensen, P., Morales, A., et al.: 'Compatibility of IEC 61400-27-1 Ed 1 and WECC 2nd generation wind turbine models'. 15th Wind Integration Workshop, Vienna, Austria, 2016
- [37] Lorenzo-Bonache, A., Villena-Ruiz, R., Honrubia-Escribano, A., et al.: 'Comparison of a standard type 3B WT model with a commercial build-in model'. IEEE Int. Electric Machines & Drives Conf., Miami, USA, 2017
- [38] WECC REMTF: 'WECC second generation of wind turbines models guidelines' (WECC, USA, 2014)
- [39] Pourbeik, P., Sánchez-Gasca, J.J., Senthil, J., et al.: 'Value and limitations of the positive sequence generic models of renewable energy systems', This is a brief white-paper prepared by an Ad hoc group within the WECC Renewable Energy Modeling Task Force, 2015
- [40] Pourbeik, P.: 'Model user guide for generic renewable energy system models' (Electric Power Research Institute, USA, 2015)
- [41] Fortmann, J.: 'Modeling of wind turbines with doubly fed generator system' (Department for Electrical Power Systems, University of Duisburg-Essen, 2014)
- [42] Jiménez-Buendía, F., Barrasa-Gordo, B.: 'Generic simplified simulation model for DFIG with active crowbar'. 11th Wind Integration Workshop, Lisbon, Portugal, 2012, p. 6
- [43] WECC REMTF: 'WECC wind power plant dynamic modeling guidelines' (WECC, USA, 2014)
- [44] Li, Q., He, J., Qin, S., et al.: 'Wind turbine model validation based on state interval and error calculation', *J. Eng.*, 2017, **2017**, pp. 762–767. Available at: <http://digital-library.theiet.org/content/journals/10.1049/joe.2017.0434>, accessed 21 February 2019

4.1.3. Paper III - Type 4 Validation

Paper III presents a validation study for the IEC and WECC generic Type 4 model. It is based on 10 different test cases obtained from a real FC WT. The four magnitudes of active and reactive currents and power are validated for the two generic models, dealing with a total of 320 error magnitudes. Not only the accuracy with respect to field data is studied, but also the performance obtained with each model. Additionally to the errors calculation, specific behaviors that cannot be emulated by the generic models are addressed as well.

The objective of this work is to conduct the first conjoined IEC and WECC generic Type 4 model validation work following the IEC 61400-27-1 guidelines, assessing their accuracy and comparing their performance.

The metrics of the indexed journal in which the paper was published is shown in Table 4.3. The paper is currently in-press status (publication in a future issue of the journal). The accepted version of the paper is included below.

Table 4.3: Journal Metrics – Paper III.

Journal Name	IEEE Transactions on Energy Conversion
Impact Factor (2017)	3.767
Category	Engineering, Electrical & Electronic
Quartile in category	Q1
Position in category	43/260
ISSN	0885-8969

Field Validation of Generic Type 4 Wind Turbine Models Based on IEC and WECC Guidelines

A. Lorenzo-Bonache, A. Honrubia-Escribano, F. Jiménez-Buendía, E. Gómez-Lázaro, *Senior Member, IEEE*

Abstract—The generic wind turbine models developed in recent years by the International Electrotechnical Commission (IEC) and the Western Electricity Coordinated Council (WECC) are intended to meet the needs of public, standard, and relatively simple (small number of parameters and computational requirements) wind turbine and wind farm models used to conduct transient stability analysis. Moreover, the full-scale converter (FSC) wind turbine technology referred to as Type 4 by IEC and WECC, is increasingly used in current power systems due to its control benefits. Hence, the development of this generic model has become a priority.

This study presents the validation of two generic Type 4 wind turbine models, which have been developed in accordance with the IEC and WECC guidelines, respectively. Field data collected from a real wind turbine located in a Spanish wind farm was used to validate both generic Type 4 wind turbine models following the IEC validation guidelines. Ten different test cases are considered, varying not only the depth and duration of the faults but also the load of the wind turbine. The parameters of the models were kept constant for all the simulation cases, aiming to evaluate the accuracy of the models when facing different voltage dips.

Index Terms—Full-scale converter, Generic model, IEC 61400-27, Power system stability, Type 4, WECC, Wind turbine.

I. INTRODUCTION

FOR MANY YEARS, power system operators have had to deal with the lack of wind turbine (WT) and wind farm (WF) models adapted to their needs. Each WT model is usually provided by the manufacturer, and is defined to cover its own needs, but not to conduct transient stability analysis of large networks, as required by TSOs and DSOs (transmission and distribution system operators, respectively). Moreover, these vendor models are usually confidential [1], complex, and specifically defined for each WT configuration. These characteristics present a major problem for power system operators who have to work with a huge amount of information to perform their power system studies.

To contribute to the integration of wind energy into power systems, and aiming to solve these issues, the International Electrotechnical Commission (IEC) and the Western Electricity Coordinating Council (WECC) have developed generic, also known as standard or simplified, wind turbine and wind farm models [2]. These models are intended to be public, are defined by a limited number of parameters, are easily implemented in any simulation software, and use relatively low computational resources. These two organizations classify the

different topologies of WTs in four types, mainly according to the electrical generator [3]. In 2009, the IEC started to develop generic WT models, publishing the first Edition of the IEC 61400-27-1 in February 2015 [4]. This edition described the four WT model types [5], omitting the WF modeling for the 27-2, currently under development. The WECC guidelines were firstly published in 2010 [6], and included the modeling of WTs and WFs. However, as their response was unsatisfactory [7], the “Second Generation of Wind Turbine Models” [8] was released in 2014. These two organizations aim to provide generic models of WT and WF, which can emulate any vendor topology, and which can be used to perform transient stability analysis with sufficient accuracy, without the need for more complex models. In this sense, one of the most interesting fields of study is the compatibility between the generic WT models defined by the two entities. At first, both working groups developed the models in conjunction, with the assistance of a certain group of manufacturers. However, notable differences related to approaches adopted in the aim of these models have been identified. The IEC focuses on ensuring the most accurate response, while the WECC focuses on minimizing the number of parameters, as well as the simulation time. This difference in approaches has led to a number of similarities and differences between these generic models, which require further attention [9].

Under this framework, the present paper first presents the implementation of the generic Type 4 WT models defined by IEC and WECC in MATLAB/Simulink. Type 4 represents a wind turbine with full-scale converter (FSC) technology [10]. This WT configuration is now increasingly used, because it permits the possibility of not including gearbox, and due to the electrical control facilities provided by the full-scale converter [11]. The main drawback is the need for a converter sized to the WT rated power, which is more expensive than the commonly used doubly-fed induction generator (DFIG) configuration, composed of a converter rated to 25-30% of the WT rated power. In fact, the validation of a generic DFIG model was performed by the authors in [12]. Once implemented, both Type 4 models are tested in 10 different cases: 5 three-phase voltage dips when the WT is injecting its nominal power, and then 5 three-phase voltage dips with the same voltage parameters, but with the WT injecting 10-20% of its nominal power. Each pair of voltage dips is defined with different values of depth and duration. Since neither of these guidelines have developed a negative-sequence model, these models can only be tested in the case of three-phase faults [13]. Subsequently, the responses of four different magnitudes (active power, active current, reactive power, and reactive current) are compared with the real responses of a

A. Lorenzo-Bonache, A. Honrubia-Escribano and E. Gómez-Lázaro are with the Renewable Energy Research Institute and DIEEAC-EDII-AB. Universidad de Castilla-La Mancha, 02071 Albacete, Spain (email: alberto.lorenzo@uclm.es; andres.honrubia@uclm.es; emilio.gomez@uclm.es)

F. Jiménez-Buendía is with Siemens Gamesa Renewable Energy. Pamplona, Spain (email: fjimenez@gamesacorp.com)

Type 4 WT located in a Spanish wind farm (provided by the wind turbine manufacturer Siemens GAMESA). Finally, the validation method defined by the IEC is applied to the comparison of the two models with the field data. IEC 61400-27-1 has defined three categories of parameters: “*Type*”, which is specific to a WT model; “*Project*”, which is specific to the project (e.g. the control parameters to comply with a grid code); and “*Use case*”, which can be modified for each simulation (e.g. depending on the load of the WT). Since most of the WT model parameters are *Type* or *Project*, the authors prioritized keeping them constant for all study cases, guaranteeing that once the model is adjusted, it can be used for any simulation test case.

The scientific literature includes several works focused on the implementation of the IEC [14], [15] and the WECC [16], [17] generic Type 4 WT models. Furthermore, the validation of the WECC generic Type 4 WT model has been discussed in [18]–[20] (in fact, the WECC guidelines provide validation responses for their models [8]). However, the IEC generic Type 4 model validation has not been analyzed in depth, with only a few works being published before the IEC 61400-27-1 [21], [22]. Moreover, none of these includes a wide range of voltage dips or considers different operating conditions. Therefore, the present work aims to fill this gap with the following main contributions: *i*) Providing guidelines in the modeling of the generic Type 4 WT model proposed by IEC and WECC, *ii*) Testing the capability of the generic models to emulate the behavior of a real Type 4 WT facing 10 different test cases, *iii*) Studying the order of magnitude of the validation errors which should be considered when working with generic WT models, *iv*) Testing the compatibility between the models defined by the IEC and WECC when facing the same event.

Following this introduction, the paper is structured as follows: Section II presents the main characteristics and the implementation of the generic Type 4 WT model following the IEC and WECC guidelines. Section III describes the methodology followed to obtain the field measurements and the model simulations, as well as the IEC validation method. The results are then presented in Section IV. Finally, the conclusions of the paper are presented in Section V.

II. GENERIC TYPE 4 WT MODEL

The generic Type 4 WT model represents a full-scale converter WT. Both international organizations, the IEC and the WECC, subdivide Type 4 in two types, depending on the simulation of the mechanical oscillations. These oscillations mainly depend on the characteristics of the real WT. The real Type 4 WT used for this work was a full converter equipped with a brake chopper, which absorbs the excess power. Thus, pitch and speed are unaffected since the generator experiences no change in power generation. Consequently, the authors modeled a generic IEC Type 4A and a generic WECC Type 4B, which neglect the mechanical and aerodynamic parts, and thus no power oscillations are simulated.

The modular structure of a generic Type 4 WT is shown in Fig. 1. Both Type 4 models include a *Control System* (CS), which comprises the control systems shown in Fig. 1 (*Reactive*

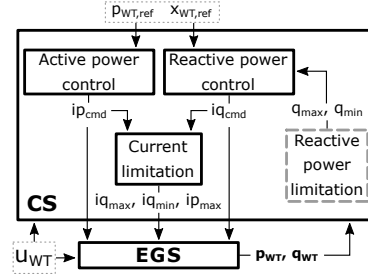


Fig. 1. Modular structure of a generic Type 4 WT.

power limitation system is only included in the IEC model). These systems provide both an active and a reactive current command signal ($i_{p,cmd}$ and $i_{q,cmd}$, respectively), which are the main inputs to the *Electrical Generator System* (EGS), as well as the active and reactive current limits. The CS actuates following the active and reactive power references ($p_{WT,ref}$ and $x_{WT,ref}$, respectively), which are set manually. The wind turbine terminal (WTT) voltage (u_{WT}), defined as the profile of its module and angle, is an input to the CS and the EGS. Finally, the EGS provides the responses of active and reactive currents and power. In the present paper, $p_{WT,ref}$ is defined by measuring the steady-state value from the real WT. With regard to the reactive power, three different control modes can be selected: voltage in the WTT, reactive power injected, or power factor. For this work, the reactive power injected is directly controlled, the value being set in the same way as that of the active power. In this sense, this behavior is followed by the real WT during steady or dynamic state (no voltage dip operation).

Since the present paper analyzes the behavior of a real WT facing voltage dips, the transient control strategies used by the models are described as follows. Regarding reactive power transient control, the main scheme is shown in Fig. 2. F_{UVRT} is a variable with a value of 0 during normal operation, 1 during the fault ($u_{WT} < 0.9 pu$) and 2 during a certain post-fault period. $i_{q,base}$ is the reactive current commanded by the normal operation controller. Hence, during steady-state operation, current $i_{q,cmd}$ is commanded by the current controller (i.e. $i_{q,cmd} = i_{q,base}$); during the fault it is calculated as $i_{q,base}$ plus a value proportional to the depth of the dip (T_{uss} is sufficiently large to maintain the steady-state value during the fault, e.g. 100 s), and after the fault, a constant value $i_{q,post}$ is added to $i_{q,base}$ for a certain time. The real WT follows this behavior, but the relationship between the dip depth and the current injected (Kqv) is defined as a curve, not as a constant. Furthermore, the it injects no additional reactive power during the fault ($i_{q,post} = 0$).

With regard to active power, none of the documents specifies any transient control systems in CS (WECC includes one in the EGS). This involves difficulties when modeling certain behaviors of a real WT. In the particular case of this paper, the real wind turbine includes a control system modifying the active power reference at a certain time after the dip, consisting

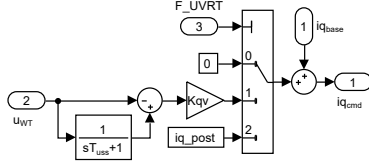


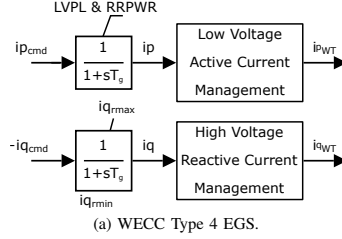
Fig. 2. Reactive power transient control system.

in recording active current just before the dip and later keeping an active current reference constant to this value during the voltage dip and 500 ms after. Then, the steps in active power performance shown in Section IV are due to this active power set point, as well as the limitation on active current due to reactive current priority during the dip and 500 ms after the voltage dip. With the aim of obtaining the most accurate response possible, the authors modeled a system similar to the one shown in Fig. 2, modifying the reference after the fault proportionally to the dip depth.

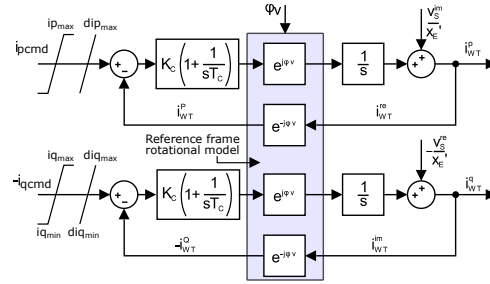
In fact, generic models should have an active control system during the faults that is proportional to voltage magnitude, since it is implemented in real WTs. This behavior is consistent with the performance required by some grid codes, such as those in the UK and Ireland, which require that active power proportional to voltage is delivered during a voltage dip. This is equivalent to freezing active current before the dip together with active power priority during the fault. The authors have considered issuing a comment to the current CDV version of the IEC 61400-27-1 (of which two of the authors are Committee members) for its consideration in Ed. 2 of the Standard.

The implementation of the Type 4 WT model following the IEC or WECC guidelines is similar because both organizations use a simple CS due to the facilities provided by full-scale converter technology. This is accentuated by the lack of mechanical model or pitch control system [23]. However, the EGS differs considerably between the two models, Fig. 3. The WECC EGS is modeled as a filtering and saturation system with the inputs provided by CS (Fig. 3a), whereas the IEC EGS is a simplification of an actual electrical generator (Fig. 3b), further explained in [24]–[26]. Hence, the IEC EGS is a more complicated system, but with higher control possibilities.

The transient control system used in EGS also differs between the two documents. As shown in Fig. 3a, the WECC model includes the *Low Voltage Active Current Management* system, which multiplies the active current by a value dependent on the dip depth. Moreover, the upper limit can also be defined by LVPL (Low Voltage Power Logic). The IEC transient control system is only included in the *Reference frame rotational model*, and allows the voltage angle (φ_v) to be filtered and/or frozen during the fault. Nevertheless, this is generally used for very severe faults (i.e. voltage under 10%, because of the difficulties of measuring the angle with low voltages), and hence is not used in this work. Active and reactive ramp limiters are implemented in the real WT as well. Nevertheless, it does not use LVPL or *Low Voltage Active Current Management* included within WECC EGS.



(a) WECC Type 4 EGS.



(b) IEC Type 3A EGS.

Fig. 3. Implementation of EGS for IEC and WECC.

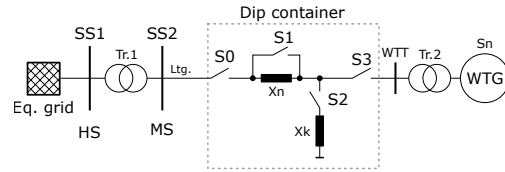


Fig. 4. Single line diagram of the FRT mobile test unit used.

III. DESCRIPTION OF THE FIELD MEASUREMENTS AND DYNAMIC MODEL SIMULATIONS

A fault ride-through (FRT) mobile test unit was connected to a wind turbine located in a Spanish wind farm to perform the field tests and measurements. The use of these devices as a tool to test the FRT capability of wind turbines connected to the power system is also found in [27]–[30].

The voltage dips were forced in the medium voltage (MV) side of the transformer Tr.2 by a dip container (Fig. 4). With the aim of decreasing the current peaks, one second before applying the fault ($t = 0.5$ s in the figures shown in Section IV), a series impedance (X_n), is connected by opening a switch (S1). To generate the voltage dip, a parallel impedance (X_k) is connected by closing switch S2 at $t = 1.5$ s. The value of this parallel impedance will affect the dip depth. Finally, one second after the fault is cleared, the series impedance is disconnected by closing switch S1. The connection and disconnection of S1 may cause perturbations in the behavior of the WT, as shown in Section IV, and can cause large maximum errors in some cases.

The FRT test unit is equipped with a current transformer and a voltage transformer connected to the MV side of the wind turbine. The measurement sampling rate was set to

TABLE I
PARAMETERS OF THE TEST CASES

Test	Depth (pu)	Duration (s)	$p_{WT,ref}$	$x_{WT,ref}$	Legend
PL1	0.65	0.62	0.15 pu		+
PL2	0.5	0.92	0.25 pu		○
PL3	0.35	1.20	0.12 pu	≈ 0 pu	*
PL4	0.2	1.70	0.15 pu		×
PL5	0.1	2.00	0.13 pu		□
FL1	0.65	0.62			◇
FL2	0.5	0.92			△
FL3	0.35	1.20	≈ 1 pu	≈ 0 pu	▷
FL4	0.2	1.70			☆
FL5	0.1	2.00			☆

10 kHz. An anti-aliasing filter of the measurement system with a cutoff frequency equal to 4.2 kHz was also implemented. The magnitudes obtained from the mobile test unit are: voltage in the WTT (u_{WT}), active current (ip_{WT}), reactive current (iq_{WT}), active power (P_{WT}), and reactive power (Q_{WT}).

The FRT mobile unit and the test procedure previously described were used to perform ten different three-phase balanced voltage dip test cases. Specifically, voltage dip depth and duration, as well as wind turbine load conditions, were taken into account for validation purposes. Table I summarizes the parameters of all the test cases, including the voltage dip parameters, as well as the active and reactive power references ($p_{WT,ref}$ and $x_{WT,ref}$, respectively). Half of the cases correspond to test cases in which the WT is operating under partial load conditions (PL), whereas in the other 5 cases the WT is operating at full load (FL). The cases for PL and FL are set in pairs (i.e. cases PLx and FLx share voltage dip parameters), as shown in Table I. Therefore, the experimental tests performed in this work allow for a comprehensive analysis of the Type 4 WT behavior when subjected to balanced power system faults.

The generic WT models based on both IEC and WECC guidelines, were modeled in MATLAB/Simulink. Following the IEC guidelines, the values of the parameters which define the behavior of the WT models (“Type” and “Project”) are maintained constant for both models and for all the simulations. Therefore, a certain error is assumed in the responses instead of a fine adjustment for each test case. This is especially relevant for each pair of cases, in which the voltage dip has the same parameters, but the active power reference drastically changes, involving a fine adjustment of the parameters (particularly those included in the *Current Limitation System*).

Following the playback validation methodology defined in IEC 61400-27-1, the measured voltage profile (u_{WT}) was directly used as input to the WT generic models, thus avoiding any uncertainty related to approximated signals. The simulations were conducted with a time step of 1 ms. Subsequently, the responses of the four signals previously mentioned, as well

as the field data, went through a filter with a cut-off frequency of 15 Hz, according to IEC 61400-27-1. Despite the validation method not being fully developed, as it will be in IEC 61400-27-2, it has already been used in certain works, such as [12], [31], [32]. The validation method was applied between the IEC-Field and WECC-Field pairs, instead of comparing the responses of both generic models. Each pair of signals for each of the four magnitudes considered is subtracted, obtaining the error signal, as shown in Eq. (1).

$$x_{err}(n) = x_{sim}(n) - x_{field}(n) \quad (1)$$

Then, three different statistic indicators are obtained: the mean error (ME - Eq. (2)), the mean absolute error (MAE - Eq. (3)), and the maximum error (MXE - Eq. (4)), where n represents each individual sample and N the total number of samples.

$$x_{ME} = \frac{\sum x_{err}(n)}{N} \quad (2)$$

$$x_{MAE} = \frac{\sum |x_{err}(n)|}{N} \quad (3)$$

$$x_{MXE} = \max(|x_{err}(n)|) \quad (4)$$

Furthermore, the IEC 61400-27-1 defines different windows during the fault to calculate these errors, which are shown in Fig. 5 and depicted in Table II. Parameters W_{fault} , $W_{faultQS}$, W_{post} , and W_{postQS} refer to the measurement windows, and are defined in the IEC 61400-27-1 as follows [4]:

- W_{fault} : Time window covering the fault period from t_{fault} to t_{clear} .
- W_{post} : Time window covering the post-fault period from t_{clear} to t_{end} .
- $W_{faultQS}$: Quasi steady state part of W_{fault} , covering from $t_{faultQS}$ to t_{clear} , where $t_{faultQS} = t_{fault} + 140$ ms
- W_{postQS} : Quasi steady state part of W_{post} , covering from $t_{clearQS}$ to t_{end} , where $t_{clearQS} = t_{clear} + 500$ ms

Where t_{fault} is the beginning of the dip, t_{clear} is the end of the dip, t_{end} is the end of measurements.

t_{fault} and t_{clear} are followed by transient time periods which cannot be appropriately simulated by fundamental frequency models. Thus, MAE during the fault and MXE during and after the fault are calculated in these quasi steady windows. The behaviors that cannot be emulated are not considered. These misbehaviors are due to the limitations when replicating events such as the DC-component of the generator flux, the transformer inrush or the non-linear aerodynamic effects.

Therefore, each validation error is obtained for each magnitude (ip_{WT} , iq_{WT} , P_{WT} and Q_{WT}), as well as for the fault and the post-fault periods.

For the present paper, the ME was dismissed as it can take either positive or negative values, which complicates the comparison between different cases. Moreover, the MAE represents a very similar magnitude, which always takes positive values. Hence, the MAE and the MXE were considered to test the validity of the generic models in this work.

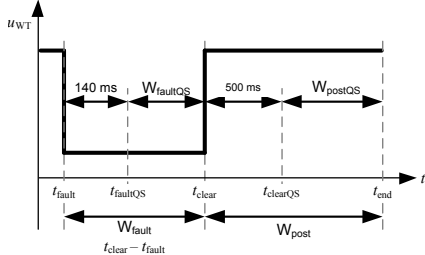


Fig. 5. Voltage dip windows.

TABLE II
WINDOWS APPLIED FOR ERROR CALCULATIONS

Period	x_{ME}	x_{MAE}	x_{MXE}
Fault	W_{fault}	$W_{faultQS}$	$W_{faultQS}$
Post-Fault	W_{post}	W_{post}	W_{postQS}

Regarding the simulation signals, the field measurements performed finished 1 s after the fault was cleared and the simulation time was set for all the test cases at 5 s. Once the field data end, the final value is kept constant until 5 s is reached. However, the validation is only conducted within the period in which there are real measurement values (i.e. $W_{postQS} = 0.5$ s).

IV. RESULTS

The results are presented in 3 parts: *i*) subsection IV-A shows the validation error distribution during the fault and the post-fault period, distinguishing between the results obtained by the IEC and WECC models; *ii*) subsection IV-B shows a statistical analysis in box plots, in which the aggregate errors of IEC and WECC models are compared with PL and FL test cases; *iii*) subsection IV-C focuses on analyzing the most relevant test case results, emphasizing those which complement the previous results.

A. IEC and WECC validation error comparison

Fig. 6 and Fig. 7 show the MAE and the MXE for all the test cases listed in Table I. The legend for these graphics is shown in the last column of Table I. For each validation error column, the left-hand symbol represents the error obtained with the IEC model, while the right-hand symbol represents the error obtained with the WECC model. For example, in Fig. 6, the MAE for active power in test case PL1 (symbol +) takes values of 0.70% and 0.80% for the IEC and WECC models, respectively. The dotted line between the validation error of both models is a visual aid, representing no further relationship. It is worth noting that both figures represent a total of 320 data.

Regarding Fig.6, the validation error obtained is very similar for the IEC and WECC generic models, except for certain cases, such as the MXE in Q and iq for PL4 (\times). For the MAE of Q and iq , a slight tendency is observed in which the

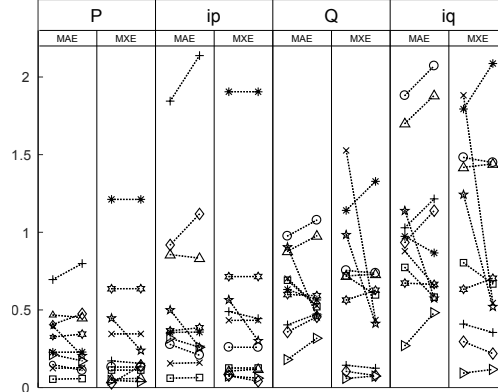


Fig. 6. Validation error distribution during fault period.

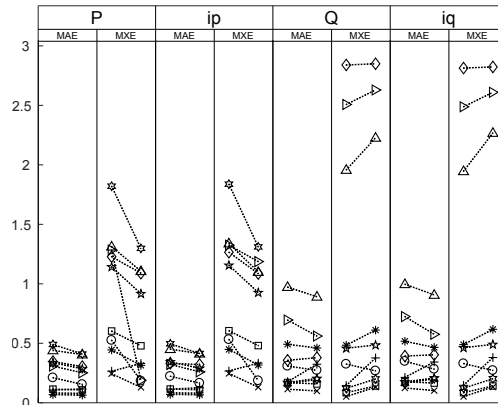


Fig. 7. Validation error distribution during post-fault period.

IEC validation error is smaller than the WECC error. During the fault period, the error between the magnitudes $P - ip$ and $Q - iq$ is related to the depth of the voltage dip, as the power magnitude is essentially the current magnitude multiplied by the voltage. Finally, it can be seen that the maximum errors during the fault period are just over 2%, as will be discussed in the following subsection.

With regard to the validation errors obtained during the post-fault period, Fig. 7, a more significant trend is observed between the errors obtained for both models. For P and ip , in most of the test cases, the MAE and MXE for the IEC generic model present higher values than the WECC model, as well as the MAE in Q and iq . In contrast, the MXE in these last two magnitudes presents higher values for the WECC model. It is also worth noting that during the post-fault period, the MXE usually takes higher values (just under 3% in some cases) than the MAE. This behavior will be discussed in depth in subsection IV-C.

B. Comparison between PL and FL test cases

In this subsection, the distribution of the validation errors of the generic models is analyzed using the box plots shown in Fig. 8 and Fig. 9. In each box, the 25th and 75th percentiles are represented by the bottom and top edges of the box respectively, while the central mark represents the median of the data. The most extreme values are represented by the extension of the whiskers, except the outliers (i.e. data which are distant from the rest), which are individually marked as '+'. In this case, the errors from the IEC and WECC models are analyzed together, as well as the group of errors which are obtained from the set of studies at partial load (PL) or full load (FL). As an example, in Fig. 8, the box of the MAE during the fault for PL studies comprises the errors obtained in tests PL1-PL5 for WECC and IEC (i.e. each box is formed by 10 samples), and the two crosses representing outlier values correspond to the MAE for test case PL1 (+), as can be observed in Fig. 6. In this sense, the authors considered only the statistics of active and reactive power, because of the relationship between current and power magnitudes explained in the previous subsection.

For both magnitudes, P and Q , it is observed that test cases at PL present smaller errors than FL cases, during both fault and post-fault periods. This behavior can be analyzed as follows:

- Regarding P (Fig. 8), in FL test cases, the response must decrease from a value of $\sim 1 pu$ to values within the range of the depth of the fault (for example, for FL2, $depth = 0.5$ and hence P decreases from $1 pu$ to $0.3 pu$). In the PL test cases, the reference is much closer to the dip value (for example, for the same dip, in PL2, P decreases from $0.25 pu$ to $0.15 pu$). Hence, the adjustment may be fitter for PL test cases. In some cases, as shown in the following section, even if the signal does not change at all during the fault, the error would be $< 1\%$.
- Regarding Q (Fig. 9), the difference between PL and FL errors is due, not only, to similar reasons, but also because of the existence of more disturbances in the FL test cases, as shown in the following subsection.

The only set which differs from this trend is the MXE during the fault for both P and Q , in which the PL error is higher than the FL error. This is mainly due to test PL3 (*), which presents a large perturbation during the fault for both signals, as described in the following subsection. This large error, compared to the others in the same series, unbalances its box.

C. Representative test cases analysis

Aiming to complement results presented in the previous subsections, this subsection analyzes the most representative responses of the ten test cases considered in this work.

First, the active and reactive power from test PL3 are shown in Fig. 10 and Fig. 11, respectively, considering the three data sources (measured in field, IEC model response and WECC model response). Both these figures show the perturbation that unbalances the MXE during the fault period observed in the

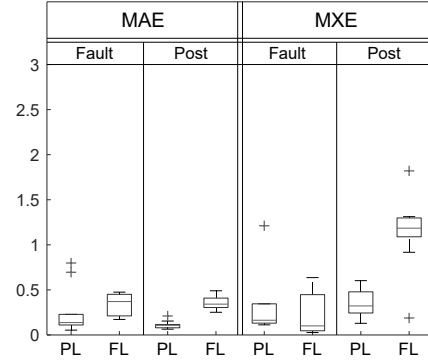


Fig. 8. Validation error analysis. Active power box plot.

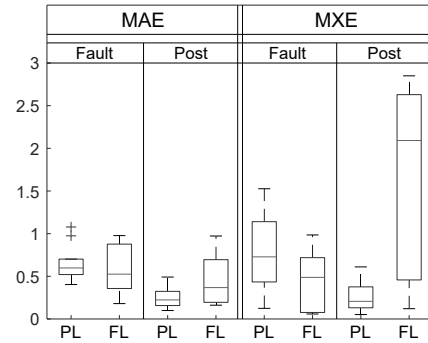


Fig. 9. Validation error analysis. Reactive power box plot.

box plots shown in the previous subsection. Specifically, in Fig. 10, it can be seen that the measured peak occurring at $2.5 s$ cannot be emulated by either of the generic models, leading to an MXE of 1.21% during the fault period for both cases. Moreover, the zoom in Fig. 11 shows that, for reactive power, the error is also $> 1\%$. Furthermore, can not only the decreasing peak not be simulated by the generic models, but also their response increases, generating even larger validation errors. This measured peak is due to a small decrease in the voltage at the WTT occurring at that time, which significantly influences the real response of the WT. Nevertheless, the active power response of the generic models is unaffected. With regard to the increase in reactive power, as shown in Fig. 2, the reactive current command during the dip is calculated adding a component that is proportional to the depth of the dip. As the voltage decrease at that moment, this additional component increases, compensating for the drop caused by the voltage perturbation.

Fig. 12 shows the active power response of test PL5, in which the depth of the dip was equal to $0.1 pu$. This figure shows that for these non-severe faults with small active power references, the validation error obtained is considerably low. Even if the active power response not to vary during the fault, the mean error would be 0.5% , which is negligible. This

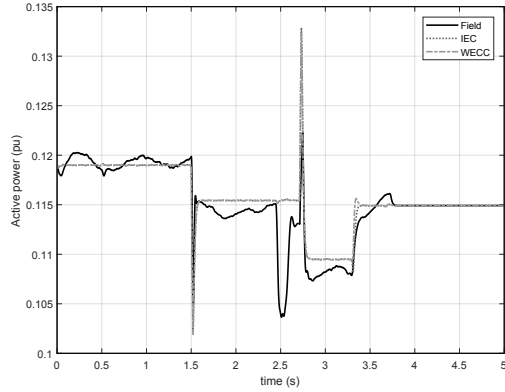


Fig. 10. Test case PL3. Active power.

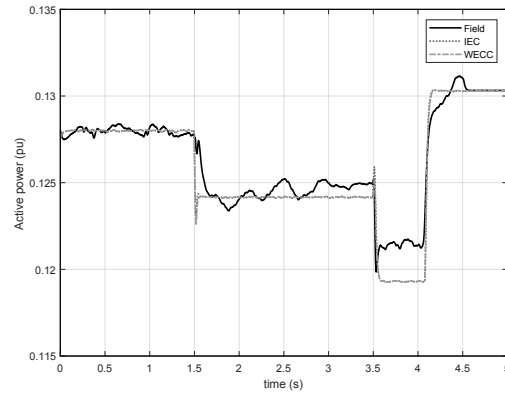


Fig. 12. Test case PL5. Active power.

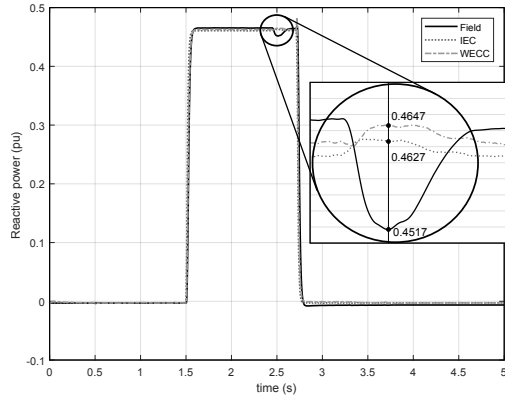


Fig. 11. Test case PL3. Reactive power.

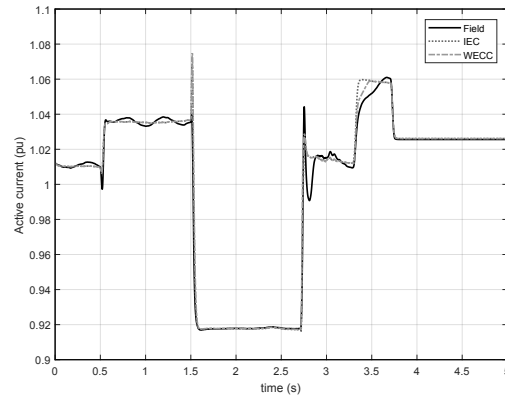


Fig. 13. Test case FL3. Active current.

explains the differences between the PL and FL test case boxes shown in Fig. 8.

Finally, an example of the relatively high post-fault validation errors observed under FL conditions is provided. Fig. 13 shows the active current response of the test FL3. On one hand, it can be observed that the current signal increases during the pre-fault period, due to a decrease in u_{WT} in which the CS has to maintain the active power constant. On the other hand, the transient period experienced in the field by the WT, which occurs between $3.25\text{ s} < t < 3.75\text{ s}$ cannot be simulated by either of the generic models, meaning $\text{MXE} > 1.2\%$. Regarding the reactive power, the zoom in Fig. 14 shows two oscillations of the WT during the post-fault period, which cannot be emulated by the generic models. A more similar response is observed for the IEC model, due to the higher control possibilities offered by its EGS. However, both models present post-fault $\text{MXE} > 2.5\%$. Furthermore, the high dispersion of MXE for FL tests shown in Fig. 9 is due to the differences between tests with and without these oscillations (i.e. the MXE is almost negligible for these cases).

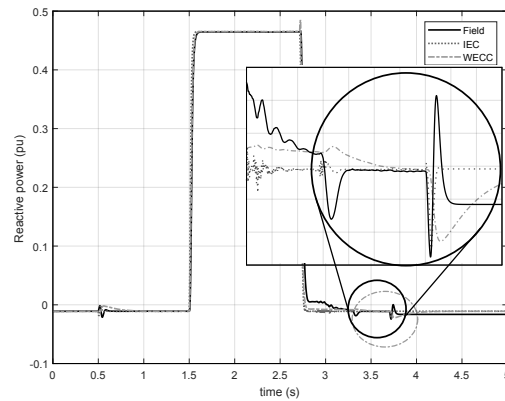


Fig. 14. Test case FL3. Reactive power.

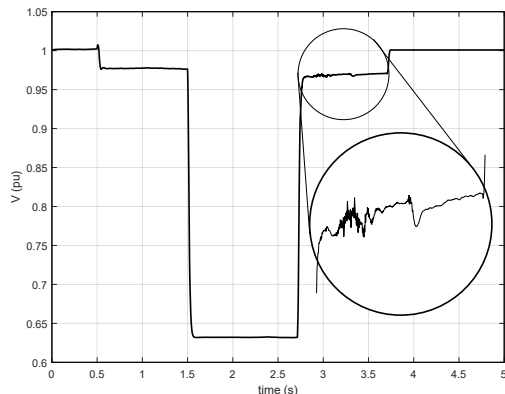


Fig. 15. Test case FL3. Voltage profile.

Both phenomena can be explained observing the voltage profile for FL3 test case, Fig. 15. When series impedance X_n is connected at 0.5 s, the voltage decreases, generating an increase in active current, as previously explained. Furthermore, comparing Figs. 14 and 15, it can be observed that when X_n is disconnected at 3.75 s, the perturbations causing a large MXE occur. Thus, these small fast variations of voltage cause perturbations in the responses of the WT which cannot be properly emulated by the model. Furthermore, the zoom in Fig. 15 shows the perturbations after the fault causing the irregular response in Figs. 13 and 14. It should be noted that certain real behaviors caused by small voltage perturbations cannot be reproduced by generic models.

V. CONCLUSIONS

The present paper validates, for the first time, the generic Type 4 WT models proposed by two international organizations: the IEC and the WECC. Both models were tested under ten different test cases, considering partial and full load conditions, as well as different voltage dip parameters. Using the validation methodology proposed in IEC 61400-27-1 (which will be fully developed in the Edition 1 of 27-2), the response of the models was compared to the response of a real Type 4 WT located in a Spanish WF. It is shown in three different ways that both generic models can accurately reproduce the general behavior of the real WT, with small validation errors for most cases ($< 1\%$). However, some transient periods and specific responses of the WT cannot be reproduced by these generic models, leading to a number of uncommon maximum errors lower than 3% for these cases. It is also worth noting that the IEC approach, which focuses on accuracy despite the use of more parameters, allows higher control possibilities. Hence, some transient periods can be more appropriately adjusted.

Following the IEC guidelines, the authors have maintained the values of the model parameters constant for all study cases. This fact is important as all the validation errors could be reduced if the parameters were adjusted for each test. WECC

guidelines do not mention this issue. However, to validate both models properly, the authors have followed the same consideration for both models.

Regarding the IEC validation method, some of the test cases show that depending on the load of the WT, the active power error may not accurately represent the variations when the dip occurs. Therefore, the validation methodology defined by IEC 61400-27-1 could include some modification considering the load of the WT, in order to obtain a more similar range of validation errors regardless of the operating condition. However, due to the recent publication of this Standard, experimental validation works, such as the present contribution, are needed to assess the capability of the validation approach.

To sum up, the generic Type 4 WT models can provide a relatively accurate response, except in particular transient periods. Nevertheless, their low computational requirements, as well as their reduced number of parameters, mean the use of these generic models is highly recommended for analysis which can accept these errors. The present paper shows a complete validation and compatibility study for Type 4 generic WT models. Thus, this work may result of particular interest to researchers, organizations, WT manufacturers or system operators considering the use of these generic models to conduct transient stability analysis. Moreover, this study might also be of interest to the IEC and WECC working groups as it contributes to testing the compatibility between both approaches, as well as the IEC validation method, which is currently under development.

ACKNOWLEDGMENT

This work was supported by the "Ministerio de Economía y Competitividad" and European Union FEDER, which supported this work under project ENE2016-78214-C2-1-R.

REFERENCES

- [1] S. Seman, "Need for confidentiality. A converter manufacturer's view," *1st Wind Integration Symposium*, p. 30pp, 2011.
- [2] A. Honrubia Escrubano, E. Gomez-Lazaro, J. Fortmann, P. Sørensen, and S. Martín-Martínez, "Generic dynamic wind turbine models for power system stability analysis: A comprehensive review," *Renewable & Sustainable Energy Reviews*, vol. 81, pp. 1939 – 1952, 2018.
- [3] J. Fortmann, "Generic aerodynamic model for simulation of variable speed wind turbines," in *Proceedings of 9th International Workshop on Large-Scale Integration of Wind Power into Power Systems*. Quebec (Canada): Energynautics GmbH, 2010.
- [4] *IEC 61400-27-1. Electrical simulation models - Wind turbines*. International Electrotechnical Commission Std., Rev. Edition 1, February 2015.
- [5] P. Sørensen, J. Fortmann, F. Jiménez Buendía, J. Bech, A. Morales, and C. Ivanov, "Final draft international standard IEC 61400-27-1. Electrical simulation models of wind turbines," *13th Wind Integration Workshop*, p. 5pp, 2014.
- [6] WECC REMTF, "WECC wind power plant dynamic modeling guide," WECC, Tech. Rep., 2010.
- [7] P. Pourbeik, "Proposed modifications to the WT3 and WT4 generic models," Electric Power Research Institute, Tech. Rep., 2011.
- [8] WECC REMTF, "WECC second generation of wind turbines models guidelines," WECC, Tech. Rep., 2014.
- [9] Ömer Göksu, P. Sørensen, A. Morales, S. Weigel, J. Fortmann, and P. Pourbeik, "Compatibility of IEC 61400-27-1 Ed 1 and WECC 2nd Generation Wind Turbine Models," *15th Wind Integration Workshop*, 2016.
- [10] T. T. Cristina Vázquez Hernández and A. V. Pradas, "JRC Wind Energy Status Report 2016 Edition," Market, technology and regulatory aspects of wind energy. JRC Science for policy report, 2017.

- [11] N. M. Salgado-Herrera, A. Medina-Ros, R. Tapia-Sánchez, and O. Anaya-Lara, "Reactive power compensation through active back to back converter in type-4 wind turbine," in *2016 IEEE International Autumn Meeting on Power, Electronics and Computing (ROPEC)*, Nov 2016, pp. 1–6.
- [12] A. Honrubia-Escribano, F. Jiménez-Buendía, E. Gómez-Lázaro, and J. Fortmann, "Field validation of a standard Type 3 wind turbine model for power system stability, according to the requirements imposed by IEC 61400-27-1," *IEEE Transactions on Energy Conversion*, vol. PP, no. 99, pp. 1–1, 2017.
- [13] P. Pourbeik, J. J. Sánchez-Gasca, J. Senthil, J. Weber, A. Ellis, S. Williams, S. Seman, K. Bolton, N. Miller, R. J. Nelson, K. Nayebi, K. Clark, S. Tacke, and S. Lu, "Value and limitations of the positive sequence generic models of renewable energy systems," December 2015.
- [14] P. Sørensen, B. Andresen, J. Fortmann, and P. Pourbeik, "Modular structure of wind turbine models in IEC 61400-27-1," *IEEE Power and Energy Society General Meeting*, pp. 1–5, 2013.
- [15] P. Pourbeik, A. Ellis, J. Sanchez-Gasca, Y. Kazachkov, E. Muljadi, J. Senthil, and D. Davies, "Generic stability models for type 3 & 4 wind turbine generators for WECC," *IEEE Power and Energy Society General Meeting*, pp. 1–5, 2013.
- [16] A. Ellis, Y. Kazachkov, E. Muljadi, P. Pourbeik, and J. Sanchez-Gasca, "Description and technical specifications for generic WTG models – A status report," *IEEE/PES Power Systems Conference and Exposition (PSC)*, pp. 1–8, 2011.
- [17] P. Pourbeik, "Model user guide for generic renewable energy system models," Electric Power Research Institute, Tech. Rep., 2015.
- [18] M. Behnke, A. Ellis, Y. Kazachkov, T. McCoy, E. Muljadi, W. Price, and J. Sánchez-Gasca, "Development and validation of WECC variable speed wind turbine dynamic models for grid integration studies," in *AWEA's 2007 WindPower Conference*, California, USA, Jun. 2007.
- [19] M. Asmine, J. Brochu, J. Fortmann, R. Gagnon, Y. Kazachkov, C. E. Langlois, C. Larose, E. Muljadi, J. MacDowell, P. Pourbeik, S. Seman, and K. Wiens, "Model validation for wind turbine generator models," *IEEE Transactions on Power Systems*, vol. 26, no. 3, pp. 1769–1782, 2011.
- [20] J. Bech, "Siemens experience with validation of different types of wind turbine models," *IEEE Power and Energy Society General Meeting*, 2014.
- [21] S. Seman, J. Simolin, J. P. Matsinen, and J. Niiranen, "Validation of Type 4 wind turbine generic simulation model by full-scale test," *9th Wind Integration Workshop*, p. 6pp, 2010.
- [22] J. Fortmann, S. Engelhardt, J. Kretschmann, M. Janben, T. Neumann, and I. Erlich, "Generic simulation model for DFIG and full size converter based wind turbines," *9th Wind Integration Workshop*, p. 8pp, 2010.
- [23] A. Lorenzo-Bonache, A. Honrubia-Escribano, F. Jiménez-Buendía, A. Molina-García, and E. Gómez-Lázaro, "Generic Type 3 wind turbine model based on IEC 61400-27-1: Parameter analysis and transient response under voltage dips," *Energies*, vol. 10, no. 9, p. 23, 2017.
- [24] C. Subramanian, D. Casadei, A. Tani, P. Sørensen, F. Blaabjerg, and P. McKeever, "Implementation of electrical simulation model for IEC Standard Type-3A generator," in *2013 European Modelling Symposium*, Nov 2013, pp. 426–431.
- [25] J. Fortmann, "Modeling of wind turbines with doubly fed generator system," Ph.D. dissertation, Department for Electrical Power Systems, University of Duisburg-Essen, 2014.
- [26] A. Lorenzo-Bonache, R. Villena-Ruiz, A. Honrubia-Escribano, and E. Gómez-Lázaro, "Comparison of a standard type 3B WT model with a commercial build-in model," *IEEE International Electric Machines & Drives Conference*, 2017.
- [27] F. Jiménez Buendía and B. Barrasa Gordo, "Generic simplified simulation model for DFIG with active crowbar," *11th Wind Integration Workshop*, p. 6pp, 2012.
- [28] F. Jiménez, E. Gómez-Lázaro, J. A. Fuentes, A. Molina-García, and A. Viguera-Rodríguez, "Validation of a DFIG wind turbine model submitted to two-phase voltage dips following the spanish grid code," *Renewable Energy*, vol. 57, pp. 27–34, 2013.
- [29] F. Jimenez, E. Gómez-Lázaro, J. A. Fuentes, A. Molina-García, and A. Viguera-Rodríguez, "Validation of a double fed induction generator wind turbine model and wind farm verification following the spanish grid code," *Wind Energy*, vol. 15, no. 4, pp. 645–659, 2012.
- [30] H. Zhao, Q. Wu, I. Margaritis, J. Bech, and A. B. Sørensen, P. E., "Implementation and validation of IEC generic Type 1A wind turbine generator model," *International Transactions on Electrical Energy Systems*, vol. 25, no. 9, pp. 1804–1813, 2014.
- [31] A. Honrubia-Escribano, F. Jiménez-Buendía, E. Gómez-Lázaro, and J. Fortmann, "Validation of generic models for variable speed operation

wind turbines following the recent guidelines issued by IEC 61400-27," *Energies*, vol. 9, 2016.

- [32] M. Meuser and M. Brennecke, "Analysis and comparison of national and international validation methods to assess the quality of DG simulation models," in *International ETG Congress 2015; Die Energiewende - Blueprints for the new energy age*, Nov 2015, pp. 1–7.



Alberto Lorenzo Bonache received the degree in electrical engineering (2015) and the master degree in industrial engineering (2017) from Universidad de Castilla-La Mancha (UCLM), Albacete, Spain. He is currently a Ph.D. student in Science and Technologies applied to Industrial Engineering.

Since 2015 he has been working as a researcher in the Renewable Energy Research Institute. His main research interest is the modeling of wind turbines and wind farms for the integration of wind energy into power systems and applications of real time

simulation for renewable energies.



Andrés Honrubia Escribano received the degree in electrical engineering from the Polytechnic University of Madrid (UPM), Madrid, Spain, in 2008 and the Ph.D. degree in Renewable Energy from the Polytechnic University of Cartagena, Cartagena, Spain, in 2012.

Since 2008 he has worked for several research entities, publishing more than 50 articles in journals, books and specialized conferences, collaborating in more than 30 R&D projects. Currently he is a Associate Professor in the Department of Electrical, Electronics, and Control Engineering, Castilla La Mancha University, Albacete, Spain. His main research interest is the integration of wind energy into power systems.



Francisco Jiménez Buendía received the M.Sc. degree in industrial engineering and the Ph.D. degree in electrical engineering from the Technical University of Cartagena, Cartagena, Spain, in 2001 and 2008, respectively.

Since 2003 he has been with GAMESA in grid integration and modeling projects. He is currently Chief Electrical Engineer for G5x product platform at SIEMENS GAMESA in Pamplona, Spain. He is a member IEC TC88 WG27. His research interests include grid integration of wind turbines into power systems, modeling of wind turbines for transient stability and development of wind power plants controllers.



Emilio Gómez Lázaro (SM10) received the M.Sc. and Ph.D. degrees in electrical engineering from the Universidad Politécnica de Valencia, Valencia, Spain, in 1995 and 2000, respectively.

He is currently a Professor in the Department of Electrical, Electronics, and Control Engineering, Castilla La Mancha University, Albacete, Spain, where he is also the Director of the Renewable Energy Research Institute. His research interests include modeling of wind turbines and wind farms, grid codes, power system integration studies, steady-state and dynamic analysis, and O&M of renewable energy power plants.

4.2. Additional analysis - Transient response study

The differences between the IEC and WECC modeling approaches for a generic Type 3 model were studied in Paper II (Section 4.1.2). Once both models were working properly, the following step was their parametrization and validation. Six different test cases, obtained from a real DFIG WT were used. The characteristics of these cases are depicted in Table 4.4.

Table 4.4: Characteristics of the test cases analyzed.

Case	Load of the WT	Residual voltage	Dip duration
PL1	0.25 pu	0.80 pu	2.0 s
FL1	1.00 pu		
PL2	0.20 pu	0.50 pu	1.0 s
FL2	1.00 pu		
PL3	0.27 pu	0.30 pu	0.7 s
FL3	1.00 pu		

Independent validation works for the IEC and WECC generic Type 3 WT models were already published in current literature (see Section 2). Nevertheless, this work is the first to validate both generic models using a full set of test cases. Furthermore, in order to conduct a novel study, a focus on transient periods was decided, which had been dismissed until this work. The two models (IEC and WECC) were fitted to the 6 test cases, and the transient response was compared with the real behavior. However, at the time of quantitatively analyze the performance, it was realized that the IEC 61400-27-1 methodology was unable to provide conclusive results, due to the disregard of transient periods for validation calculations (see Section 3.2). Thus, an extension of the current validation methodology to transient periods, nowadays dismissed, is proposed. With the extended methodology, the additional accuracy of the IEC model is demonstrated, as well as the inability to emulate some transient responses.

4.2.1. Proposal of extension of the IEC 61400-27-1 validation methodology

The validation methodology proposed in the IEC 61400-27-1 has been depicted in Section 3.2. Despite this methodology being valid for studying the general behavior of the models, the IEC validation methodology has an important issue regarding transient periods. Accepting that generic models are not designed to model transient periods properly, the IEC guidelines propose neglecting a certain time after the fault occurs and after it ends. For the fault period, the first 140 ms are neglected to calculate MAE and MXE.

For the post-fault period, the following 500 ms when the fault clears are neglected to calculate MXE. The full post-fault window is used to calculate MAE, but since it is recommended that it lasts 5 s, the transient error is diffused. These windows, which do not include transient periods, are referred to as Quasi Steady State (QSS).

The issue here is that most features included in the IEC generic model to improve its response are designed to emulate transient behaviors (e.g., the crowbar system, the detailed electrical generator system or the complex electromagnetic torque control system). In QSS, the IEC generic model provides slightly better results, but both approaches are valid, as shown in the literature [44, 106]. Nevertheless, important differences exist between the two models, especially during transient periods. IEC is more accurate, yet the IEC validation method is unable to demonstrate this appropriately. Furthermore, this validation system, which completely neglects transient periods, has a greater number of issues. On the one hand, for short faults (shorter than 280 ms according to [30]), errors during the fault period cannot be validated. On the other hand, generic models tend to simulate large reactive current spikes at the end of the fault (which is partially countered with the IEC detailed generator system) [82]. These spikes can cause instability issues, since they can be large enough to fire protections. More critically, users unfamiliar with this specific behavior may tend to see an actual problem in the grid while, in reality, this is simply a simulation issue. Thus, ignoring these responses when conducting a model validation may involve a passed test with a model causing problems in the grid.

It is proposed to calculate these error magnitudes during transient periods, as a different window. In this way, the validation method would show the overall picture of the behavior of the generic model. The values obtained in these transient windows may not be binding, since these models are not designed to cover these periods. However, anyone using these models would have a complete insight of the behavior of the generic model. In addition, defining transient periods as different windows allows the behavior analyzed in each of them to be specified (e.g., regarding active power post-fault period, its rise during transient window and the oscillations in QSS). With the current methodology, the consequences of these behaviors may overlap. A large amount of data is already provided by the IEC validation approach. Adding more data may render the information more difficult to interpret. On the other hand, valuable additional information could be made available to the user, reducing the risk of misinterpreting the data provided. In fact, despite generic models not being designed to accurately emulate transient periods, obviating them does not mean they do not exist, with the subsequent impact on the grid model in which they are connected.

In conclusion, this extension of the current methodology allows the identification of critical transient response issues. Furthermore, in the current

work, this extension is necessary to demonstrate the advantages of the more complex generic model from the IEC during transient periods. In the following section, all the transient behaviors not covered by the current methodology are depicted and the benefits of the proposal are demonstrated. Finally, it is worth mentioning that, despite further comparison and validation methodologies existing, it has been considered the extension of the current IEC methodology as the most appropriate for the generic models. This work aims to provide the IEC Committee with the necessary information to improve its methodology. Hence, the extension of the current work, instead of a completely new formulation, facilitates its inclusion in future editions of the IEC Standard.

4.2.2. Results

This section is divided in three parts. Parts 4.2.2.1 and 4.2.2.2 compare field data and models responses of active and reactive power, respectively. The transient behavior of each model is analyzed, as well as those field performances which cannot be addressed by either of both models. Those transient responses which cannot be assessed by the IEC validation methodology are especially highlighted. Finally, Part 4.2.2.3 shows the results of applying the current validation methodology and the proposed extension. The benefits of the proposal are depicted in this last Part.

4.2.2.1. Active power response

This subsection shows the active power responses of the two generic Type 3 WT models (IEC and WECC), compared to field data. Not only are the transient responses analyzed, but also the QSS behaviors that cannot be addressed by either of the generic models. In the figures shown in this section, the green shaded area represents the transient period when the fault occurs (140 ms) and the orange shaded area represents the transient period when the fault clears (500 ms). Finally, a vertical red dashed line indicates the end of the post-fault QSS window.

First, one of the most complicated situations to be emulated by the WECC model is the behavior produced by the crowbar system, due to the lack of such control in the WECC Type 3 model. When the crowbar system actuates, the rotor terminals of the DFIG WT are short-circuited, thus protecting the rotor-side converter from high currents. This involves the active power of the actual WT decreasing close to, or even below, zero. Regarding the models' transient response when the fault occurs, the IEC model can adjust its response more accurately because of the inclusion of the crowbar system. The active power of the IEC system is able to decrease to almost zero, whatever the fault is (i.e. non-severe faults may also reduce the active power significantly). The WECC response decreases proportionally to the

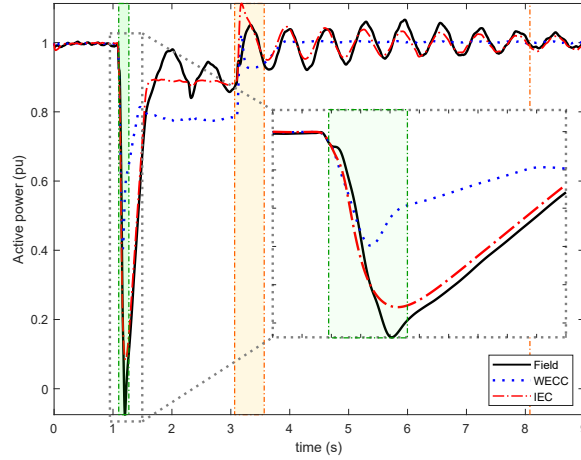


Figure 4.1: Active power for case FL1.

decrease in voltage and the consequent current saturation. An example of this behavior is shown in FL1 test case, the active power of which is shown in Fig. 4.1. The WECC response (dotted blue) only decreases to 0.4 pu due to the low severity of the fault, while the IEC active power (dashed red) is able to decrease close to 0 pu, representing a more accurate response compared to field data (solid black).

However, none of the systems can emulate the negative active power in the case of a fault during partial power operation, when the generator operates in under-synchronous mode (i.e., it absorbs active power, working as a motor for a short period). This failure when modeling the motor behavior of the actual WT is significant for case PL2 (Fig. 4.2), in which the crowbar is activated at the beginning and the end of the fault and the WT injects 0.2 pu of active power during pre-fault conditions. Indeed, at the end of the fault, the negative spike of active power cannot be emulated at all. In fact, the lower limits from active current and power saturators are usually set to zero, since negative active power may cause models to suffer instability issues. Nevertheless, Fig. 4.2 shows that the active power response of the IEC model decreases to almost 0 pu when the fault ends (crowbar activation), while the WECC's response directly increases due to the voltage recovery, thus resulting in a larger validation error.

Finally, the case of the rise to nominal power after the fault, when the crowbar is not activated, is addressed. This transient behavior when the fault is cleared is found in case FL2 (Fig. 4.3). When the voltage recovers, the IEC model is able to emulate the rise of the active power with great accuracy, due to the complex electromagnetic control system. Nevertheless, the WECC model's response is an abrupt increase (because of the voltage recovery) and subsequently a rise with a constant rate ramp. It can be observed that most of this rise is included within the 500 ms of the transient period, and hence,

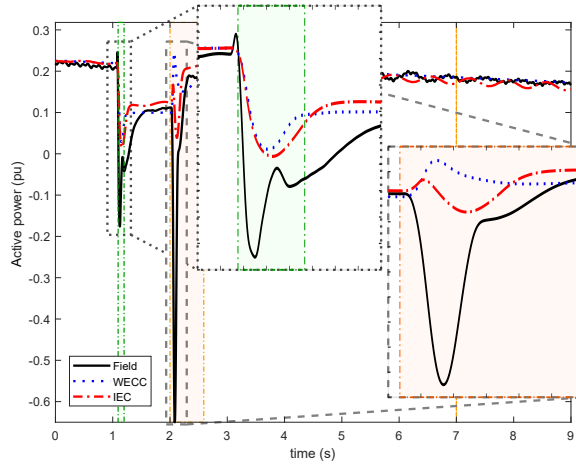


Figure 4.2: Active power for case PL2.

is not considered by the IEC validation methodology.

Additionally, Fig. 4.3 shows another response which cannot be emulated by either of the two generic Type 3 WT models, after the fault is cleared. When the active power recovers its nominal value, the actual WT response shows an undershoot from 2.5 s to 6.5 s. The mean value of the generic model is constant once it recovers the nominal value, and, thus, this response cannot be emulated. This is likely a consequence of some short-term aerodynamic imbalance, which cannot be simulated by generic models since they are designed to work with constant wind. Since this behavior is included in the post-fault QSS period, it is correctly analyzed by the IEC validation methodology.

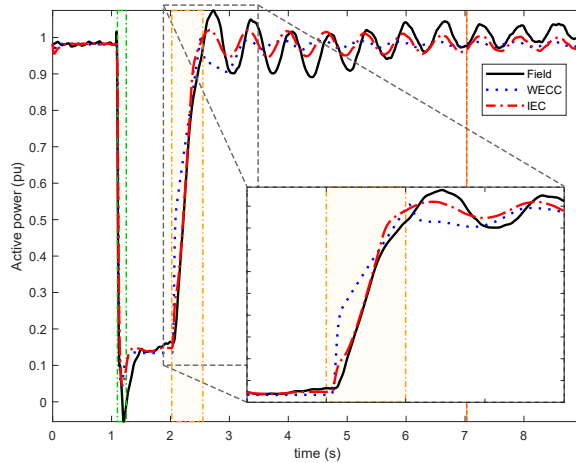


Figure 4.3: Active power for case FL2.

In fact, the IEC validation methodology is useful to compare other dif-

ferences in the behavior of the models, most of them occurring in QSS. For example, case FL1 (Fig. 4.1), shows how, during the fault QSS period, the WECC response is unable to adjust the active power value to the actual one. The active and electromagnetic torque control model for the IEC is a complex system, which controls the values of these magnitudes during the fault, depending on the voltage and the load of the WT. For the WECC model, these systems maintain the reference of active current constant during the fault, which is only modified by the *Current saturation system* and the *LVPL* (Low Voltage Power Logic). Both of these systems depend only on the voltage, and directly modify the command current, not allowing either to differentiate between cases with full or partial load WT condition or to control the rise of active power accurately. It is worth remembering that the models' parameters are kept constant for all simulation cases, thus obtaining the minimum error for all cases at a time. For example, if only case FL1 was taken into account, the LVPL system could have been adjusted so that the average active current value during the fault coincided with that of the field response.

Another response which can be measured by the IEC validation methodology is the ability to control the oscillations after the fault. The IEC generic model, which includes the active drive-train damping system [99] is able to emulate these oscillations more accurately, as shown in Fig. 4.1. These oscillations mostly occur in QSS post-fault period, and thus the error is correctly measured by the IEC methodology.

Summarizing this part, generic DFIG WT models present certain limitations in emulating the active power response. Responses such as the absorption of active power in under-synchronous mode when the crowbar operates or short-term aerodynamic imbalances cannot be accurately emulated by either of the two models. Additionally, the lack of crowbar system in the WECC model constitutes an important drawback for simulating this behavior. In contrast, the IEC model's response more accurately approaches that of the real WT because of its additional complexity. Finally, it is worth mentioning that most of these differences occur during transient periods, and hence the IEC validation methodology is not able to assess them.

4.2.2.2. Reactive power response

This subsection analyzes the differences between the two models and field data regarding reactive power response, most of which occur in the transient periods when the fault starts and ends. As previously explained, the IEC electrical generator system, with the inclusion of the crowbar system and the dynamics of the generator reactance, is able to emulate the response of these transient periods more correctly.

First, as mentioned above, the main difference between the models is the lack of crowbar system in the WECC model. Figs. 4.4 and 4.5 show the

response of reactive power for cases FL3 and PL3, respectively, in which the crowbar system actuates. Regarding the first transient period, when the voltage dip occurs, the differences are substantial. The effects of the crowbar system are clearly shown in field measurements, and mostly emulated by the IEC system. However, since the WECC model does not include this system, the rise in reactive power is unable to emulate this transient behavior. It is worth noting that this behavior is fully included within the transient period window (shaded green), and thus, neglected by the IEC validation methodology.

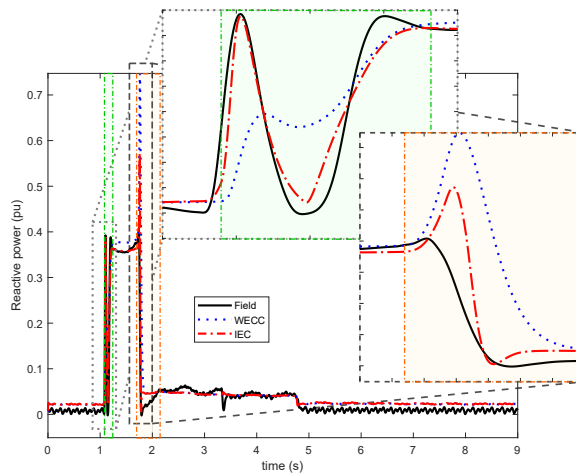


Figure 4.4: Reactive power for case FL3.

When the fault clears, the modeling of the dynamics of the generator reactance allows a deeper control of the spikes in reactive power [99]. The inclusion of this transient reactance has proven to avoid the spikes, generating a more accurate and stable response than a first-order lag model [82]. This is shown for case FL3 (Fig. 4.4), in which the crowbar system is not activated when the fault is cleared. The reactive power spike of the WECC model is much larger than that of the IEC.

Additionally, the fact that the IEC crowbar system actuates multiplying by zero the command reactive current should reduce the reactive power spikes even more. However, for the cases in which the crowbar actuates at the end of the fault, the actual WT response shows a significant negative spike which cannot be modeled by generic models. This is shown in Fig. 4.5 for case PL3, and also occurs in case PL2. This negative spike does not allow good results to be obtained when compared to the actual WT. The spike of the IEC response and the falling rate are, however, more precise.

Finally, the reactive power response for case PL1 is shown in Fig. 4.6. In this case, the crowbar system actuates neither at the beginning nor the end of the fault. The similar behavior when the fault takes place for both models

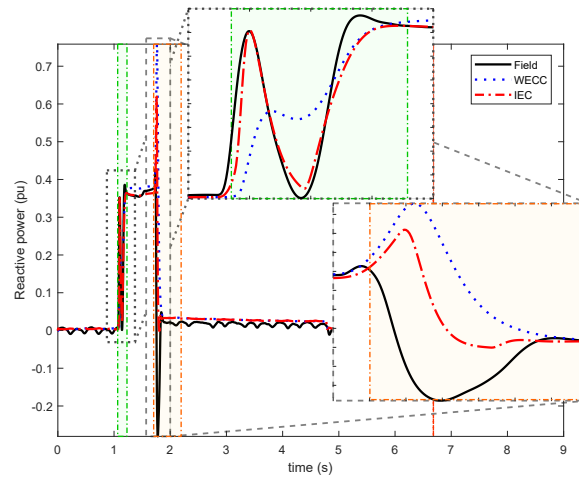


Figure 4.5: Reactive power for case PL3.

is notable, the WECC model being more accurate in this case. Nevertheless, when the fault ends, despite none of the systems showing any significant spikes, the IEC model fits the actual response more accurately.

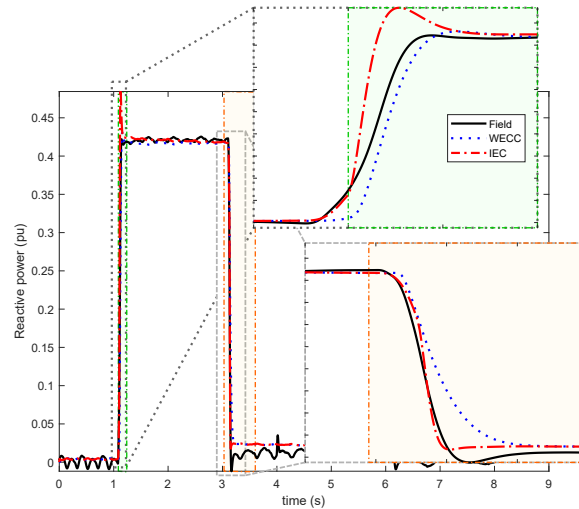


Figure 4.6: Reactive power for case PL1.

Recapitulating, the QSS reactive power responses are modeled with great accuracy by both models. Thus, the largest differences occur during transient periods. The lack of crowbar system or the ability to control the reactive current spikes via the consideration of the generator reactance by the WECC model means the rise and fall of reactive current when the fault begins and ends is uncontrolled. Hence, the IEC model is able to represent these operations more precisely. Regarding the IEC validation methodology, in the

case of reactive power, it is even more ineffective in the comparison, because most differences occur during transient periods. The following subsection demonstrates this fact, addressing the need to numerically analyze transient periods.

4.2.2.3. Application of the proposed validation methodology

This subsection underlines the need to analyze the transient periods to assess the ability of generic models to bring their behavior closer to that of actual WTs. It has been shown that both approaches present accurate behavior during QSS. Thus, based only on the IEC validation methodology results, no significant differences are found. In contrast, errors during transient periods are considerable. To justify these statements, the QSS and transient errors have been calculated for all test cases (Table 4.4), following the considerations from Section 4.2.1. Bar graphs show the errors calculated by the IEC methodology (QSS) and those calculated during transient periods (Tran.). Additionally, the numerical values of the error are also detailed aiming for a deeper analysis.

Regarding active power errors, Fig. 4.7 shows the different error magnitudes, the values of which are depicted in Table 4.5 (fault period) and Table 4.6 (post-fault period). First, it is shown how, during the fault period (Figs. 4.7a and 4.7b and Table 4.5), the IEC methodology and the transient period analysis yield similar results. The responses shown in Section 4.2.2.1 show that the transient period when the fault occurs mostly includes the decrease in active power. The peak of the response occurs near the boundary that divides the transient period and the QSS, implying that MXE is similar for both analyses. In essence, during the fault, the cases that do not adjust properly to the QSS response do not adjust to the transient response, either (e.g., case FL1, Fig. 4.1).

In contrast, the behaviors analyzed during the transient period and the QSS when the fault clears differ significantly (Figs. 4.7c and 4.7d and Table 4.6). The transient period includes the activation of the crowbar system (for the cases in which it activates) and the rise in active power. The QSS analysis mostly analyzes the oscillations after the fault. Two different scenarios may occur, depending on whether the crowbar is deactivated or activated. On the one hand, these cases in which the crowbar is not activated and the rise in active power is not correctly modeled by the WECC model (e.g. cases FL2, Fig. 4.3, and FL3), are addressed. The IEC validation methodology shows significant differences in these cases, but larger errors for the WECC model are due to the inability to emulate active power oscillations. In this sense, mean errors smaller than 0.05 pu are usually acceptable. In contrast, the MAE calculated during the transient period (Table 4.6 and Fig. 4.7c) is able to demonstrate the inability of the WECC model to follow the rise precisely. This is why the QSS and the transient error are similar

for the IEC model, while it may be tripled for the WECC model. On the other hand, when the crowbar is activated after the fault (cases PL2 and PL3), the active power for the IEC model decreases almost to 0. However, for the WECC model, the active power response recovers along with the voltage magnitude (see Fig. 4.2). This different operation inevitably involves a larger MXE in the post-fault transient period for the WECC model. Nevertheless, as shown in Table 4.6 and Fig. 4.7d, the difference between IEC and WECC MXE QSS errors for these cases is lower than 0.01 pu (which can easily be negligible). Conversely, the study of transient periods shows that the error can even be doubled by the WECC model.

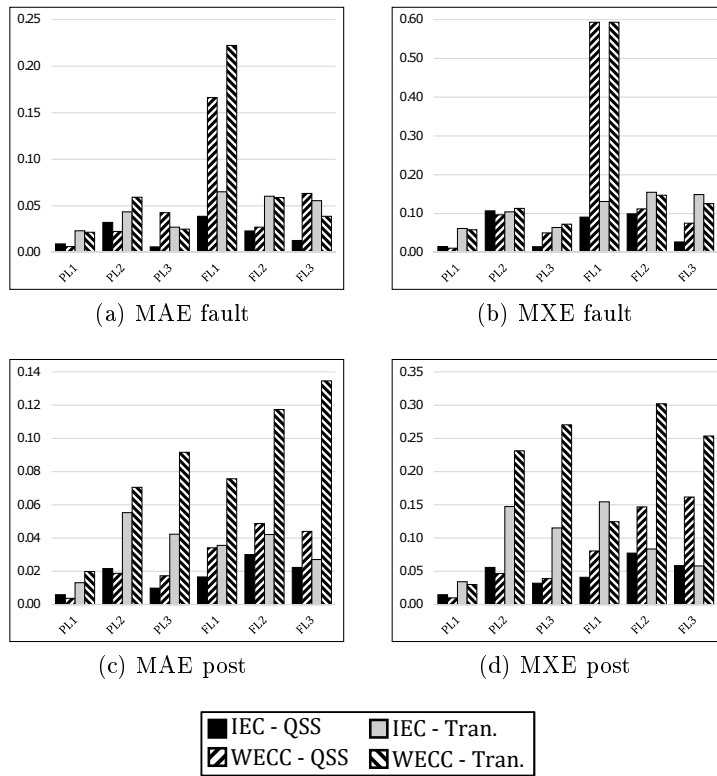


Figure 4.7: Active power errors calculated according to IEC methodology and transient errors, in pu.

Regarding reactive power, graphics showing error magnitudes calculated according to the IEC methodology and the extended methodology are shown in Fig. 4.8 and depicted in Table 4.7 (fault period) and Table 4.8 (post-fault period). For reactive power, the modeling of transient period response especially differs between both models, as previously explained. Nevertheless, errors calculated in QSS show no significant differences, since both models are highly accurate in these periods. This accentuates the lack of an analytical

Table 4.5: Active power MAE and MXE during fault period with IEC and transient validation methodology.

Case	Model	MAE		MXE	
		QSS error (pu)	Transient error (pu)	QSS error (pu)	Transient error (pu)
PL1	IEC	0.0090	0.0232	0.0148	0.0616
	WECC	0.0062	0.0216	0.0106	0.0582
PL2	IEC	0.0322	0.0435	0.1067	0.1043
	WECC	0.0224	0.0592	0.0965	0.1133
PL3	IEC	0.0058	0.0271	0.0142	0.0641
	WECC	0.0425	0.0249	0.0500	0.0724
FL1	IEC	0.0387	0.0651	0.0907	0.1311
	WECC	0.1662	0.2222	0.5931	0.5930
FL2	IEC	0.0229	0.0602	0.0994	0.1547
	WECC	0.0270	0.0589	0.1119	0.1469
FL3	IEC	0.0127	0.0554	0.0269	0.1489
	WECC	0.0632	0.0387	0.0751	0.1255

Table 4.6: Active power MAE and MXE during post-fault period with IEC and transient validation methodology.

Case	Model	MAE		MXE	
		QSS error (pu)	Transient error (pu)	QSS error (pu)	Transient error (pu)
PL1	IEC	0.0059	0.0131	0.0147	0.0343
	WECC	0.0036	0.0198	0.0099	0.0300
PL2	IEC	0.0216	0.0552	0.0557	0.1474
	WECC	0.0188	0.0705	0.0466	0.2311
PL3	IEC	0.0098	0.0423	0.0319	0.1152
	WECC	0.0172	0.0916	0.0389	0.2701
FL1	IEC	0.0166	0.0356	0.0408	0.1545
	WECC	0.0340	0.0756	0.0805	0.1245
FL2	IEC	0.0300	0.0420	0.0771	0.0835
	WECC	0.0487	0.1173	0.1468	0.3019
FL3	IEC	0.0223	0.0271	0.0585	0.0578
	WECC	0.0440	0.1345	0.1616	0.2533

tool that shows the advantages of the IEC model.

The activation of the crowbar system at the beginning of the fault (all cases except PL1), as shown in Section 4.2.2.2, involves significant differences in the transient period when the fault occurs. This is shown in both the MAE and MXE of the transient period, but is not an observation in the IEC methodology. Table 4.7 summarizes these values, which are shown in Figs. 4.8a and 4.8b. The MAE errors calculated with IEC methodology are lower than 0.01 pu for most cases, which demonstrates how accurate the models are in QSS. However, the MAE in the transient period shows how different models actually behave, with the WECC error being two to three

times larger than that of the IEC. Furthermore, the analysis of the transient period shows that the MXE for the WECC model almost triples that of the IEC for almost every case (except PL1, in which crowbar does not activate).

Regarding the post-fault error (Table 4.8 and Figs. 4.8c and 4.8d), a similar situation can be observed. The crowbar and the transient reactance of the IEC system allow greater control of the spikes after the fault. Except for case PL3, in which a large negative spike occurs in the actual response due to the activation of the crowbar system, most transient MXEs for the IEC model are around 0.20 pu or lower. Nevertheless, this magnitude is around 0.5 pu for the WECC model. The control of these spikes can be crucial for the analysis of the stability of the power system (e.g., a grid protection can be activated due to the increase of voltage caused by the sudden injection of capacitive power). The control of the spikes affects not only the maximum value of the spike, but also the falling time. Thus, the MAE of the transient post-fault period also shows significant differences between the two models.

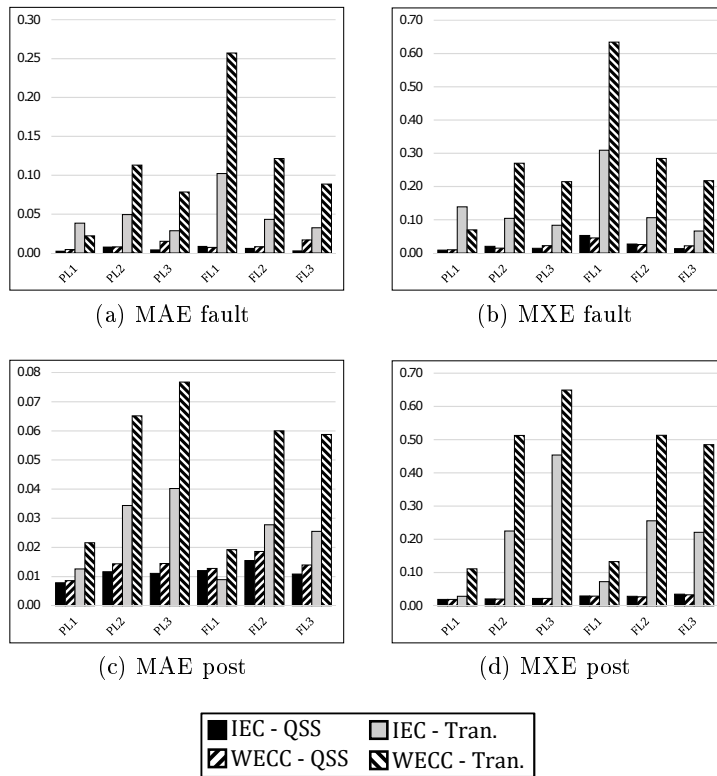


Figure 4.8: Reactive power errors calculated according to IEC methodology and transient errors, in pu.

Summarizing, it can be concluded that the IEC validation methodology is unable to properly expose either the limitations of the generic models

Table 4.7: Reactive power MAE and MXE during fault period with IEC and transient validation methodology.

Case	Model	MAE		MXE	
		QSS error (pu)	Transient error (pu)	QSS error (pu)	Transient error (pu)
PL1	IEC	0.0028	0.0383	0.0084	0.1387
	WECC	0.0043	0.0219	0.0097	0.0693
PL2	IEC	0.0082	0.0493	0.0202	0.1042
	WECC	0.0077	0.1130	0.0147	0.2697
PL3	IEC	0.0046	0.0285	0.0139	0.0832
	WECC	0.0150	0.0783	0.0218	0.2147
FL1	IEC	0.0089	0.1022	0.0529	0.3088
	WECC	0.0072	0.2572	0.0451	0.6340
FL2	IEC	0.0065	0.0432	0.0267	0.1059
	WECC	0.0080	0.1213	0.0256	0.2841
FL3	IEC	0.0032	0.0323	0.0129	0.0658
	WECC	0.0166	0.0886	0.0213	0.2174

Table 4.8: Reactive power MAE and MXE during post-fault period with IEC and transient validation methodology.

Case	Model	MAE		MXE	
		QSS error (pu)	Transient error (pu)	QSS error (pu)	Transient error (pu)
PL1	IEC	0.0079	0.0126	0.0189	0.0284
	WECC	0.0086	0.0216	0.0192	0.1111
PL2	IEC	0.0117	0.0344	0.0200	0.2251
	WECC	0.0143	0.0651	0.0206	0.5126
PL3	IEC	0.0111	0.0402	0.0219	0.4533
	WECC	0.0145	0.0767	0.0222	0.6488
FL1	IEC	0.0121	0.0090	0.0287	0.0725
	WECC	0.0128	0.0192	0.0296	0.1328
FL2	IEC	0.0155	0.0277	0.0270	0.2556
	WECC	0.0186	0.0600	0.0283	0.5132
FL3	IEC	0.0108	0.0255	0.0329	0.2208
	WECC	0.0139	0.0587	0.0347	0.4846

or the advantages of using their own generic model. Especially for reactive power, but also for some behaviors of active power, the current method shows no significant differences that allow the advantages and limitations of either of the models to be established. Conversely, the proposed transient period analysis is able to explicitly reveal both properties, complementing the current methodology.

4.2.3. Conclusions

Assuming the limitations of generic WT models, the study of transient periods is usually dismissed. In fact, the IEC validation methodology focuses

on the QSS analysis, disregarding most calculations during transient periods when the fault begins and ends. Nevertheless, the generic Type 3 models from the IEC and the WECC include systems that attempt to emulate these transient periods. This is especially relevant in the IEC model, which includes systems such as the crowbar, a detailed electrical generator model and a complete electromagnetic torque control. In fact, the improvement in accuracy offered by the inclusion of these complex systems is mainly shown in the transient periods. In contrast, and in line with the IEC validation methodology (i.e., considering that the important response occurs in QSS), the WECC focuses on reducing simulation time and number of parameters, considering that the complexity introduced by these systems does not outweigh the improvement in performance. Indeed, if the inability to emulate these responses is accepted, the inclusion of the systems that increase the simulation time and complexity, as the WECC concluded, may be worthless.

To the best of the author's knowledge, this work is the first to focus on the study of the emulation ability of these transient periods by generic WT models. Nevertheless, when quantitatively analyzing this feature, the current IEC validation methodology is unable to provide the expected results. According to the IEC validation methodology, the behavior of both models (IEC and WECC) is so similar (except in a few exceptional cases) that stakeholders may find difficulties in discerning which model fits their needs. Hence, the additional features in the IEC model, with their consequent challenges in the modeling task and the increase in simulation time, do not clearly show benefits compared to the current methodology. With the aim of illustrating the differences between the two modeling approaches, as well as providing better validation results, it is proposed not to dismiss these transient periods, but to include them in the analysis. Section 4.2.2 demonstrates the usefulness of studying these periods, which provide data on behaviors that cannot be assessed by current methodology. Results show that the most complex systems included in the IEC generic WT model allow the emulation of the actual phenomena with greater accuracy. Furthermore, it is worth mentioning that the WECC model works properly in QSS. However, the greatest differences occur mainly during transients, rather than during QSS. Thus, the analysis of transient periods is not only useful to evaluate behaviors which may cause simulation and stability problems, but also to discern the benefits of modeling a more complex system.

In conclusion, the greatest impact of the different approaches of the IEC and WECC regarding the key focus of the generic WT models (accuracy or simplicity, respectively) is found when transient periods are compared. The WECC's acceptance of the inability of generic models to model the physical phenomena which occur during these periods, with the subsequent gains in simplicity and simulation time, clashes with the IEC focus, which attempts to emulate the full response of the WT as accurately as possible, involving a

complex model which takes considerably longer to simulate. However, these differences are not correctly shown in the existing validation methodology proposed by the IEC committee. The proposal of this work aims to clarify the possibilities of generic WT models when modeling an actual WT. With the addition of the proposed extension of the current method, stakeholders may make an informed decision on which generic model fits their purpose, and the limitations they can accept. Lastly, it is worth mentioning that this study is the first to validate the responses of two generic Type 3 models by the IEC and WECC, using the same set of cases.

Conclusions, summary of contributions and future work

The final Chapter of this Doctoral Thesis summarizes the main conclusions from the different scientific contributions, which are: the IEC Type 3 model parameter analysis (Paper I), the IEC and WECC Type 3 models comparison (Paper II), the IEC and WECC Type 4 validation study (Paper III), and the additional study of the IEC validation methodology. After these conclusions, all the contributions developed during the present Doctoral Thesis are listed, divided into two categories: journal papers, and conference and seminar contributions. Additionally, the contributions made to the 2nd Edition of the IEC 61400-27-1 are depicted. Finally, future work lines are detailed.

5.1. Conclusions

Three are the main goals set out in the current Doctoral Thesis, as stated in its title: the modeling, the simulation and the validation of generic WT models based on international guidelines. The point of departure of the current Doctoral Thesis was the National Project “*Análisis y simulación de nuevos requisitos de regulación en parques eólicos y su integración como servicios complementarios en sistemas eléctricos con elevada presencia eólica (ENE 2012-34603)*”, with which the author was hired during the last months of 2015. The task developed was a first implementation of the four WT types defined in the IEC 61400-27-1, which was published in February 2015. During the subsequent months, thanks to the grants “*Iniciación a la investigación para estudiantes de máster (UCLM)*” and “*Prácticas en empresas asociadas al programa Internship CYTEMA (UCLM)*”, the modeling of the IEC generic models continued. Finally, from March 2017, the author of the current Doctoral Thesis is hired to the National Project “*Operación y mantenimiento de*

grandes plantas de energías renovables on time (ENE 2016-78214-C2-1-R)”, period during which the current Doctoral Thesis was finished.

The first work line followed during the development of the present Doctoral Thesis was the modeling of the IEC generic WT models. During the development of this task, a lack of descriptive works detailing the internal operation of those recently published models was detected in literature. Furthermore, in contrast with the WECC guidelines, the IEC 61400-27-1 provides no values for the models’ parameters, which leads to considerable difficulties at the time of developing the IEC models. Aiming to cover this issue, thus providing a detailed study on the operation of an IEC generic Type 3 model, Paper I (Section 4.1.1) was developed. This paper describes with high detail four of the most important systems which contribute to the active power response: the two mass model, the active power control, the torque PI controller and the pitch control. Not only a theoretical description is conducted, but also a parameter estimation and a sensitivity analysis, providing common ranges of parameters, as well as showing the consequences of their variation in active power and rotational speed responses. This work aims at supporting stakeholders who are beginning with the development of this type of WT, offering a detailed theoretical clarification of its operation, and providing parameter ranges and values.

In order to complement the IEC generic models, the WECC generic models were modeled as well. This work resulted in a new research line: the comparison between both approaches. A detailed study of the differences between IEC and WECC perspectives for the generic Type 3 model was conducted for Paper II (Section 4.1.2). This work depicts the generic Type 3 models developed following the two guidelines, remarking the differences and similarities on their operation. Snapshots of the Simulink[®] models of five of the most relevant systems of the generic models (for both guidelines) are shown. Furthermore, this theoretical approach is complemented with a series of simulations in which the flexibility provided by the most complex models of the IEC system is acknowledged. Values of more than 40 parameters for both guidelines, as well as a sensitivity analysis of the 7 parameters which most influence their response, are detailed. Additionally, the main advantage of the WECC model, the smaller simulation time, is assessed. The IEC model is indeed more flexible and accurate, but it takes twice as long to simulate. Hence, this work evaluates the consequences of the different approaches by the part of the IEC (accuracy) and the WECC (simplicity), thus allowing stakeholders to select the model which better fits their needs.

Apart from Type 3, Paper III (Section 4.1.3) deals with the validation of the IEC and WECC generic Type 4 WT models. To the best of the author’s knowledge, this work is the first in literature to apply the IEC 61400-27-1 validation methodology to both generic Type 4 WT models using a large set of field measurements. Furthermore, since the two guidelines models are

considered, a comparison work was conducted as well. A total of 10 field measurements (5 with full load condition and another 5 with partial load condition) are used to conduct the parametrization of both models. It is worth noting that all parameters were adjusted to be equal for every simulation. Hence, these parameters were those that involved the smaller validation error for all cases at a time. Each case may have been adjusted particularly, but this does not cover the IEC 61400-27-1 requirements, which remark that most parameters (known as *Type*) should be constant, independently from the study case. Additionally, the lack of a more complex system that controls the active power response after a fault is acknowledged. The simplified systems proposed by the two guidelines are not able to emulate the response of the real WT from which the field data was obtained. Thus, a detailed system that models this behavior was developed for this work. With these regards, three issues were assessed: *a)* the different accuracy obtained with each model: the IEC model provides slightly better results, but for Type 4 both models are highly precise; *b)* the general accuracy of the generic Type 4 models: since no remarkable difference was observed between both guidelines, the validation errors were evaluated jointly. For active power, there is a tendency for the error at partial load to be less than that at nominal load. For reactive power, this tendency is not observed; *c)* specific behaviors which cause the largest errors are analyzed using the graphics of the field and models responses. In conclusion, the generic Type 4 models are highly accurate, with both generic systems providing similar results.

Finally, an additional analysis regarding the IEC 61400-27-1 validation methodology is presented in Section 4.2. The original idea for this work was to study the emulation of transient periods when a fault starts and ends by using of the IEC and WECC generic Type 3 WT models. When both systems were adjusted and parametrized, a clear advantage was shown by the IEC model, being considerably more accurate during these periods. However, at the time of quantitatively analyze these results, the IEC 61400-27-1 validation methodology was not enough enlightening. This methodology disregards the first 140 ms after the occurrence of the fault and the following 500 ms when it ends for most error calculations. It is demonstrated that most of the features that make the difference between the IEC and WECC model have its impact during these transient periods. Thus, the proposal to extend the current validation methodology to analyze these transient periods is made. This extension, instead of a new formulation, is proposed in order to be easily included in future editions of the IEC 61400-27. Furthermore, to the best of the author's knowledge, this work is the first validating the IEC and WECC Type 3 models with a set of 6 test cases, including full and partial load. Summarizing, this work not only analyzes the transient operation of the generic Type 3 WT models, but also proposes a quantitatively approach to its analysis, extending the current IEC 61400-27-1 methodology.

In conclusion, the present Doctoral Thesis has served to establish the knowledge regarding IEC and WECC generic WT models. The aims of the presented publications have had two main perspectives. On the one hand, there is a theoretical focus showing, detailing and describing the operation of the generic WT models as deeply as possible, aiming at supporting new users with the development of their own models. On the other hand, a practical approach has been taken, validating the developed models with field responses obtained from real WTs. These validation tasks have concluded with the analysis of the limitations of the current validation methodology and the proposal of its extension.

5.2. Summary of contributions

This Chapter shows the main contributions of the present Doctoral Thesis. First, the journal, conference and seminar contributions are summarized. Then, the contributions to the 2nd Edition of the IEC 61400-27-1 are described.

5.2.1. Contributions to journals, conferences and seminars

The contributions developed during the current Doctoral Thesis are shown in this Chapter. The journal paper contributions are as follows:

- Alberto Lorenzo-Bonache, Andrés Honrubia-Escribano, Jens Fortmann, Emilio Gómez-Lázaro, “Generic Type 3 Wind Turbine Models’ Transient Response: Limitations and Extension of the Validation Methodology”. Under second review, submitted April 2018.
- Alberto Lorenzo-Bonache, Andrés Honrubia-Escribano, Jens Fortmann, Emilio Gómez-Lázaro, “Generic Type 3 WT models: comparison between IEC and WECC approaches”. IET Renewable Power Generation, 2019.
- Alberto Lorenzo-Bonache, Andrés Honrubia-Escribano, Francisco Jiménez -Buendía, Emilio Gómez-Lázaro, “Field Validation of Generic Type 4 Wind Turbine Models Based on IEC and WECC Guidelines”. IEEE Transactions on Energy Conversion, In press, 2018.
- Alberto Lorenzo-Bonache, Andrés Honrubia-Escribano, Francisco Jiménez -Buendía, Ángel Molina-García, Emilio Gómez-Lázaro, “Generic Type 3 Wind Turbine Model Based on IEC 61400-27-1: Parameter Analysis and Transient Response under Voltage Dips”. Energies, Vol. 10, No. 9, pp1441, 2017.

The conference and seminar contributions are:

- International Conference on Renewable Energies and Power Quality (ICREPQ'17). Málaga (Spain), 4th to 6th April, 2017. Alberto Lorenzo-Bonache, Raquel Villena-Ruiz, Andrés Honrubia-Escribano, Emilio Gómez-Lázaro. Contribution: “Real time simulation applied to the implementation of generic wind turbine models”.
- International Conference on Renewable Energies and Power Quality (ICREPQ'17). Málaga (Spain), 4th to 6th April, 2017. Raquel Villena-Ruiz, Alberto Lorenzo-Bonache, Andrés Honrubia-Escribano, Emilio Gómez-Lázaro. Contribution: “Implementation of a Generic Type I Wind Turbine Generator for Power System Stability Studies”.
- 11th International Conference on Compatibility & Power Electronics and 7th on Power Engineering, Energy & Electrical Drives (IEEE Conference CPE-POWERENG 2017), Cádiz (Spain), 4th to 6th April, 2017. Alberto Lorenzo-Bonache, Raquel Villena-Ruiz, Andrés Honrubia-Escribano, Emilio Gómez-Lázaro. Contribution: “Operation of Active and Reactive Control Systems of a Generic Type 3 WT Model”.
- IEEE International Electric Machines and Drives Conference (IEEE IEMDC 2017). Miami (EEUU), 21st to 24th May, 2017. Alberto Lorenzo-Bonache, Raquel Villena-Ruiz, Andrés Honrubia-Escribano, Ángel Molina-García, Emilio Gómez-Lázaro. Contribution: “Comparison of a Standard Type 3B WT Model with a Commercial Build-in Model”.
- 16th International Workshop on Large-Scale Integration of Wind Power into Power Systems as well as on Transmission Networks for Offshore Wind Power Plants, 25th to 27th October, 2017, Berlin, Germany. Alberto Lorenzo-Bonache, Raquel Villena-Ruiz, Andrés Honrubia-Escribano, Emilio Gómez-Lázaro, Estefanía Artigao-Andicoberry. Contribution: “Implementation of Standard Type 1 Wind Turbine Models in Different Power System Analysis Tools”.
- *I Jornadas Doctorales en Energías Renovables*, Jaén, Spain, 9th to 11th May, 2018. Poster contribution and debates with other PhD students. “Modeling and Simulation of Generic Wind Turbine Models. Implementation in Real-Time Simulation Platform”.
- ELECTRIMACS 2019. Salerno (Italy), 21st to 23rd April, 2019. Alberto Lorenzo-Bonache, Raquel Villena-Ruiz, Andrés Honrubia-Escribano, Emilio Gómez-Lázaro. Contribution: “Simulation Optimization of Generic Wind Turbine and Wind Farm Models”.
- Wind Energy Science Conference 2019, Cork (Ireland), 17th to 20th June, 2019. Alberto Lorenzo-Bonache, Raquel Villena-Ruiz, Andrés Honrubia-Escribano, Estefanía Artigao-Andicoberry, Emilio Gómez-

Lázaro. Contribution: “Generic DFIG wind turbine model approach to transient periods”.

- Wind Energy Science Conference 2019, Cork (Ireland), 17th to 20th June, 2019. Raquel Villena-Ruiz, Alberto Lorenzo-Bonache, Andrés Honrubia-Escribano, Estefanía Artigao-Andicoberry, Emilio Gómez-Lázaro. Contribution: “Analysis of Transient Responses of a Generic Type 3 WT model Implemented in DIgSILENT PowerFactory ”.
- The International Conference on Power Systems Transients (IPST 2019), Perpignan (France), 16th to 20th June, 2019. Alberto Lorenzo-Bonache, Raquel Villena-Ruiz, Andrés Honrubia-Escribano, Emilio Gómez-Lázaro. Contribution: “Electromagnetic Torque Transient Control System of a Generic DFIG Wind Turbine Model”.
- The International Conference on Power Systems Transients (IPST 2019), Perpignan (France), 16th to 20th June, 2019. Raquel Villena-Ruiz, Alberto Lorenzo-Bonache, Andrés Honrubia-Escribano, Emilio Gómez-Lázaro. Contribution: “Analysis of the Active and Reactive Power Transient Responses of a Generic Type 3 Wind Turbine Model”.

5.2.2. Contributions to the 2nd Edition of the IEC 61400-27-1

The 1st Edition of the IEC 61400-27-1 supposed an important achievement towards the establishment of generic WT models. The additional accuracy provided by the IEC models, as demonstrated in the current Doctoral Thesis, allowed stakeholders to have a more complete alternative to those generic WT models developed by the WECC. Nevertheless, this 1st Edition, which is currently applicable, presents some issues that lead to misbehaviors of the generic WT models. In order to solve these concerns, the members of the WG 27 of the TC 88 have had the opportunity to provide feedback to the IEC Committee during the last years, which will be accounted for the 2nd Edition of the Standard. During the development of the current Doctoral Thesis, some of these issues have been identified and communicated to the IEC Committee, and will be included in the future Edition of the IEC 61400-27-1. In the following Parts, those problems detected are depicted, as well as the proposed solution. It is worth noting that all these considerations are included in the FDIS version of the 2nd Edition of the Standard.

5.2.2.1. Delay flags

IEC generic WT models use delay flags to control the behavior during and after a voltage dip. These systems are included in all WT types, and can be divided in two types: *a)* The post-fault period depends on the fault depth; *b)* The post-fault period is constant regardless of the fault. Nevertheless, the

IEC 61400-27-1 only describes one system to be used for both cases, as shown in Fig. 5.1a. The timer behavior included in Fig. 5.1a is shown in Fig. 5.1b. However, the proposed system is not functional for any of both cases:

- a) Variable post-fault period** This case is shown for generic Type 2 WT model. The post-fault period depends on the voltage dip depth, calculated via a look-up table. However, if the behavior of the IEC delay flag is analyzed, there is no system able to store this post fault time (T_d). In steady-state period, F_i and T_d value 0. When a fault occur, F_i values 1, and T_d is calculated by the look-up table, depending on the voltage magnitude (it can increase with the time if the fault gets deeper). During this fault period, $F_o = F_i = 1$. Then, when the fault clears ($F_i = 0$ again), the output F_o should be equal to 2 during a time equal to the maximum T_d , since the timer output should continue increasing until $time > T_d$. However, since T_d depends on the fault depth and the fault is cleared, $T_d = 0$. Thus, there is no post-fault period with this implementation.
- b) Fixed post-fault period** This case is shown for generic Types 3 and 4 WT models. If T_d is constant (i.e., it does not depend on the fault depth), an initialization issue exists. At the beginning of the simulation, $F_i = 0$ and T_d has its constant value (e.g., 3 s). Since the input to the timer is 0 (no fault), it starts counting. Hence, until the timer output reaches T_d , the comparator output is 1, and then $F_o = 2$. This would activate the post-fault behavior at the beginning of the simulation, when no fault has happened. A new system is needed for a correct initialization.

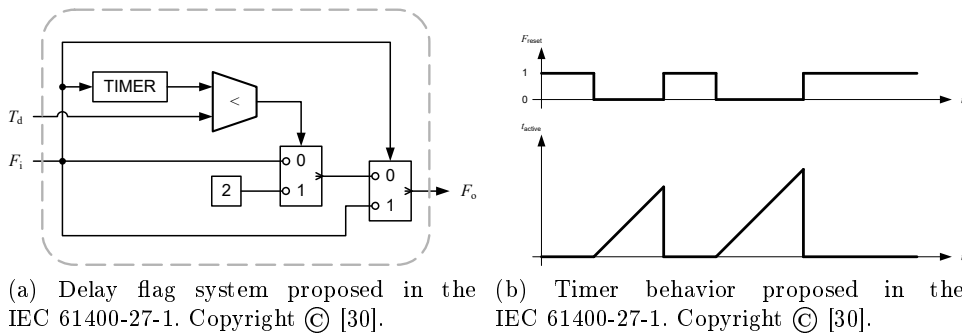


Figure 5.1: IEC 61400-27-1 Delay flag and timer.

The proposals developed in the current Doctoral Thesis are shown in Fig. 5.2a for the case *a*) and in Fig. 5.2b for case *b*). For both systems, the basic structure is the same than that from the IEC 61400-27-1. What has been added are the systems that store the time used for post-fault time, using

a looped switch. The blocks e^{-sT_s} represent unit delays to break algebraic loops. In the case of variable post fault time, the time used to compare with the timer is updated each time T_d increases. The maximum value is maintained until timer exceeds it. Then F_o decreases (from 2 to 0), and T_d is updated again, becoming 0 due to the absence of fault. For case of constant post-fault time (Fig. 5.2b), the scheme used is a simplification from the previous case, since T_d does not need to be updated depending on the dip depth. In this case, the initial time used for comparison is 0 (avoiding the initialization problem), and the constant value T_d is updated when the fault occurs, keeping it constant until the end of the simulation.

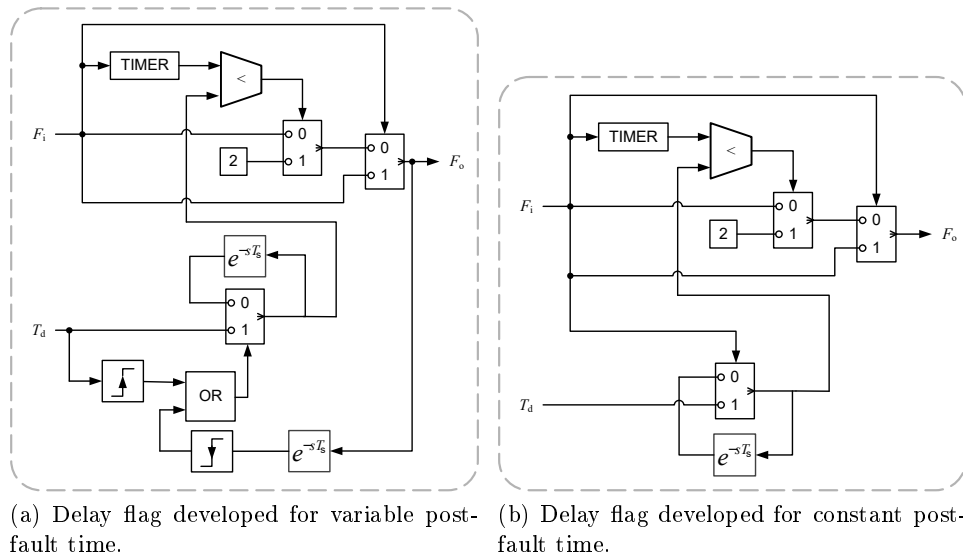


Figure 5.2: Proposals for delay flag systems.

5.2.2.2. Pitch control system

Two issues were identified in the Pitch control system of the IEC generic Type 3 WT model (Fig. 3.11b). The system depicted in the IEC 61400-27-1 is shown in Fig. 5.3. As it is shown, each branch of the PI controllers, as well as the integrators, are saturated with the parameters $\Theta_{max/min}$ and $d\Theta_{max/min}$. These parameters are the same that saturate the pitch angle output (Θ). The highest concern is by the part of Θ_{min} . It is not mandatory, but usually the minimum pitch angle for a WT is 0° . Thus, usually, $\Theta_{min} = 0$. The problem of using this value for saturating the integral parts of the PI controllers is that it does not allow the controllers to reduce pitch angle correctly. An example showing this concern is shown in page 18 of Paper I (Section 4.1.1). Thus, the FDIS version of the 2nd Edition of the IEC 61400-27-1 includes different saturation parameters for both PI controllers and the output of the

system (red in Fig. 5.3). This solution has the inconvenience to increase the number of parameters from 2 to 6.

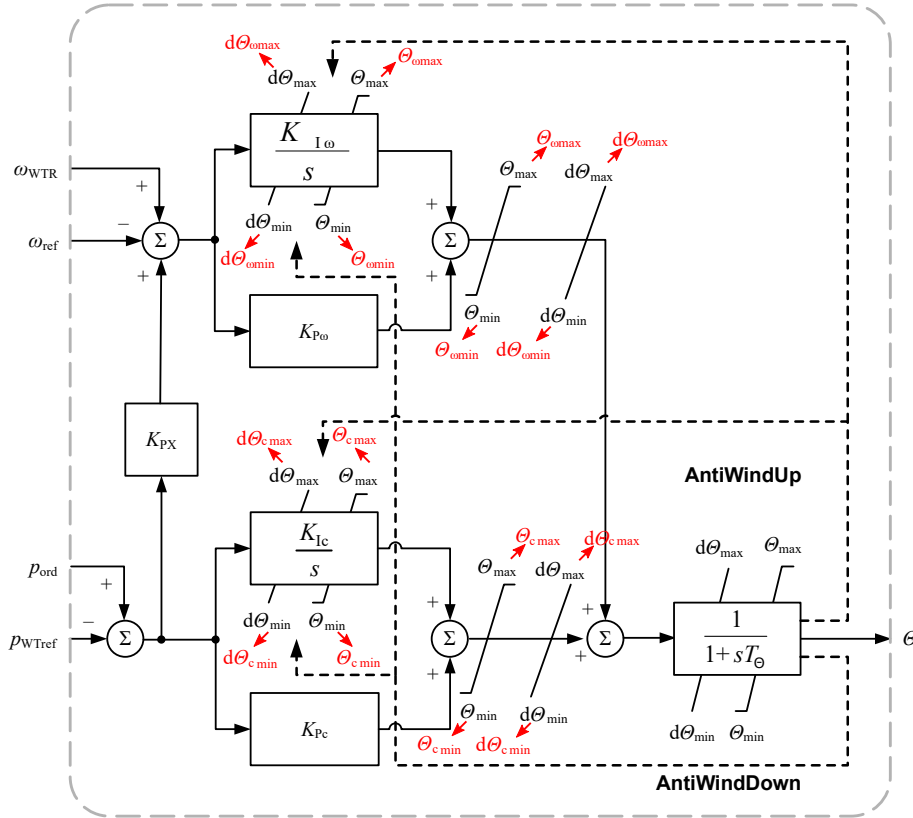


Figure 5.3: IEC 61400-27-1 Pitch control system. Copyright © [30].

Finally, another implementation issue is found into the first order filter with limitation detection, used in Pitch control system for the activation of the AntiWindUp protection system. The IEC 61400-27-1 system is shown in Fig. 5.4. The problem in this system is related with the encircled comparators. The inputs to these blocks are the input and output from a saturator block. The point is that, in normal condition, the input and output from a saturator block are equal. Since the comparator considers the equal sign, the AntiWindUp protection system will be active during normal condition, thus freezing the integral actuation of the PI controllers. The problem does not affect with the other comparator used for the activation of the AntiWindUp system, since the comparison is conducted with a fixed value ($y_{max/min}$). The solution proposed and adopted for this problem is deleting the equal sign of the comparator (i.e., it goes from \leq to $>$). This issue is treated in Paper I (Section 4.1.1) as well.

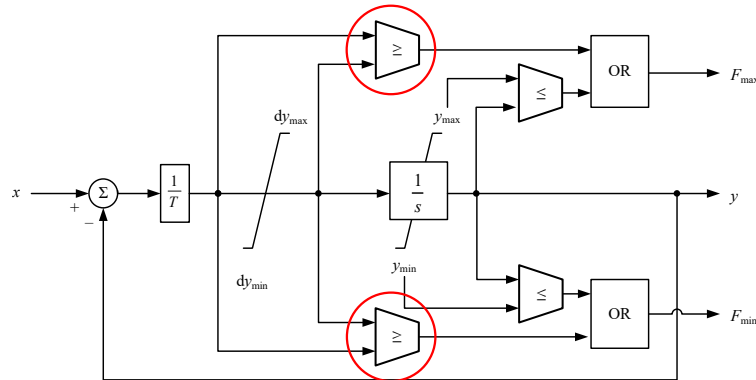


Figure 5.4: IEC 61400-27-1 First order filter with limitation detection (G.10). Source [30].

5.3. Future work

With the close publication of the future Editions of the IEC 61400-27 Parts 1 and 2 (expected in 2020), the modeling of those new generic WT models is one of the most important future works. Furthermore, the comparison between the 1st and 2nd Edition IEC WT models will be an interesting study with which to assess the modifications performed in the models. Additionally, the publication of the complete validation methodology in the IEC 61400-27-2 will allow to conduct complete validation studies, which will be more and more important for real WTs and WPPs.

Additionally, the modeling of generic WPP following the IEC and WECC guidelines will involve a new range of studies. With the international grid codes being more and more strict with the integration of wind energy in power systems, a complete WPP model will allow TSOs and DSOs to conduct new analysis. Furthermore, the WPP behavior facing secondary or tertiary regulation commands may be modeled, covering grid codes such as the Spanish, that considers this operation.

Finally, new studies are being considered using generic WT models. For example, their use to study voltage flicker, and the effect that WTs have on it, is currently being studied. The different control modes allowed by the generic WT models allow different studies to be conducted, aiming to improve the grid integration of wind energy in current power systems, thus promoting the use of renewable energies worldwide.

Bibliography

- [1] GWEC. Global Wind Statistics 2018. Technical report, Global Wind Energy Council, 2018.
- [2] A. Sedaghat, A. Hassanzadeh, J. Jamali, A. Mostafaeipour, and W.-H. Chen. Determination of rated wind speed for maximum annual energy production of variable speed wind turbines. *Applied Energy*, 205:781–789, 2017.
- [3] M.M. Savino, R. Manzini, V. Della Selva, and R. Accorsi. A new model for environmental and economic evaluation of renewable energy systems: The case of wind turbines. *Applied Energy*, 189:739–752, 2017.
- [4] United Nations. Kyoto protocol to the United Nations framework convention on climate change, 1998.
- [5] European Commission. Horizon 2020 - Work Programme 2018-2020: 10. Secure, clean and efficient energy, 2018.
- [6] H. Holttinen, P. Meibom, A. Orths, B. Lange, M. O'Malley, J. O. Tande, A. Estanqueiro, E. Gómez-Lázaro, L. Soder, G. Strbac, J. C. Smith, and F. V. Hulle. Impacts of large amounts of wind power on design and operation of power systems, results of IEA collaboration. *Wind Energy*, 14, no. 2:179 – 192, 2011.
- [7] A. Basit, A.D. Hansen, M. Altin, P. Sørensen, and M. Gamst. Wind power integration into the automatic generation control of power systems with large-scale wind power. *The Journal of Engineering*, 2014:538–545(7), October 2014.
- [8] M. Tsili and S. Papathanassiou. A review of grid code technical requirements for wind farms. *IET Renewable Power Generation*, 3(3):308–332, 2009.

-
- [9] R. Guerrero. Grid code interrelation, wind generation evolution and reactive compensation. special topics inside a grid code. In *CIREN 2012 Workshop: Integration of Renewables into the Distribution Grid*, pages 1–4, May 2012.
- [10] I. Erlich, H. Wrede, and C. Feltes. Dynamic behavior of DFIG-Based wind turbines during grid faults. *Power Conversion Conference*, pages 1195–1200, 2007.
- [11] C. Vázquez Hernández, T. Telsnig, and A. Villalba Pradas. JRC Wind Energy Status Report 2016 Edition. Market, technology and regulatory aspects of wind energy. JRC Science for policy report, 2017.
- [12] I. Erlich, F. Shewarega, C. Feltes, F. W. Koch, and J. Fortmann. Off-shore wind power generation technologies. *Proceedings of the IEEE*, 101(4):891–905, April 2013.
- [13] J. Carroll, A. McDonald, and D. McMillan. Reliability comparison of wind turbines with DFIG and PMG drive trains. *IEEE Transactions on Energy Conversion*, 30(2):663–670, June 2015.
- [14] T. Petru. Modelling of wind turbines for power system studies. Technical report, Chalmers University of Technology, Sweden, 2001.
- [15] V. Akhmatov. Modelling and ride-through capability of variable speed wind turbines with permanent magnet generators. *Wind Energy*, 9:313–326, November 2006.
- [16] S. K. Salman, B. Badrzadeh, and J. Penman. Modelling wind turbine-generators for fault ride-through studies. In *Proc. 39th Int. Universities Power Engineering Conf. UPEC 2004*, volume 2, pages 634–638, 2004.
- [17] V. Akhmatov, J.N. Nielsen, K.H. Jensen, J. Thisted, M. Frydensbjerg, and B. Andresen. Siemens wind power variable-speed full scale frequency converter wind turbine model for balanced and unbalanced short-circuit faults. *Wind Engineering*, 34(2):139–156, 2010.
- [18] R. Zavadil, N. Miller, A. Ellis, E. Muljadi, P. Pourbeik, S. Saylor, R. Nelson, G. Irwin, M.S. Sahni, and D. Muthumuni. Models for change. *IEEE Power and Energy Magazine*, 9(6):86–96, 2011.
- [19] A. I. Estanqueiro. A dynamic wind generation model for power systems studies. *IEEE Transactions on Power Systems*, 22(3):920–928, 2007.
- [20] J. Hu, Y. Huang, D. Wang, H. Yuan, and X. Yuan. Modeling of grid-connected DFIG-based wind turbines for DC-link voltage stability analysis. *IEEE Transactions on Sustainable Energy*, 6(4):1325–1336, Oct 2015.

- [21] G. P. Prajapat, N. Senroy, and I. N. Kar. Wind turbine structural modeling consideration for dynamic studies of DFIG based system. *IEEE Transactions on Sustainable Energy*, 8(4):1463–1472, Oct 2017.
- [22] S. Seman. Need for confidentiality. A converter manufacturer’s view. *1st Wind Integration Symposium*, page 30pp, 2011.
- [23] A. Perdana. *Dynamic Models of Wind Turbines. A Contribution towards the Establishment of Standardized Models of Wind Turbines for Power System Stability Studies*. PhD thesis, Chalmers University of Technology, 2008.
- [24] A. Ellis, Y. Kazachkov, E. Muljadi, P. Pourbeik, and J.J. Sanchez-Gasca. Description and technical specifications for generic WTG models – A status report. *IEEE/PES Power Systems Conference and Exposition (PSCE)*, pages 1–8, 2011.
- [25] Y.L. Hu and Y.K. Wu. Comparative analysis of generic and complex models of the Type-3 wind turbine. In *2016 IEEE PES Asia-Pacific Power and Energy Engineering Conference (APPEEC)*, pages 392–396, Oct 2016.
- [26] P.K. Keung, Y. Kazachkov, and J. Senthil. Generic models of wind turbines for power system stability studies. *8th International Conference on Advances in Power System Control, Operation and Management*, pages 1–6, 2009.
- [27] WECC REMTF. WECC Wind Power Plant Dynamic Modeling Guide. Technical report, WECC, 2010.
- [28] P. Pourbeik. Generic models and model validation for wind and solar PV generation: Technical update. Technical report, Electric Power Research Institute, 2011.
- [29] WECC REMTF. WECC Second Generation of Wind Turbine Models Guidelines. Technical report, WECC, 2014.
- [30] IEC 61400-27-1 ed. 1. *Wind turbines - Part 27-1: Electrical simulation models for wind power generation – Wind turbines*. International Electrotechnical Commission, Geneva, Switzerland, February 2015.
- [31] A. Timbus, P. Korba, A. Vilhunen, G. Pepe, S. Seman, and J. Niiranen. Simplified model of wind turbines with doubly-fed induction generator. *10th International Workshop on Large-Scale Integration of Wind Power into Power Systems as well as on Transmission Networks for Offshore Wind Power Farms*, page 6pp, 2011.

- [32] P. Sørensen. Introduction to IEC 61400-27. Electrical simulation models for wind power generation. *EERA Workshop on Generic electric models for wind power*, 2012.
- [33] P. Pourbeik, J. J. Sánchez-Gasca, J. Senthil, J. Weber, A. Ellis, S. Williams, S. Seman, K. Bolton, N. Miller, R. J. Nelson, K. Nayebi, K. Clark, S. Tacke, and S. Lu. Value and limitations of the positive sequence generic models of renewable energy systems, December 2015.
- [34] P. Pourbeik. Proposed modifications to the WT3 and WT4 generic models. Technical report, Electric Power Research Institute, 2011.
- [35] P. Sørensen, J. Fortmann, F. Jiménez Buendía, J. Bech, A. Morales, and Chavdar Ivanov. Final draft international standard IEC 61400-27-1. Electrical simulation models of wind turbines. *13th Wind Integration Workshop*, page 5pp, 2014.
- [36] A. Honrubia-Escribano, F. Jiménez-Buendía, E. Gómez-Lázaro, and J. Fortmann. Validation of generic models for variable speed operation wind turbines following the recent guidelines issued by IEC 61400-27. *Energies*, 9, 2016.
- [37] A. Honrubia-Escribano, F. Jiménez-Buendía, E. Gómez-Lázaro, and J. Fortmann. Field validation of a standard type 3 wind turbine model for power system stability, according to the requirements imposed by iec 61400-27-1. *IEEE Transactions on Energy Conversion*, 33(1):137–145, March 2018.
- [38] M. Asmine, J. Brochu, J. Fortmann, R. Gagnon, Y. Kazachkov, C. E. Langlois, C. Larose, E. Muljadi, J. MacDowell, P. Pourbeik, S.A. Seman, and K. Wiens. Model validation for wind turbine generator models. *IEEE Transactions on Power Systems*, 26(3):1769–1782, 2011.
- [39] F. J. Buendía, A. Viguera-Rodríguez, E. Gomez-Lazaro, J. A. Fuentes, and A. Molina-Garcia. Validation of a mechanical model for fault ride-through: Application to a Gamesa G52 commercial wind turbine. *IEEE Transactions on Energy Conversion*, 28(3):707–715, 2013.
- [40] P. Pourbeik. Proposed changes to the WECC WT3 generic model for Type 3 wind turbine generators. Technical report, Electric Power Research Institute, 2014.
- [41] P. Pourbeik. Proposed changes to the WECC WT4 generic model for Type 4 wind turbine generators. Technical report, Electric Power Research Institute, 2013.

- [42] P. Pourbeik. Model validations attempts for the Type 3 generic model structure-review of proposed changes by Gamesa. Technical report, EPRI, 2012.
- [43] NERC. Standard models for variable generation. Technical report, North American Electric Reliability Corporation, 2010.
- [44] Ö. Göksu, P. Sørensen, A. Morales, S. Weigel, J. Fortmann, and P. Pourbeik. Compatibility of IEC 61400-27-1 Ed 1 and WECC 2nd Generation Wind Turbine Models. *15th Wind Integration Workshop*, 2016.
- [45] J. Fortmann, S. Engelhardt, J. Kretschmann, M. Janben, T. Neumann, and I. Erlich. Generic simulation model for DFIG and full size converter based wind turbines. *9th Wind Integration Workshop*, page 8pp, 2010.
- [46] P. Pourbeik. Proposed changes to the WECC WT3 generic model for Type 3 wind turbine generators. Technical report, Electric Power Research Institute, 2012.
- [47] WECC REMTF. WECC Wind Power Plant Dynamic Modeling Guidelines. Technical report, WECC, 2014.
- [48] International Electrotechnical Commission. Approval stage - Final Draft International Standard (FDIS). <https://www.iec.ch/standardsdev/how/processes/development/approval.htm>.
- [49] International Electrotechnical Commission. FDIS documents. https://www.iec.ch/standardsdev/resources/draftingpublications/overview/drafting_process/fdis_doc.htm.
- [50] M. Pöller. Doubly-fed induction machine models for stability assesment of wind farms. In *Proceedings of the IEEE Power-Tech Conference*, Bologna, Italy, 2003.
- [51] Miller N. W., Sanchez-Gasca J.J., Price W. W., and Delmerico R. W. Dynamic modeling of GE 1.5 and 3.6 MW wind turbine-generators for stability simulations. *IEEE Power Engineering Society General Meeting*, 3:1977–1983, 2003.
- [52] W.W. Price and J.J. Sanchez-Gasca. Simplified wind turbine generator aerodynamic models for transient stability studies. *IEEE PES Power Systems Conference and Exposition*, pages 986 – 992, 2006.
- [53] J.N. Nielsen, V. Akhmatov, J. Thisted, E. Grondahl, P. Egedal, M.N. Frydensbjerg, and K.H. Jensen. Modelling and fault-ride-through tests of Siemens wind power 3.6 MW variable-speed wind turbines. *Wind Engineering*, 31(6):441–452, 2007.

- [54] M. Martins, A. Perdana, P. Ledesma, E. Agneholm, and O. Carlson. Validation of fixed speed wind turbine dynamic models with measured data. *Renewable Energy*, 32(8):1301–1316, 2007.
- [55] M. Behnke, A. Ellis, Y. Kazachkov, T. McCoy, E. Muljadi, W. Price, and J. Sánchez-Gasca. Development and validation of WECC variable speed wind turbine dynamic models for grid integration studies. In *AWEA's 2007 WindPower Conference*, California, USA, June 2007.
- [56] C.E. Langlois, D. Lefebvre, L. Dube, and R. Gagnon. Developing a Type-III wind turbine model for stability studies of the hydro-quebec network. *8th International Workshop Large-Scale Integration of Wind Power Into Power Systems*, pages 674–679, 2009.
- [57] J. Fortmann, S. Engelhardt, J. Kretschmann, C Feltes, and I. Erlich. Validation of an RMS DFIG simulation model according to new german model validation standard FGW TR4 at balanced and unbalanced grid faults. In *8th International Workshop on Large-Scale Integration of Wind Power into Power Systems as well as on Transmission Networks for Offshore Wind Farms*, 2009.
- [58] J. Fortmann. Generic aerodynamic model for simulation of variable speed wind turbines. *9th International Workshop on Large-Scale Integration of Wind Power into Power Systems as well as on Transmission Networks for Offshore Wind Power Plants*, page 7pp, 2010.
- [59] K. Clark, N.W. Miller, and J. Sánchez-Gasca. Modeling of GE wind turbine-generators for grid studies. Technical Report 4.5, General Electric International, Inc., 2010.
- [60] M. Mata Dumenjó, J. Sánchez Navarro, V. Casadevall Benet, J. Gil Cepeda, and L. García Caballero. Simplified model of DFIG. *10th International Workshop on Large-Scale Integration of Wind Power into Power Systems as well as on Transmission Networks for Offshore Wind Power Farms*, page 5pp, 2011.
- [61] A. Ellis, E. Muljadi, J. Sanchez-Gasca, and Y. Kazachkov. Generic models for simulation of wind power plants in bulk system planning studies. *IEEE Power and Energy Society General Meeting*, pages 1–8, 2011.
- [62] S. Seman, J. Simolin, J. P. Matsinen, and J. Niiranen. Validation of Type 4 wind turbine generic simulation model by full-scale test. *9th Wind Integration Workshop*, page 6pp, 2010.
- [63] I.A. Hiskens. Dynamics of type-3 wind turbine generator models. *IEEE Transactions on Power Systems*, 27(1):465–474, 2012.

- [64] P. Pourbeik. Example case of using field data for model calibration of a type 4 wind turbine generator. Technical report, Electric Power Research Institute, 2011.
- [65] P. Pourbeik, A. Ellis, J. Sanchez-Gasca, Y. Kazachkov, E. Muljadi, J. Senthil, and D. Davies. Generic stability models for type 3 & 4 wind turbine generators for WECC. *IEEE Power and Energy Society General Meeting*, pages 1–5, 2013.
- [66] P. Pourbeik. Specification of the second generation generic models for wind turbine generators. Technical report, Electric Power Research Institute, 2014.
- [67] M. P. Richwine, J. J. Sanchez-Gasca, and N. W. Miller. Validation of a second generation type 3 generic wind model. *IEEE Power Energy Society General Meeting*, pages 1–4, 2014.
- [68] A. Aziz, M. Amanullah, A. Vinayagam, and A. Stojcevski. Modelling and comparison of generic type 4 WTG with EMT type 4 WTG model. In *2015 Annual IEEE India Conference (INDICON)*, pages 1–6, Dec 2015.
- [69] A. Ellis, P. Pourbeik, J. J. Sanchez-Gasca, J. Senthil, and J. Weber. Generic wind turbine generator models for WECC — A second status report. *IEEE Power and Energy Society General Meeting*, pages 1–5, 2015.
- [70] P. Pourbeik. Model user guide for generic renewable energy system models. Technical report, Electric Power Research Institute, 2015.
- [71] P. Sørensen, B. Andersen, J. Fortmann, K. Johansen, and P. Pourbeik. Overview, status and outline of the new IEC 61400 -27 - Electrical simulation models for wind power generation. *10th International Workshop on Large-Scale Integration of Wind Power into Power Systems as well as on Transmission Networks for Offshore Wind Power Farms*, page 6pp, 2011.
- [72] I. Margaritis, A.D. Hansen, J. Bech, B. Andresen, and P. Sørensen. Implementation of IEC standard models for power system stability studies. *11th International Workshop on Large-Scale Integration of Wind Power into Power Systems*, page 6pp, 2012.
- [73] P. Sørensen, B. Andersen, J. Bech, J. Fortmann, and P. Pourbeik. Progress in IEC 61400 -27. Electrical simulation models for wind power generation. *11th International Workshop on Large-Scale Integration of Wind Power into Power Systems as well as on Transmission Networks for Offshore Wind Power Farms*, page 7pp, 2012.

- [74] P. Sørensen. Generic wind power modelling. *CIGRE 7th Southern Africa Regional Conference*, page 62pp, 2013.
- [75] P. Sørensen, B. Andresen, J. Fortmann, and P. Pourbeik. Modular structure of wind turbine models in IEC 61400-27-1. *IEEE Power and Energy Society General Meeting*, pages 1–5, 2013.
- [76] S.T. Cha, Q. Wu, H. Zhao, I. Margaritis, P. Sørensen, and J. Østergaard. Implementation of IEC generic model type 1 wind turbine generators using RTDS. *International Conference on Wind energy Grid-Adaptive Technologies*, page 8pp, 2012.
- [77] H. Zhao, Q. Wu, P. Sørensen, J. Bech, and B. Andresen. Implementation of draft IEC generic model of type 1 wind turbine generator in powerfactory and simulink. *12th International Workshop on Large-Scale Integration of Wind Power into Power Systems as well as on Transmission Networks for Offshore Wind Power Plants*, page 8pp, 2013.
- [78] H. Zhao, Q. Wu, I. Margaritis, J. Bech, P. Sørensen, and B. Andresen. Implementation and validation of IEC generic Type 1A wind turbine generator model. *International Transactions on Electrical Energy Systems*, 25(9):1804–1813, 2014.
- [79] A. Honrubia Escribano, E. Gómez-Lázaro, A. Viguera-Rodríguez, A. Molina-García, J. A. Fuentes, and E. Muljadi. Assessment of DFIG simplified model parameters using field test data. *IEEE Symposium on Power Electronics & Machines for Wind Application*, pages 1 – 7, 2012.
- [80] C. Subramanian, D. Casadei, A. Tani, P. Sorensen, F. Blaabjerg, and P. McKeever. Implementation of electrical simulation model for IEC Standard Type-3A generator. In *2013 European Modelling Symposium*, pages 426–431, Nov 2013.
- [81] F. Jiménez Buendía and B. Barrasa Gordo. Generic simplified simulation model for DFIG with active crowbar. *11th Wind Integration Workshop*, page 6pp, 2012.
- [82] J. Fortmann. *Modeling of Wind Turbines with Doubly Fed Generator System*. PhD thesis, Department for Electrical Power Systems, University of Duisburg-Essen, 2014.
- [83] J. Fortmann, S. Engelhardt, J. Kretschmann, C. Feltes, and I. Erlich. New generic model of DFG-Based wind turbines for rms-type simulation. *IEEE Transactions on Energy Conversion*, 29(1):110–118, 2014.

- [84] X.S. Han and Q.H. Liu. Research on IEC type3 wind turbine generator. *Applied Mechanics and Materials*, 556-562:2021–2026, 2014.
- [85] J. Fortmann. Generic aerodynamic model for simulation of variable speed wind turbines. In *Proceedings of 9th International Workshop on Large-Scale Integration of Wind Power into Power Systems*, Quebec (Canada), 2010. Energynautics GmbH.
- [86] A. Honrubia-Escribano, S. Martín-Martínez, A. Estanqueiro, F. Jiménez Buendía, and E. Gómez Lázaro. Simplified wind turbine models for wind energy integration into power systems. *European Wind Energy Conference*, page 6pp, 2015.
- [87] J. Bech. Siemens experience with validation of different types of wind turbine models. *IEEE Power and Energy Society General Meeting*, 2014.
- [88] M. Meuser and M. Brennecke. Analysis and comparison of national and international validation methods to assess the quality of DG simulation models. In *International ETG Congress 2015; Die Energiewende - Blueprints for the new energy age*, pages 1–7, Nov 2015.
- [89] Q. Li, J. He, S. Qin, and X. Shi. Wind turbine model validation based on state interval and error calculation. *The Journal of Engineering*, 2017(13):762–767, 2017.
- [90] A. Honrubia Escribano, E. Gomez-Lazaro, J. Fortmann, P. Sørensen, and S. Martín-Martínez. Generic dynamic wind turbine models for power system stability analysis: A comprehensive review. *Renewable & Sustainable Energy Reviews*, 81:1939 – 1952, 2018.
- [91] Ö. Göksu, M. Altin, J. Fortmann, and P. Sorensen. Field validation of IEC 61400-27-1 wind generation Type 3 model with plant power factor controller. *IEEE Transactions on Energy Conversion*, 2016.
- [92] P. Pourbeik, N. Etzel, and S. Wang. Model validation of large wind power plants through field testing. *IEEE Transactions on Sustainable Energy*, 9(3):1212–1219, July 2018.
- [93] J. Fortmann, N. Miller, Y. Kazachkov, J. Bech, B. Andresen, P. Pourbeik, and P. Sørensen. Wind plant models in IEC 61400-27-2 and WECC - latest developments in international standards on wind turbine and wind plant modeling. *14th International Workshop on Large-Scale Integration of Wind Power into Power Systems as well as on Transmission Networks for Offshore Wind Power Plants*, page 5pp, 2015.

-
- [94] MATLAB. Version 9.5 R2018b. <https://www.mathworks.com/products/matlab.html>, 2018.
- [95] Simulink. Version 9.2 R2018b. <https://www.mathworks.com/products/simulink.html>, 2018.
- [96] Simscape. Version 4.5 R2018b. <https://www.mathworks.com/products/simscape.html>, 2018.
- [97] M. B. C. Salles, K. Hameyer, J. R. Cardoso, A. P. Grilo, and C. Rahmann. Crowbar system in doubly fed induction wind generators. *Energies*, 3:738–753, 2010.
- [98] J.M. Rodriguez, D. Alvira, and S. ; Bañares. The spanish experience of the grid integration of wind energy sources. In *Power Tech, 2005 IEEE Russia*, 2005.
- [99] A. Lorenzo-Bonache, A. Honrubia-Escribano, J. Fortmann, and E. Gómez-Lázaro. Generic Type 3 WT models: comparison between IEC and WECC approaches. *IET Renewable Power Generation*, February 2019.
- [100] REE. *P.O. 12.3 Requisitos de respuesta frente a huecos de tensión de las instalaciones eólicas (in Spanish)*. Red Eléctrica de España, October 2006.
- [101] I. P. Girsang, J. S. Dhupia, E. Muljadi, M. Singh, and L. Y. Pao. Gearbox and drivetrain models to study dynamic effects of modern wind turbines. In *2013 IEEE Energy Conversion Congress and Exposition*, pages 874–881, Sep. 2013.
- [102] A. Lorenzo-Bonache, A. Honrubia-Escribano, F. Jiménez-Buendía, A. Molina-García, and E. Gómez-Lázaro. Generic Type 3 wind turbine model based on IEC 61400-27-1: Parameter analysis and transient response under voltage dips. *Energies*, 10(9):23, 2017.
- [103] A. Lorenzo-Bonache, R. Villena-Ruiz, A. Honrubia-Escribano, and E. Gómez-Lázaro. Operation of active and reactive control systems of a generic Type 3 WT model. *IEEE International Conference on Compatibility, Power Electronics and Power Engineering*, 2017.
- [104] A. Lorenzo-Bonache, R. Villena-Ruiz, A. Honrubia-Escribano, and E. Gómez-Lázaro. Comparison of a standard type 3B WT model with a commercial build-in model. *IEEE International Electric Machines & Drives Conference*, 2017.
- [105] E. Artigao, S. Martín-Martínez, A. Honrubia-Escribano, and E. Gómez-Lázaro. Wind turbine reliability: A comprehensive review

- towards effective condition monitoring development. *Applied Energy*, 228:1569 – 1583, 2018.
- [106] A. Lorenzo-Bonache, A. Honrubia-Escribano, F. Jimenez, and E. Gomez-Lazaro. Field validation of generic Type 4 wind turbine models based on IEC and WECC guidelines. *IEEE Transactions on Energy Conversion*, pages 1–1, 2018.
- [107] IEC 61400-21. *Wind turbine generator systems. Part 21. Measurement and assessment of power quality characteristics of grid connected wind turbines*. International Electrotechnical Commission, Geneva, Switzerland, August 2008.
- [108] Simulink Design Optimization tool. Version 3.5 R2018b. https://www.mathworks.com/products/sl-design-optimization.html?s_tid=srchtitle, 2018.

Acknowledgment to the IEC

The author thanks the International Electrotechnical Commission (IEC) for permission to reproduce Information from its International Standards. All such extracts are copyright of IEC, Geneva, Switzerland. All rights reserved. Further information on the IEC is available from www.iec.ch. IEC has no responsibility for the placement and context in which the extracts and contents are reproduced by the author, nor is IEC in any way responsible for the other content or accuracy therein

Acronyms

DFIG Doubly Fed Induction Generator

DSOs Distribution System Operators

EID International Doctoral School

EMT Electromagnetic Transients

EPRI Electric Power Research Institute

FC Full-Converter

FDIS Final Draft International Standard

GWEC Global Wind Energy Council

IEC International Electrotechnical Commission

JCR Journal Citation Report

LVRT Low Voltage Ride Through

MAE Mean Absolute Error

ME Mean Error

MXE Maximum Absolute Error

NERC North American Electric Reliability Corporation

PI Proportional-Integral

QSS Quasi Steady State

RMS Root Mean Square

TC Technical Committee

TSOs Transmission System Operators

UCLM University of Castilla – La Mancha

WECC Western Electricity Coordinating Council

WG Working Group

WPP Wind Power Plants

WT Wind Turbine

WTR Wind Turbine Rotor

